The Role of Periostin in ErbB2-Driven Mammary Tumorigenesis and Its Gene Regulation in ErbB2+ Cancer Cells

Cédrik Labrèche

Department of Cellular and Molecular Medicine

Faculty of Medicine

University of Ottawa

Ottawa, Ontario, Canada

July 2021

This thesis is submitted as a partial fulfilment of the

Ph.D. Program in Cellular and Molecular Medicine

Abstract

Breast cancer is a highly heterogeneous disease with multiple drivers and a complex regulatory network. Periostin (Postn) is a matricellular protein involved in a plethora of cancer types and other diseases. More specifically, Postn has been shown to be involved in various processes of tumor progression such as angiogenesis, cell survival, invasion, and metastasis. A high Postn level in breast cancer has been corelated with a more aggressive phenotype. Despite extensive research, it remains unclear what Postn is doing to the cancer environment and how cancer cells regulate Postn. Here, we assessed the role and regulation mechanisms of Postn in ErbB2-mediated tumorigenesis. By crossing Postn deficient animals into the oncogenic NeuNDL model of ErbB2-positive breast cancer, we have shown that Postn deletion delays tumor onset and increases overall survival by affecting proliferation and apoptosis. These tumors also showed a decrease in collagen deposition which is the proposed mechanism for its effect *in vivo*. Using isolated cancer cells from the Postn deficient background we assessed re-expression of Postn which had no effect on *in vitro* tumorigenesis processes or *in vivo* subcutaneous growth in immunodeficient mice. Furthermore, we established an *in vitro* model to study the regulation of Postn using a bovine pituitary gland derived extract as a natural repressor of Postn. Using mass spectrometry and RNA sequencing, we identified potential regulators of Postn gene expression. We also showed a cross regulation between FGFR, TGFβ and PI3K/AKT pathways to regulate Postn expression. In ErbB2-mediated murine breast cancer cells, we found that TGFβ can induce Postn expression in a SMAD-independent manner while bFGF can repress Postn expression through a PKC-dependent pathway. Postn induction and repression by TGFβ and bFGF respectively, are both dependent on PI3K/AKT signaling. Overall, these results suggest a cancer-driving function for Postn and reveal a novel mechanism for regulating Postn expression.

Table of Contents

Lists of figures

Chapter 1

Chapter 3

Chapter 4

Chapter 5

Chapter 6

Lists of tables

Chapter 2

Chapter 4

Abbreviations

AKT	Protein kinase B
ALDH	Aldehyde dehydrogenase
AR	Amphiregulin
BME	Basement membrane extract
BMP	Bone morphogenetic protein
BPE	Bovine pituitary extract
BSA	Bovine serum albumin
BTC	betacellulin
CAF	Cancer-associated fibroblast
CSC	Cancer stem cell
DAB	Diaminobenzidine
DAG	Diacylglycerol
DAPI	4’,6-diamidino-2-phenylindole
DMEM	Dulbecco’s modified Eagle medium
DMSO	Dimethyl sulfoxide
DNA	Desoxyribonucleic acid
dNTP	Deoxynucleoside triphosphate
DTT	Dithiothreitol
ECM	Extracellular matrix
EDTA	Ethylenediaminetetraacetic acid
EGF	Epidermal growth factor

EGFR	Epidermal growth factor receptor
EMT	Epithelial-mesenchymal transition
EPG	Epigen
EPR	Epiregulin
ESR	Estrogen receptor
FAK	Focal adhesion kinase
FBS	Fetal bovine serum
FGF	Fibroblast growth factor
FGFR	Fibroblast growth factor receptor
GAB	GRB2 Associated Binding Protein
GRB	Growth factor receptor-bound protein
GSK	Glycogen synthase kinase
HB-EGF	Heparin-binding EGF-like growth factor
HER	Human epidermal growth factor receptor
HPSG	Heparan sulphate proteoglycans
HRP	Horseradish peroxidase
IGF	Insulin-like growth factor
IgG	Immunoglobulin G
IHC	Immunohistochemistry
IL	Interleukin
IRES	Internal ribosome entry site
JNK	c-Jun N-terminal kinase
LC-MS	Liquid chromatography–mass spectrometry

LOX	Lysyl Oxidase
MAPK	Mitogen-activated protein kinase
MEGS	Mammary epithelial growth supplement
MMTV	Mouse mammary tumor virus
NDL	Neu Deletion2-5
NIC	Neu Deletion2-5 internal ribosome entry site Cre
NRG	Neuregulin
OSF-2	Osteoblast specific factor
PARP	Poly [ADP-ribose] polymerase
PBS	Phosphate buffered saline
PCR	Polymerase chain reaction
PDGF	Platelet-derived growth factor
PDGFR	Platelet-derived growth factor receptor
PDK	3-Phosphoinositide-dependent kinase
PFA	Paraformaldehyde
PGR	Progesterone receptor
PI3K	Phosphoinositide 3-kinase
PIP_2	Phosphatidylinositol 4,5-bisphosphate
PIP_3	Phosphatidylinositol (3,4,5)-trisphosphate
PKC	Protein kinase C
PLC	Phospholipase C
PMA	Phorbol 12-myristate 13-acetate
PMSF	Phenylmethylsulfonyl fluoride

POSTN	Periostin
PVDF	Polyvinylidene fluoride
PyMT	Polyoma virus middle T antigen
RNA	Ribonucleic acid
RSK	Ribosomal protein S6 kinase
RTK	Receptor tyrosine kinase
SDS	Sodium dodecyl sulfate
SEM	Standard error of the mean
SMA	Smooth muscle actin
SOS	Son of the Sevenless
STAT	Signal transducer and activator of transcription
TBS	Tris-buffered saline
TGF	Transforming growth factor
TMA	Tissue microarray
TME	Tumor microenvironment
TNBC	Triple negative breast cancer
TNM	Tumor Nodes Metastasis
TNF	Tumor necrosis factor
VEGF	Vascular endothelial growth factor
WT	Wildtype

Significant Contributions

David P. Cook generated all the data analysis scripts and analyzed RNA-sequencing data shown in Figure 4.11. David also analyzed single-cell RNA-sequencing from a TNBC dataset shown in Figure 4.3.

Christiano Tanese de Souza performed subcutaneous injection shown in Figure 3.13.

Sabina Sarvan performed on-column size exclusion and ion-exchange chromatography shown in Figure 4.8 and 4.9, respectively.

John L. Holmes Mass Spectrometry Facility processed the samples, performed and analyzed the mass spectrometry shown in Table 4.1.

The Louise Pelletier Histology Core Facility performed the paraffin embedding and sectioning of all tissues and performed the Masson's trichrome staining on mammary tumors.

Acknowledgments

Throughout the progression of this research project and thesis writing, I have received a great amount of support and assistance from a wide range of people.

I would like to first thank my supervisor, Dr. Luc Sabourin, for his consistent support and guidance through times when things were going great and times when things were not going too well. Through the ups and downs, Luc's down-to-earth personality and openness to try new approaches really allowed me to put my own personal touch into my research project.

To my family, especially my mother, father, and brother, I am eternally grateful for your continuous support and for always being there for me. I dedicate this thesis to the three of you as I would not have been able to achieve this without your unceasing encouragements, motivation and pushing for me to reach my full potential.

To all my present and former lab mates, more specifically John, Khalid and Ben, thanks for showing me much more than techniques and principles. You guys showed me that hard work and success is possible while still having a blast in the lab. From the overly serious scientific discussions to the goofy conversations, you guys made the laboratory feel like home, and for that I am forever grateful.

Thanks to all my friends who I might have neglected at times, to be so understanding and supportive through the struggles and challenges.

Finally, thanks to Valerie, who has been with me through it all from the beginning and offered me support and distraction in the times I needed it most, and for it I am extremely thankful.

Chapter 1

General Introduction

1.1 Breast Cancer

1.1.1 Breast Cancer Classification Systems

Breast cancer is the most common type of cancer in women worldwide, excluding non-melanoma skin cancer [1]. Breast cancer is a complex and highly heterogeneous disease which is generally classified in several molecular subtypes [2, 3]. Those subtypes are generally identified by distinct gene expression profiles and molecular markers. The expression of Estrogen Receptor (ESR1), Progesterone Receptor (PGR) and Human Epidermal Growth Factor Receptor 2 (HER2) are used as the basis for the classification system [4]. The Luminal A and Luminal B subtypes are characterized by the expression of ESR1 and PGR, the difference between those two subtypes being that the Luminal B usually has higher proliferation index (Ki67-positive) [5, 6]. The Luminal subtypes are the most common with approximately 65% of all breast cancer cases and these tend to have a better prognosis than other subtypes, with Luminal A having a significantly better outcome than Luminal B [7, 8]. The HER2-positive subtype is characterized by an overexpression of the HER2 receptor with low or no expression of ESR1 and PGR. This subtype has a prevalence of approximately 30% and is strongly associated with a highly metastatic disease and a poor prognosis in patients [9-11]. Finally, the triple negative breast cancer (TNBC) subtype is characterized by the lack of ESR1, PGR and HER2 and accounts for approximately 10-15% of all breast cancer cases [7, 12]. This subtype has the worst survival rate and prognosis since there are currently no targeted therapies available as no critical therapeutic targets have been identified for this subtype [13]. A summary of breast cancer subtype classification along with their receptor expression pattern and overall prognosis is presented in Figure 1.1.

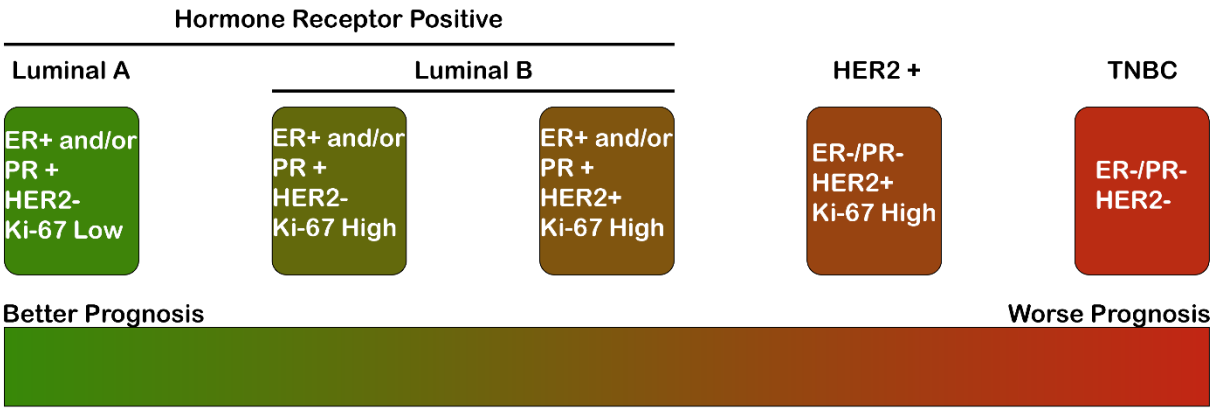

Figure 1.1 Classification of breast cancer subtype.

Subtype of breast cancer are presented along with their receptor status for Estrogen Receptors (ER), Progesterone Receptors (PR), Human Epidermal Growth Factor Receptor 2 (HER2) and Ki-67. Overall prognosis is ordered with a gradient from green (better prognosis) to red (worse prognosis). Figure adapted from [14].

Alongside subtype identification, physicians also use the TNM staging system which is based on anatomic information relating to the size of the primary tumor (T), the extent of lymph node involvement (N) and the presence or lack of metastases at distant sites (M), the most common for breast cancers being the bones, the lungs, the brain and the liver [15, 16]. Another way to classify tumors is by their histologic characteristics. Pathologists will make a histologic diagnosis on a biopsy or a fully resected tumor using standardized criteria. The most common breast cancer histology diagnosis is invasive ductal carcinoma which affects between 50 and 75% of all patients, followed by invasive lobular carcinoma making up 5 to 15% of cases. The remainder of patients are affected by a mixed of ductal and lobular carcinomas or other much rarer pathologies [17].

Cancer cells are also given a histological grade when they are resected from the primary site and analysed in the laboratory. The differentiation index of the cells is assessed and graded from 1 to 3, grade 1 being the most differentiated and 3 being poorly differentiated. The grade is an indication of how fast the cells are growing and spreading. Cells that are well differentiated tend to grow slowly and look more like normal breast tissue while poorly differentiated cells look different from normal breast cells and tend to grow and spread faster [18].

1.1.2 Breast Cancer Treatment

The goal for therapy in non-metastatic patients is to eradicate the tumor from breast tissues and regional lymph nodes. The standard of care for this type of cancer is local surgery to resect the tumor and assessment of lymph node involvement sometimes leading to removal of axillary lymph nodes, often combined with radiotherapy post-surgery. Systemic therapy is guided by subtype determination. Endocrine therapy is used for all hormone receptor positive

cancers (Luminal A and B) in combination with general chemotherapy. HER2-directed antibody therapy is used for all HER2-positive cancer (HER2- positive subtype) in combination with endocrine therapy (if hormone-receptor positive) and general chemotherapy. Chemotherapy alone is used for tumors that are negative for hormone receptor and HER2 (triple negative) [19]. These treatments can be given preoperatively (neoadjuvant), which shrinks the tumor before surgery, postoperatively (adjuvant), which reduces resurgence by killing the remaining cells, or both [20]. The therapeutic goal in metastatic patients is completely different since metastatic breast cancer is virtually incurable in all affected patients. The overall goal becomes focused on prolonging lifespan and improving the quality of life through symptom mitigation. The same treatment approach is used for systemic therapy, although, local therapy (surgery and radiation) are only used as palliative measures [19].

1.2 HER2-positive Breast Cancer

1.2.1 HER/ErbB Family

HER2/ErbB2/Neu (human, mouse and rat homolog, respectively) is a member of the HER family of transmembrane tyrosine kinase receptors (RTKs) [21]. This family contains four members which are EGFR/HER1/ErbB1, HER2/ErbB2, HER3/ErbB3 and HER4/ErbB4 [22]. These receptors require homodimerization or heterodimerization in order to be activated [23, 24] . Each member has distinctive characteristics that make them unique. Classically, RTKs contain a N-terminal ligand-binding domain, a transmembrane domain containing a single helix, a cytoplasmic tyrosine kinase domain and a C-terminal regulatory domain [25]. EGFR (HER1) contains all the classical components of RTKs while HER2 does not bind any ligand but remains in an open conformation for dimerization whereas HER3 can bind heregulin ligands but has impaired kinase activity [26, 27]. HER4 is a fully functional RTK but has a

unique property following ligand binding whereby HER4 undergoes proteolytic cleavage releasing an 80kDa intracellular domain that can enter the nucleus and regulate gene expression [28]. Consequently, in order to have proper activation of its downstream effectors following ligand binding, heterodimerization is critical for ligand binding and kinase activity for the transduction of intracellular signals [29]. Peptide growth factors of the EGF family act as ligands of the HER family and are segregated into categories depending on which receptors they are interacting with. The first group contains the ligands who specifically bind EGFR (HER1) which comprises Epithelial Growth Factor (EGF), transforming growth factor α (TGFα), amphiregulin (AR) and epigen (EPG) [30-33]. The second category includes factors that bind to both EGFR and HER4, namely epiregulin (EPR), β-cellulin (BTC) and heparin-binding EGF-like growth factors (HB-EGF) [34-36]. The third and last category regroups all the neuregulins that include NRG1 and NRG2 which can bind to HER3 and HER4 whereas NRG3-NRG5 can specifically only bind to HER4 [37-41]. More recently, Neuroglycan C, was shown to be a direct ligand of HER3, making it part NRG-6 [42]. A summary of the structure of the HER family members along with specific ligands for each is presented in Figure 1.2.

Upon ligand binding to the extracellular domain of HER, the receptor goes through conformational changes from tethered (unable to dimerize) to extended (able to dimerize) [25]. The receptors then undergo dimerization and subsequent transphosphorylation of tyrosine residues located in their intracellular domains. These phosphorylated residues can interact with various intracellular signaling adapter molecules which in turn activate numerous downstream second messenger pathways as well as cross-talk with other signaling pathways ultimately leading to a plethora of biological effects [43]. As HER2 is an orphan receptor (no endogenous ligand has been identified) and unable to undergo ligand-dependent conformational change, it

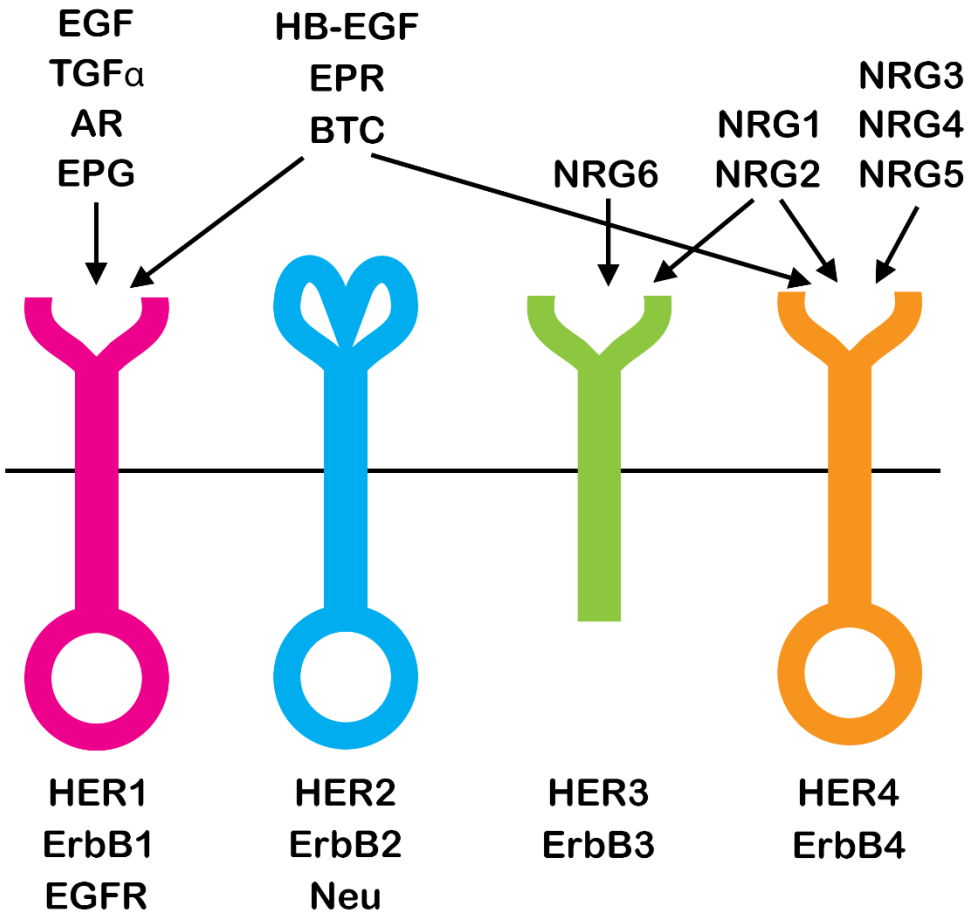

Figure 1.2 Schematic of HER family receptors and their respective ligands

HER1, the prototypical receptor of its family contains all important domains. HER2 does not have any activating soluble ligands while HER3 has impaired kinase activity and HER4 contains all important domains. HER1 specific ligands are Epithelial Growth Factor (EGF), transforming growth factor α (TGFα), amphiregulin (AR) and epigen (EPG). Epiregulin (EPR), β-cellulin (BTC) and heparin-binding EGF-like growth factors (HB-EGF) are specific for both HER1 and HER4. Neuregulin 1 (NRG1) and 2 (NRG2) can act as a ligand for both HER3 and HER4. NRG6 is specific to HER3 while NGR3-5 are specific to HER4.

exists in an open activated form [44]. Consistent with its constitutively active conformation, HER2 has been identified as the preferred heterodimerization partner of all HER receptors [45]. The HER family is extensively expressed and important in non-hematopoietic tissues responsible for diverse functions [46, 47]. This family of receptors is critical for mammalian development as murine gene disruption models showed in multiple instances their involvement in the development of multiples organs including the nervous system, skin, lungs, and gastrointestinal tract [48-50]. Due to the embryonic lethality of these models, the functional importance of HER proteins in adult mammary gland development could not be established in early models. However, mammary gland developmental defects were depicted using alternative conditional knockout models that inactivate HER1 or HER2 [51, 52].

1.2.2 HER2/neu Oncogenes

The transforming potential of HER2/*Neu* is undeniable considering the extensive amount of supporting data. The rat *Neu* oncogene was identified and shown to transform NIH3T3 and mammary epithelial cells [53, 54]. There are a few significant differences in the way human and rodent versions of this oncogene induce transformation. First and foremost, it has been determined that the transformation functions of *Neu* were due to a V664E point mutation found in the transmembrane domain termed *NeuT* (or *NeuNT*) [55]. This specific mutation favors receptor dimerization and tyrosine kinase activity [56]. The wildtype *c-Neu* was also able to promote mammary tumor transformation in mouse models, but in most tumors, it occurred after the acquisition of deletion mutations in the extracellular region which similarly increased kinase activity and dimerization potential [57, 58].

In contrast, the human HER2 oncogene transforming potential is equally convincing, but its mechanisms are quite different. The rodent oncogene requires mutational activation to

induce transformation, the human counterpart can induce transformation through overexpression alone. Although engineered mutations of HER2 were able to replicate the results seen with the rodent *NeuNT* in terms of enhanced dimerization and kinase activity, these mutations do not occur spontaneously [59]. In a similar fashion, HER2 overexpression was tested in a plethora of cell lines, from mouse fibroblast cells to human mammary epithelial cancer cells with a similar effect on cell transformation, tumorigenic growth, 2D and 3D proliferative advantage and anti-apoptotic changes [60-63].

These experiments are highly relevant when comparing to the clinical data on the human disease. HER2 overexpression occurs in 25-30% of breast and ovarian cancers through amplification or transcriptional deregulation and its expression is associated with a worse prognosis [64]. It has been determined that in breast cancer, 25 to 50 copies of the HER2 gene can be present in the genome and a 40- to 100-fold increase in HER2 protein expression often leading to up to 2 million receptors on the surface of each tumor cell [65, 66]. The literature suggests that HER2 amplification is an early event but that its status is unchanged throughout the evolution to invasive disease and metastasis, indicating that it is a marker of the HER2 subtype and not an indicator of late-stage disease [67, 68]. Gene expression profiling studies showed that HER2 amplification is segregated into a specific disease subset containing a unique molecular pattern that is maintained throughout cancer progression [4, 69]. Along with their unique molecular portrait, HER2 amplification in breast cancer also leads to different biological characteristics that distinguish them from other subtypes of breast cancers. These include enhanced resistance to certain hormonal therapy [70, 71], sensitivity to specific chemotherapeutic agents [72] and enhanced tendency for brain metastasis [73].

1.2.3 Transgenic Models of HER2-positive Breast Cancer

Animal models depicting HER2-positive breast cancers have been widely used in the last decades. The most frequently used models have a similar structure, which is the mouse mammary tumor virus (MMTV) promoter driving expression of *Neu* or a mutated version of it [74, 75]. The MMTV promoter provides high level expression of the oncogene in the luminal epithelial and myoepithelial cells of the mammary epithelium starting at embryonic day 8.5 [74, 76]. Expression in the salivary glands and seminal vesicle, commonly referred to as leaky expression of MMTV promoter, has also been observed [74, 77]. The first reported model used a constitutively active *Neu* (*NeuNT*) containing a point mutation in the transmembrane domain [55]. This model resulted in female mice developing mammary tumors involving the entire mammary gland by 90 days of age on average [74]. Although this model is useful to study HER2-positive breast cancer, it mimics a somatic mutation of HER2. The main issue with this model is the fact that somatic mutation of HER2 happens in very rare occurrence [78]. HER2 is commonly overexpressed but not due to somatic mutations.

Another widely used murine model of breast cancer was generated by mammary-specific expression of the Polyoma Middle T antigen (PyMT). The MMTV-PyMT results in mammary gland transformation leading to the development of multifocal adenocarcinomas with a high incidence of metastases to the lymph nodes and lungs [79]. The tumors arising from this model display close similarity to human breast cancers by their gradual loss of hormone receptors such as estrogen and progesterone, which is correlated with an overexpression of ErbB2 and Cyclin D1 in late-stage breast cancers [80]. The particularity of this model is the short latency at which hyperplasia are seen (as early as 4 weeks of age).

Combined with metastasis, such a short latency makes it a model of choice to study tumorigenesis and metastasis.

In a different tumor model, *c-neu* was overexpressed under the same MMTV promoter. The resulting mice had their latency doubled compared to the *NeuNT* model even though their level of oncogene expression was similar [81]. It was found that 65% of the tumors arising from this model were carrying in-frame deletion affecting the extracellular domain of the transgene [58]. These deletions were replicated in cell lines and showed increased tyrosine kinase activity confirming these as activating mutations [58]. The high frequency of these mutations in wildtype *Neu* suggests that the tyrosine kinase activation acts as the rate-determining step for the induction of mammary tumors [58].

The observation that a rate-limiting step is controlled by the acquisition of deletions in wildtype Neu-induced mammary tumorigenesis led to the generation of the widely used MMTV-*Neu* deletion (NDL) model of breast cancer. The MMTV-NeuNDL2-5 transgenic line harbors a deletion of 5 amino acids which lead to a cysteine imbalance preventing cysteine bridge formation and promoting disulfide-stabilized dimers [82]. A splice variant of human HER2 has been observed with a 16 amino acid deletion which results in cysteine-related intramolecular disulfide bond previously described in the MMTV-NeuNDL2-5 model [58, 82]. This increase in stabilized dimers results in constitutive activation of Neu, which resulted in an average mammary tumor onset of 161 days [82]. The tumors resulting from this model resembled mammary adenocarcinomas and metastasized to the lungs in 67% of the animals.

This is still used today to study the effect of genes on mammary tumorigenesis by crossing knock-out mouse models into the MMTV-NeuNDL2-5 background. This is a powerful tool to assess the roles of other proteins *in vivo*, but gene deletions that were early

lethal could not be assessed using this model. This led to the generation of another widely used model to allow the study of conditional knockout alleles, the MMTV-NeuNDL2-5-IRES-Cre (NIC) [83]. Using a bicistronic transcript expressing NeuNDL2-5 followed by Cre recombinase under the control of an internal ribosome entry site (IRES), these animals coupled the expression of the *Neu* oncogene, along with Cre to recombine loxP sites specifically in cells expressing the oncogene [83]. These tumors, along with the NeuNDL counterpart both have high similarities with human HER2-positive tumors making them a valuable tool for studying HER2 positive breast cancer *in vivo*. These models were used to identify novel genes for their oncogenic cooperation as well as for the pre-clinical testing of multiple novel therapies prior to launching clinical trials.

Interestingly, the mouse strain has a significant effect on the penetrance of these transgenes. C57BL/6 is usually the preferred murine genetic background for gene-targeting experiments due to the capacity of 129/SvJ embryonic stem cells to facilitate germline transmission. However, it has been shown to confer resistance to MMTV infection and mammary tumorigenesis using the MMTV promoter. This specific observation was made when crossing MMTV-*Neu* transgenics from an FVB background with wild-type C57BL/6 mice. The tumor formation latency increased from 7-12 months in the FVB background to over 18 months in the C57BL/6 background [84]. A similar observation was made with MMTV-PyMT which showed a longer tumor latency and a reduced metastatic spread when the transgene was carried over from the FVB to a C57BL/6 background [85]. These data suggest that different genetic backgrounds can dramatically affect the outcomes when using the MMTV-driven oncogene expression models and that a poorly controlled background can lead to an incorrect interpretation of the role of critical genes in mammary tumorigenesis.

1.3 Periostin

1.3.1 Identification and Structure

Periostin (*Postn*) was first isolated in a mouse osteoblastic cell line using a differential screening approach and was formerly designated osteoblast-specific factor 2 (*OSF-2*) [86]. This was followed by cloning of the mouse and human *OSF-2* and initial characterisation showed homology to the insect protein Fascilin I. It was then hypothesised that it may function as a homophilic adhesion molecule in bone formation. The gene was then renamed Periostin due to the nature of its preferential expression to the periosteum, periodontal ligament and its potential involvement in bone and tooth formation [87].

The *POSTN* gene is found on the long arm of human chromosome 13 (13q13.3) and on murine chromosome 3. The genes are approximately 36 and 30kb long, respectively [88]. Both mRNA transcripts have been shown to contain a maximum of 23 exons with multiple splice variants encoding Postn proteins ranging from 83-93 kDa [89]. The structure of *Postn* comprises a signal peptide, responsible for secretion, an EMI domain (named after the EMILIN family of proteins), probably involved in protein-protein interaction, four tandem repeats of fasciclin-like domain (FAS1 domain) known to interact with integrins and a C-terminal region that interacts with other members of the extracellular matrix (Figure 1.3) [87]. These regions make *Postn* a key regulator of cell behaviour and extracellular matrix remodelling. Its interaction with specific integrins (αvβ3 and αvβ5) have been linked to activation of AKT, PI3K, and FAK signaling pathways in multiple cell types, including osteoblasts, normal, and cancer cells [90-92].

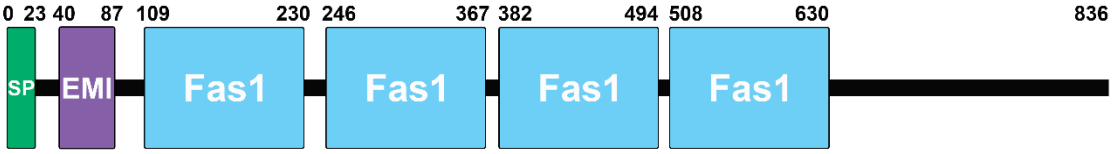

Figure 1.3: Schematic representation of the human *POSTN* gene structure.

Full length *POSTN* (isoform 1) consists of a typical small signal peptide (SP), an EMI domain (EMI), four tandem repeats of Fasciclin 1 domain (Fas1) and a C-terminal region. The numbers represent the amino acids flanking the different regions. Figure was adapted from [93].

1.3.2 Development and Homeostasis

The extracellular matrix (ECM) is an essential component of metazoan life. Complex organization of different cell types in multicellular organisms would be impossible without this non-cellular component that plays both a structural and signaling role and forms a physical environment surrounding the cells [94]. Matricellular proteins, such as *Postn*, modulate the composition of the ECM to allowing a tight regulation of cellular processes such as differentiation and migration during embryogenesis [95].

During bone development and maturation, multiple *Postn* variants have been shown to be expressed in a precise temporal and spatial pattern supporting a role for these isoforms during embryogenesis and in the neonatal bones [96]. Despite multiple attempts at identifying distinct biological activity related to specific variants, it remains controversial. Studies have shown variant specific expression patterns without providing any mechanistic interpretation [97]. Although the differential expression patterns suggest a specific role for different splice variants, more evidence is needed to confirm these claims.

The periosteum, which is a membrane that covers the outer surface of all bones, is a structure where *Postn* is preferentially expressed. This specific structure is responsible for bone growth. The activity of this structure is especially high during development and body growth. Its activity in adults is reduced but continues to contribute to bone diameter, which is intrinsically related to bone strength [98]. *Postn* transcripts were also identified in pre-osteoblasts using *in situ* hybridization, suggesting its involvement in bone development [89]. *Postn* has also been shown to be involved in the processes of bone repair, fracture healing and more specifically in the stages of early inflammation, progenitor cell recruitment, osteoblast differentiation and bone formation [99]. Multiple studies using the *Postn* knockout animal

model validated these claims by showing osteoporosis accompanied by low bone mineral density, altered microarchitecture and a reduction in bone strength in *Postn*-null mice [100-102].

Postn is also expressed in the dermis during skin development, more specifically from the embryonic to neonatal stages. Its expression is also observed in the basement membrane and hair follicles in adults [103]. Wound healing, the process by which skin wounds repair, is a multi-step process that involves several important players such as transforming growth factor-β1 (TGFβ-1), fibrin and fibronectin [104, 105]. The steps of skin wound healing have been extensively studied, starting with hemostasis (termination of hemorrhage), followed by phases of inflammation, proliferation, and remodeling [106]. A study assessed the expression pattern of Postn during wound repair and revealed that its expression starts after the inflammation step showing a negative correlation between Postn expression and inflammatory cell infiltration (CD68+ macrophages) [107]. These observations were validated by various studies using *Postn* (-/-) mice. Postn-deficient mice displayed delays in skin closure kinetics from day 3 to 9 post-injury which correlated to the transition from the inflammatory to proliferative phase of healing [108, 109].

Studies of *Postn* involvement in the cardiac system were prompted by the identification of its role in the remodeling of the myocardium following cardiac infarct [110]. *Postn* was then linked to cardiac development as it is highly expressed by embryonic fibroblasts and pericardial cells covering the heart during embryogenesis [111, 112]. Further studies showed that *Postn* was expressed exclusively in non-cardiomyocytes and had a significant role in the development of valve leaflets and cardiac fibrous scaffolding during embryogenesis [112]. Using *Postn* (-/-) mice, it was shown that insufficient collagen deposition and maturation

during valvulogenesis leads to encroachment of the myocardium around the ventricular leaflet of the tricuspid valve, suggesting a role for Postn in restricting boundary for cell types during cardiac development [113, 114].

In most tissues where *Postn* is expressed, its main role is related to the extracellular matrix structure and organization. *Postn* has been shown to modulate the ECM by stabilizing the collagen network. This process is called collagen crosslinking and is essential to stabilise collagen-rich structures such as tendons, skin, and cartilage. This process involves two main players: bone morphogenetic protein-1 (BMP-1) and lysyl oxidase (LOX). BMP-1 can cleave a pro-peptide which produces and activates LOX, which in turn can covalently crosslink intra- and extra-molecular collagen fibrils [115]. Postn can bind to BMP-1 and collagen, therefore, acting as a scaffold to accelerate collagen crosslinking by promoting the proteolytic activation of LOX [116]. *Postn* knockout models also support this model by showing that *Postn*-null animals exerted aberrant collagen fibrillogenesis [117] and a reduction in collagen crosslinking in skin, tendons and heart [118].

1.3.3 Periostin in Pathological Conditions

POSTN has been linked to several pathologies involving different tissues. *Postn* is important for structures that undergo severe mechanical stresses, and many pathological conditions involve *Postn* deregulation. These include pathologies observed in the fields of ophthalmology [119], dermatology [120], respiratory [121], otolaryngology [122], oncology [123] and several other systems. A summary of *Postn* disease involvement and regulation is shown in Figure 1.4.

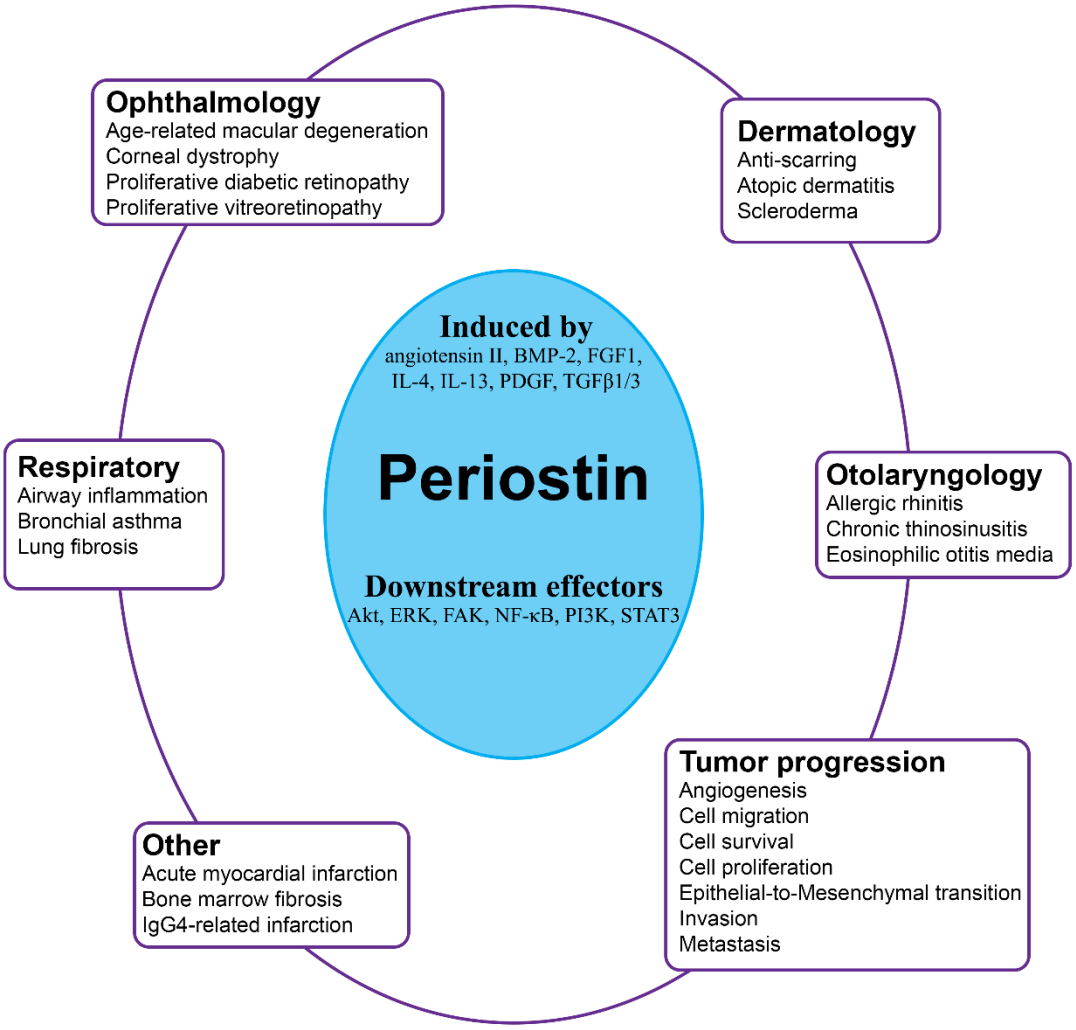

Figure 1.4: Summary of *Postn* induction, downstream effectors, and associated diseases. Studies have shown that *Postn* can be induced by multiple factors and that it acts through multiple signaling pathways. Studies also have shown involvement in multiple pathologies related to ophthalmology, dermatology, respiratory, otolaryngology, tumor progression and more. Adapted from [124].

Postn expression has been studied in limbal stem cells, also known as corneal epithelial stem cells as a prospective marker of stem/progenitor cell and potentially involved in corneal pathologies [125].

In response to allergens, bacterial and viral infection, epithelial damage is common in respiratory diseases. Acute injury in the lungs results in a decrease of *Postn* expression which is re-expressed following the initiation of repair and activation of TGFβ. Evidence supports a relationship between *Postn* and fibrogenesis following pulmonary injury [126]. An ever-increasing body of evidence is supporting a role for *Postn* in asthma and more particularly type 2 inflammation [127, 128] Consistent *Postn* upregulation in the airway epithelium contributes to airway fibrosis and consequently reduces airway distensibility [129].

Postn induction has been described in multiple tissues post-injury, such as cardiac healing following myocardial infract [130], vascular cell differentiation and migration following vascular injury [131] and regeneration of hindlimb skeletal muscle following injury [132].

1.3.4 Role of Periostin in Cancer

The general approach to understand cancer biology is focused on individual cancer cells directly and the processes leading to their malignancy. In the last 20-30 years, the basis of cancer biology was studied by implementing new concepts such as the tumor microenvironment (TME) which consists of the tumor's connective tissues, vasculature, infiltrating immune cells, and the extracellular matrix [133]. Although these components are not malignant per se, they can greatly influence cancer cells and provide an environment more or less prone to proliferation, migration or invasion. The ECM is one of the components of the TME that received the least attention initially. This has considerably changed in the last decade

or so where studies furthered our understanding of the tumor ECM and its important role in tumorigenesis and in response to therapies [134]. A role for *Postn* in the remodeling of the ECM has also been identified in multiple types of cancers establishing it as a marker of poor prognosis and metastasis.

In prostate cancer, POSTN expression has been detected in cancer epithelial cells, tumor stroma and peritumoral areas. High levels in stromal compartments is associated with shorter progression-free survival [135, 136] while low epithelial expression was associated with shorter progression-free survival [135]. This shows a different clinical prognostic value depending on the cell types expressing *POSTN*.

In non-small cell lung cancer, POSTN has been detected in tumor stroma, but not in epithelial cancer cells [137]. High levels of POSTN in the stroma was also associated with poor overall survival in non-small cell lung cancer patients [137]. Similarly, in pancreatic cancer, POSTN was detected in cancer epithelial cells, tumor stroma and pancreatic stellate cells. Its high expression levels in tumor stroma and cancer epithelial cells are both indicative of a poor prognosis [138, 139].

In ovarian cancers, POSTN expression is detected in both epithelial cancer cells and tumor stroma. High POSTN expression in the stromal compartment is associated with lower progression-free and overall survival while differential POSTN expression in epithelial cancer cells revealed no prognostic value in ovarian cancer [140]. Higher levels of POSTN have also been correlated with cancer recurrence and late clinical stages [141].

In breast cancers, elevated POSTN expression in epithelial cancer cells is correlated with poor progression-free and overall survival [142]. Another study found a role for *POSTN* in the establishment of metastatic niches in the lungs, since in the absence of POSTN, metastatic colonization of the lungs was not evident [143]. Furthermore, high POSTN expression by cancer associated fibroblasts (CAFs) is associated with higher tumor grades, suggesting that POSTN secreted by CAFs may be a key element in cancer progression [144].

In colorectal carcinoma, the expression of POSTN has been detected in the stroma, more specifically in CAFs and high levels of POSTN were also an indicator of poor prognosis [145]. Its higher expression in liver metastases appears to increase survival when compared to the primary tumors [90]. Another study, utilizing multivariate analyses showed a strong correlation between liver metastasis and *POSTN* levels, histological type, lymph node metastasis and TNM stage [146]. A positive correlation between high *POSTN* expression and clinical stage, tumor size, lymph node metastasis, serosal invasion, differentiation grade and 5-year survival rate were also observed [147]. Lastly, multivariate analyses performed in colorectal carcinoma patients revealed that high POSTN expression in the stromal compartment was an independent prognostic biomarker for poor progression-free survival and overall survival [145].

In liver cancer, POSTN expression has been detected in epithelial cancer cells and in the tumor stroma. Its expression in epithelial cancer cells is associated with reduced overall survival and is correlated with advanced tumor grade [148]. Other studies have found a correlation between high POSTN levels and TNM stage, tumor nodules, microvascular invasion, and higher levels of vascular endothelial growth factor (VEGF), as well as significantly lower overall survival rates [149, 150]. Similarly, the relationship between

POSTN and VEGF was also shown in osteosarcomas. The high levels of POSTN are also correlated with a poorer prognosis accompanied with lower overall survival when compared to tumors expressing low levels of POSTN [151]. Other cancer types such as renal carcinomas and esophageal squamous cell carcinomas have identified *POSTN* as a prognostic factor, responsible for a more aggressive behaviour [152, 153].

Unlike many cancers, POSTN expression in bladder cancers is downregulated compared to normal tissue. Surprisingly, POSTN expression is shown to be downregulated in high grade bladder cancers and POSTN has been shown to supress metastasis *in vivo* and *in vitro* [154]. Nevertheless, other studies have found an opposite role for POSTN. For example, in muscle-invasive bladder cancer, an aggressive type of tumors, higher POSTN expression has been correlated with a worse prognosis. These tumors have been shown to produce vesicles containing POSTN in the urine which could potentially be used as a biomarker of cancer progression [154].

Since *POSTN* expression in many types of cancers is associated with poor prognosis and the fact that it is a secreted protein, multiple studies have tested if the presence of POSTN in the serum of patients could be used as a prognostic tool. Depending on the type of cancer, the presence of POSTN in the serum was associated with tissue specific metastases such as bone metastasis in lung cancer [155] and breast cancer [156]. Serum POSTN levels were identified as a poor prognosis and survival factor in lung cancer [157], some subgroups of breast cancers [158], colorectal cancer [159], hepatocellular carcinoma [160] and cholangiocarcinoma (bile duct cancer) [161].

POSTN has been shown to play a role in invasion and metastasis following the activation of epithelial-to-mesenchymal transition (EMT). Succinctly, EMT is a process by

which epithelial cells acquire mesenchymal characteristics. This process was initially discovered and characterised in embryogenesis. It was later observed and assessed in tumor progression. EMT is particularly important in epithelial cancers whereby cancer cells acquire migratory characteristics which increases invasion and colonization at secondary sites. *Postn* has been shown to promote EMT in lung cancer cells by upregulating mesenchymal-specific genes such as N-Cadherin, Vimentin, Twist and Snail while also downregulating E-Cadherin [162]. A similar observation was made in PC3 and DU145 prostate cancer cells overexpressing *Postn*, leading to an increase in EMT markers and activation of the AKT and GSK-3β pathway [163]. In contrast, another study found the opposite effects in bladder cancer cells where exogenous *Postn* expression upregulated the epithelial-specific marker E-Cadherin and reduced cell migration and invasion [164]. These observations suggest that the effects of *POSTN* are cell type- and tumor-dependent.

1.4 Fibroblast Growth Factor Signaling

1.4.1 Structure and Activation

Fibroblast Growth Factor (FGF) signaling activates complex pathways comprising a panoply of functions in various organisms. The mammalian FGF family comprises 18 ligands which interact with 4 transmembrane receptors that are highly conserved (*FGFR1*, *FGFR2*, *FGFR3* and *FGFR4*). FGFs are glycoproteins which are secreted and sequestered to the ECM and the cell surface by interacting with heparan sulphate proteoglycans (HPSGs). Upon activation, FGFs are released from the ECM by one of several ways (heparinase, protease or specific FGF-binding proteins) and then bind to cell surface HPSGs [165]. These cell surface HPSGs are able to stabilize the binding between the FGF ligand and its receptor to form a FGF-FGFR-Heparin complex [166]. This ternary complex results in a conformational change

of the FGFR receptor which activates their intracellular kinase domain. Subsequent transphosphorylation of tyrosine residues on the receptor itself functions as a docking site for adaptor proteins which can in turn get phosphorylated by FGFR [167].

This activation of FGFRs triggers many signal transduction pathways. For example, recruitment of Son of Sevenless (SOS) and Growth Factor Receptor-Bound 2 (GRB2) is able to activate Ras, and therefore Raf and MAPK pathways [166]. Recruitment and formation of another complex involving GRB2-associated binding protein 1 (GAB1) and Phosphoinositide 3-Kinase (PI3K) can activate the well studied AKT-dependent cell survival pathway [168]. In addition, phospholipase Cγ (PLCγ) binds to the carboxy-terminal end of activated FGFR receptors [169]. Following PLCγ activation, it hydrolyses phosphatidylinositol-4,5-biphosphate (PIP_2) into phosphatidylinositol-3,4,5-triphosphate (PIP_3) and diacylglycerol (DAG), which in turn activates protein kinase C (PKC) and subsequently the MAPK pathway [170]. Other pathways have been shown to be activated by FGFRs in specific cellular context, such as p38 MAPK, Jun N-terminal kinase (JNK) pathways, signal transducer and activator of transcription (STAT) signaling pathways and ribosomal protein S6 kinase 2 (RSK2) [171, 172].

1.4.2 Deregulation of FGF Signaling in Cancer

Aberrant FGF signaling has been observed in multiple types of cancer, although the underlying mechanism driving the signaling is highly tumor specific. Two general types of activation have been observed: alteration driving ligand-independent activation of FGFR or changes supporting ligand-dependent activation. For example, in bladder cancer, somatic mutations in the FGFR3 coding sequence are common, more than 50% of these mutations are a S249C in the extracellular domain which leads to the formation of intermolecular cysteine

disulphide bridges that result in constitutive dimerization and subsequent activation of FGFR3 in a ligand-independent fashion [173, 174].

Ovarian cancer studies have shown frequent amplification of FGF1 which is correlated with poor survival [175]. Furthermore, higher FGF1 expression has been linked to increased microvessel density suggesting a role in promoting angiogenesis in ovarian cancer [175]. It is still unclear whether the mechanisms of FGF expression are autocrine or paracrine since it is challenging to model such an interaction *in vitro*. Interestingly, increased expression of FGF2 and other FGFs plasma levels have been found in multiple types of cancer [175]. It has also been proposed that cancer cells can induced FGF2 expression when subjected to stromal inflammatory infiltrate, promoting angiogenesis or tumor survival following a classical paracrine activation loop [176].

1.5 Thesis Objectives and Hypotheses.

It is undeniable that *POSTN* is a critical player in the development, growth, and metastasis of certain types of cancer. Furthermore, the involvement of the ECM in different processes governing tumorigenesis such as proliferation, migration and invasion has become increasingly important in the last few decades. *POSTN* interaction with multiple ECM related proteins and multiple integrins highlights the potential of *POSTN* to modulate breast cancer.

A lot of correlation studies identified *POSTN* as a promoter of tumor initiation and progression and as essential for metastatic colonization in breast cancers [143, 177]. Although these observations were made in multiple tumor models, different mechanisms were reported on how *POSTN* promotes the aggressive behaviour in breast tumors.

The observation that *POSTN* can promote EMT and metastasis by a signaling cross-talk between integrins and EGFR [178] along with the fact that *HER2* positive breast cancers are relatively aggressive cancers led us to investigate the relationship between *POSTN* and *HER2* positive mammary tumors. We hypothesized that global *Postn* deletion would significantly delay tumor initiation, progression, and metastasis in a *Neu*-driven oncogenic transgenic mouse model. Furthermore, as epithelial expression of *POSTN* appears to be a poor prognostic factor, we hypothesized that cancer cells that are devoid of *POSTN* would have reduced proliferative, migratory, and invasive potential *in vivo* and *in vitro*. To test this hypothesis, we isolated *Neu*-driven cancer cells from the *Postn* knockout background and re-expressed *Postn* in those cells to assess the effect on proliferation, migration, and invasion.

The expression pattern of Postn in breast cancers suggests that the regulation of *Postn* in epithelial cancer cells is different from the stromal compartment. This led us to investigate the regulatory mechanisms underlying *Postn* expression in epithelial cancer cells. Serendipitously, we have found a growth supplement able to repress Postn expression in isolated *Neu*-positive epithelial breast cancer cells. We have used this extract to establish an *in vitro* model to study the regulation of *Postn* in these cells. The objectives using this *in vitro* model were to identify potential repressive components of *Postn* gene expression and the signaling pathways involved in the regulation of *Postn* in *Neu*-positive epithelial breast cancer cells.

Chapter 2

Materials and Methods

2.1 Animals

2.1.1 Mouse Models and Husbandry

The mouse models used were all bred and maintained on an FVB/N background. The MMTV-NeuNDL, MMTV-NIC and MMTV-PyMT transgenic mice were a kind gift from Dr. William Muller (McGill University). *Postn*-null mice were obtained from Dr. Simon J. Conway (Indiana University School of Medicine). Only female mice were used in all experiments. MMTV-NeuNDL and Postn-null females were not used as breeders and all other female breeders were euthanized after their fifth pregnancy. All animal care and husbandry were performed with adherence to guidelines established by the Canadian Council on Animal Care under a protocol approved by University of Ottawa Animal Care Committee.

2.1.2 Genotyping

Ear clips were obtained from mice at weaning, processed using proteinase K digestion and subsequent genomic DNA was isolated following the DNeasy Blood and Tissue Kit manufacturer's protocol (QIAGEN). Genomic DNA was then used for genotyping using the PCR-based KAPA2G Fast ReadyMix (Roche/Sigma). Genotyping PCR was performed using a thermocycler as follows: 95°C denaturation step for 3 minutes, then 32 cycles of denaturation at 95°C for 15 seconds, annealing between 52-62°C (depending on the melting temperature of the primers used) for 15 seconds and elongation at 72°C for 30 seconds. An elongation step at 72°C for 4 minutes was the final step prior to cooling the samples to 4°C and running on a 2% agarose gel containing ethidium bromide to visualize the DNA. A full list of primers can be found in Table 2.1.

2.1.3 Tumor Studies

All tumors assessed, whether from injections or from a spontaneous model, were palpated and measured twice a week. Using a caliper, the longest diameter was measured, and tumor volumes were calculated assuming tumors were a spheroid using the following formula: $4/3 * \pi * (r^3)$, where r corresponds to the radius (half of the diameter measured). Tumor onset was defined as the total tumor burden reaching $0.5cm^3$ which usually corresponded to the first palpable tumor time point. The endpoint was a set volume of $1.7cm^3$ as per University of Ottawa Animal Care and Veterinary Service Guidelines.

2.1.4 Cell Injections

To perform subcutaneous injections, CD-1 nude mice were purchased from Charles River. 1.5×10^6 cells were injected in CD-1 mice aged between 8 and 12 weeks. The cells were resuspended in 100µl of a 1:1 mixture of PBS:Matrigel. The cells were injected in the right flanks while the left flanks were injected with the mixture lacking cells to use as a control. Following the injections, mice were palpated and measured twice a week to assess tumor size. Mice were sacrificed when the first mouse reached the pre-established endpoint size of $1.7cm^3$.

2.2 Histology

2.2.1 Tissue Processing

Mammary gland tumors and lungs were extracted and fixed using 10% buffered formalin phosphate for 24 hours and transferred into 70% ethanol for storage at 4ºC. Samples were then sent to the University of Ottawa Louise Pelletier Histology Core Facility for processing and embedding in paraffin. Paraffin blocks were stored at room temperature protected from light until subsequent sectioning of the samples at 5µm.

2.2.2 Immunohistochemistry

Tissue sections were deparaffinized using xylene and rehydrated using ethanol washes. Antigen retrieval was then performed on the section using 10mM citrate buffer (pH 6.0) for 10 minutes in a pressure cooker. Sections were then incubated in 3% hydrogen peroxide for 15 minutes to quench endogenous peroxidase. Sections were then blocked using 5% donkey or goat serum depending on the host of the secondary antibody in PBS for an hour. Blocking of endogenous avidin and biotin was then used following Avidin/Biotin Blocking Kit (Vector laboratories) manufacturer guidelines. The primary antibody was then added and left to incubate overnight at 4ºC. Incubation with the appropriate HRP-conjugated secondary antibody was performed for 30 minutes at room temperature. All incubations were performed in the same blocking buffer containing donkey or goat serum. The sections were then incubated in DAB substrate (MilliporeSigma) and subsequent counterstain was performed using Hematoxylin. The sections were then dehydrated and cleared using ethanol and xylene washes respectively. Slides were then mounted and imaged using ZEISS Axio Scan Z1.

2.2.3 Immunofluorescence

Cells were seeded on coverslips for the duration of treatments. The cells were then washed three times in PBS and fixed using 4% Paraformaldehyde (PFA) for 10 minutes. Cells were washed three times again and permeabilization was performed using 0.3% Triton-X for 10 minutes. Cells were then blocked in 5% donkey serum for 1 hour, followed by incubation with specified primary antibodies (Table 2.2) diluted in 5% donkey serum for 1 hour. Cells were washed three times followed by a 1-hour incubation with secondary antibody diluted in 5% goat serum (Table 2.2).

2.3 Plasmid and cloning

pMSCV plasmid was digested with BglII and EcoRI restriction enzyme. *Postn* amplification was performed by PCR from a mammary tumor single stranded cDNA preparation using primers shown in Table 2.1. Restriction enzyme sequences for EcoRI and BamHI were added to the reverse and forward primers, respectively. The PCR product was ligated into a pJET1.2/blunt plasmid using the CloneJET PCR cloning kit (Thermo Scientific) using the manufacturer's protocol. Following the ligation, the pJET1.2/blunt-*Postn* plasmid was digested using EcoRI and BamHI and the *Postn* insert was cloned into pMSCV. Purification of the digested backbone (pMSCV) and *Postn* coding sequence (2.4kb) were performed using Qiagen Gel Extraction Kit following the manufacturer's protocol.

2.4 Cell culture

2.4.1 Isolation of NeuNDL Cell Lines

To establish mammary epithelial cancer cells, tumor-bearing animal from the NeuNDL and *Postn* (-/-):NeuNDL were sacrificed at endpoint. The tumors were then extracted, and a small lump of tumor was minced in a collagenase-based digestion buffer containing 50% Accutase (Thermo Fisher Technologies), 1% Penicillin-Streptomycin (Life technologies), 1mg/mL collagenase B (Sigma) in DMEM:F12. Once minced, the mixture was transferred to a 50mL conical tube and incubated at 37 °C in a shaking incubator for 5 hours. The digested tumor was then diluted 1:1 with 0.2% bovine serum albumin (BSA) DMEM:F12 and filtered through a 40µm cell strainer to clear up the debris. Cells were pelleted and washed using 0.2% BSA DMEM:F12 twice. Using a 4:1 NH_4Cl:PBS solution containing 1% BSA, red blood cells were lysed by incubating at room temperature for 3-5 minutes. Cells were pelleted and washed in 0.2% BSA DMEM:F12 and then digested with Accutase for 10 minutes at 37 °C to remove

clumps. Neutralization of the Accutase was then performed by adding two volumes of 0.2% BSA DMEM:F12. To isolate mammary epithelial tumor cells from this mixed population, lineage marker negative (Lin^-) from the Mammary Stem Cell Enrichment Kit (Stemcell Technologies) was used according to the manufacturer's protocol without using either CD24 or CD49f antibodies from the kit. After isolation, cells were seeded in DMEM:F12 media containing 1X Mammary Epithelial Growth Supplement (MEGS), 1% Penicillin-Streptomycin, and 1% L-glutamine. The cells were washed, and the media was replenished every second day. Whenever confluency reached 80%, cultures were passaged. Experiments on cells started once their doubling time was around 24 hours.

2.4.2 Cell maintenance

Murine breast cancer cell lines were maintained in DMEM:F12 containing 10% FBS, 1X Mammary Epithelial Growth Supplement (MEGS) (Life technologies), 1% Penicillin-Streptomycin (Life technologies), and 1% L-glutamine (Life technologies). All cell lines were used up to 20 passages from initial plating. All other cell lines were maintained in 10% FBS DMEM, 1% Penicillin-Streptomycin (Life technologies), and 1% L-glutamine (Life technologies). Cells were cultured in a humidified incubator kept at 37 °C and 5% CO_2. Cells were routinely passaged every 2-3 days at a 1:5 to 1:10 dilution. Mycoplasma testing was performed routinely by PCR analysis.

2.4.3 Transient transfection

Cells were seeded on a 10 cm plate and left to grow until they reached approximately 80% confluency. Transfection were performed using Lipofectamine 3000 according to the manufacturer's protocol using 8 µg of DNA. Plasmid transfection were performed for 24 hours before replenishing the media. Expression was validated by western blotting or qRT-PCR.

2.4.4 Retroviral Production and Transduction

293T cells were plated in a 10cm plate in 10% FBS DMEM and then transfected using lipofectamine 3000 (Life Technologies) the next day using 1 µg of retroviral construct, 889 ng of pUMVC (Addgene) and 111 ng of pCMV-VSV-G (Addgene). 24 hours post-transfection, the media was removed and 5ml of serum-free DMEM:F12 was added to the plate. The next day, virus containing media was filtered through a 0.44µm filter and 3 mL of filtrate was added to the target cells along with 8 µg/mL of polybrene. 5 mL of serum free media was then added on top of the cells to allow collection for a second day following the same infection step. After the second day of virus-containing media collection, 293T cells were discarded.

Target cells (*Postn* (-/-):NeuNDL Isolate A and B) were seeded at sub-confluency and left to grow. These cells were then infected using filtered supernatant from 293T cells transfected with retroviral vectors. Infected cells were then treated 2 days post-infection with 2 µg/ml of puromycin (Sigma) for 5 days and were then maintained using 1 µg/ml.

2.4.5 Proliferation Assay

To perform proliferation assays, 50 000 cells were seeded in triplicate into 60 mm plates. Each plate represents a specific timepoint. At each time point, cells were trypsinized and pelleted. The cell pellets were washed in PBS and resuspended in 2 mL of culture medium. Cells were then stained with trypan blue and counted in triplicate using a Beckman Coulter Vi-CELL XR automated cell viability analyzer. The number of viable cells per plate was quantified. All proliferation assays were performed for at least three independent biological replicates.

2.4.6 Boyden Chamber Migration and Invasion Assays

For migration, Boyden chambers were pre-coated using 40 µg/ml of Collagen I (Thermo Fisher Scientific), the membrane were then washed in PBS prior to their usage. Cell starvation in serum-free media was performed overnight the day before the migration assay started. 50 000 cells were seeded in the top part of the chambers in a total of 400 µL and left to migrate through the membrane for 8 hours. The culture medium in the top and bottom portion of the chamber contained 1% FBS DMEM:F12. After the 8 hours, membranes were washed three times in PBS and using a cotton swab the cells on the top part of the membrane were removed. The membranes were then fixed using 10% phosphate buffered formalin for 10 minutes at room temperature. Following the fixation, the membranes were washed three times in PBS and then stained with a mixture of 0.5% crystal violet and 25% methanol for 30 minutes at room temperature. ddH_2O was used to wash the excess crystal violet from the membranes which were then left to dry overnight in a fume hood. The following day, the membranes were removed from the plastic insert using a scalpel and mounted onto slides for scanning using a ZEISS Axio Scan Z1.

For invasion, the upper chamber was coated with a layer of basement membrane extract (BME) (Cultrex 5X BME Solution) following the manufacturer's protocol. In brief, BME was thawed on ice for 30 minutes, then diluted using their coating buffer to obtain a 1X solution. 100 µL of the diluted BME solution was used to coat the upper chamber of the insert for 24 hours at 37°C in a CO_2 controlled humidifying chamber. The coating solution was aspirated just before the addition of 50 000 cells in 400 µL on top of the BME coated membrane. Cells were left to invade for 48 hours; membranes were then washed, fixed and stained as above.

2.4.7 Mammosphere Forming Assay

To establish primary mammospheres, we disaggregated cells by passing them through a 25-gauge needle three times and then plated them at 1000 cells per well in a 24-well Ultra-Low attachment Flat Bottom Plates (Corning/Costar). Cells were then washed in PBS and resuspended in 500 µL of DMEM:F12 supplemented with 1X MEGS and 1X B27 supplement (Life Technologies). Spheres were left to grow for 5 days before taking pictures and quantifying the spheres. Clumps of cells were considered mammospheres if the diameter of the clump was over 50 µm. The mammosphere forming efficiency was then obtained by calculating the percentage of spheres per well over the total number of cells seeded per well.

2.5 Protein and RNA Expression analysis

2.5.1 Protein Extraction

Cell lines and tissues were collected and homogenized in RIPA buffer (50mM Tris-HCl pH 7.5, 1% NP-40, 1% Triton-X-100, 150mM NaCl, 12mM Na-deoxycholate, 0.05% sodium dodecyl sulfate (SDS), 2mM EDTA, 1mM DTT) containing a protease inhibitor cocktail (10mM NaF, 1mM DTT, β-glycerophosphate, 1mM PMSF, 0.6mM $NaVO_3$, 100 µM benzamide, 10 µg/mL leupeptin, 10 µg/mL aprotinin and 10µg/mL pepstatin). The lysates were incubated at 4ºC for 30 minutes with intermittent vortexing or multiple freeze and thaw cycles. The resultant lysates were then centrifuged at 12,000rpm in a temperature-controlled centrifuge set at 4ºC for 10 minutes to clear the lysates of debris. Protein concentration were then determined using a Bio-Rad protein assay dye reagent and a spectrometer to read absorbance at 595nm.

2.5.2 Western Blotting

Equivalent amounts of proteins were prepared in RIPA containing SDS sample buffer (100mM DTT, 50mM Tris-HCl, 10% glycerol, 2% SDS, 0.1% bromophenol blue). The lysates were then denatured using a heat block set at 100ºC for 5 minutes. The denatured samples were then electrophoresed on polyacrylamide gels (8 to 15%) for 45 minutes at 50 milliamps in SDS running buffer (192mM glycine, 25mM Tris-HCl and 0.1% SDS). The gels were then transferred to a polyvinylidene fluoride (PVDF) membrane at 100 volts for 90 minutes in transfer buffer (48mM Tris-HCl, 39mM glycine and 20% methanol). The resulting membrane was then probed with primary antibodies at the appropriate concentration overnight at 4ºC in TBS-T (150 mM NaCl, 50mM Tris, pH 7.4, 0.05% Tween 20) with 5% BSA. The primary antibody was then removed, and three subsequent TBS-T washes were performed for five minutes each at room temperature. Corresponding HRP-conjugated secondary antibody was added at the appropriate concentration in TBS-T containing 5% BSA and incubated for 60 minutes at room temperature. The secondary antibody was then removed, and another three TBS-T washes were performed at room temperature. Visualization of target proteins was performed using Western Lightning® Plus-ECL (PerkinElmer) according to the manufacturers protocol, followed by exposure to X-ray film.

2.5.3 RNA Extraction

Tissues and cell lines were collected and homogenized in a tube containing 1 mL of Trizol buffer. The samples were processed for RNA extraction as per the manufacturer's protocol. The RNA was pelleted by centrifugation at 12000x g for 10 minutes at 4ºC. Pellets were subsequently washed with 70% ethanol and centrifugated at 7500x g for 5 minutes. The RNA pellet was then dried at room temperature for 10 minutes and resuspended using 100µL

of RNase-Free water. Sample were then cleaned using DNase included in the RNeasy Mini Kit (QIAGEN). Purified DNA was quantified, and RNA purity was assessed using A260/230 and A260/280 using a nanodrop spectrophotometer.

2.5.4 Reverse Transcription and First Strand cDNA Synthesis

First strand cDNA synthesis was performed by mixing 500ng of total RNA, 250ng of oligo$(dT)_{12-18}$, 50ng of random primers and 10 nmol of dNTP in a total of 13 µL and incubating the mixture at 65°C for 5 minutes. The reverse transcription procedure was performed using SuperScript III Reverse Transcriptase (Life Technologies) according to the manufacturer's manual. In summary, 4 µL of 5X First Strand Buffer, 1 µL of RNase OUT, 1 µL of 0.1 M DTT and 1 µL of SuperScript III reverse transcriptase were added to the 13 µL previously described. Samples were then incubated at 25°C for 5 minutes, followed by 55°C for 1 hour, and lastly 70°C for 15 minutes. Samples were then diluted by adding 180 µL of nuclease-free water to a total volume of 200 µL. These samples were then used right away or stored at -20°C until use.

2.5.5 Quantitative Realtime-PCR

For qRT-PCR, a mastermix was prepared using 17.5 µL of 2X Taq Universal SYBR Green Supermix (Bio-Rad), 11.9 µL of nuclease-free water, 3.5 µL of diluted cDNA, and 2.1 µL of the indicated primers (10 µM). Triplicate wells were then loaded with 10 µL of mastermix each in a 96-well qPCR plate. Plates were loaded on an Applied Biosystems 7500 Real-Time Fast PCR thermocycler. The PCR reaction was as follows: initial 5 minutes hold at 50°C, 10 minutes denaturation at 95°C, followed by 40 cycles of denaturation at 95°C for 15 seconds, then annealing and extension at 60°C for 60 seconds. Relative mRNA expression was determined using the ΔΔCT method and normalization was done using ribosomal 18S specific primers. All the primers used for qRT-PCR can be found in Table 2.1.

2.5.6 Library Preparation and Sequencing

This part was performed by Genome Quebec facilities as a service; the samples were processed as follows. Total RNA was quantified using a NanoDrop Spectrophotometer ND-1000 (NanoDrop Technologies, Inc.) and its integrity was assessed on a 2100 Bioanalyzer (Agilent Technologies). Libraries were generated from 250 ng of total RNA as follows: mRNA enrichment was performed using the NEBNext Poly(A) Magnetic Isolation Module (New England BioLabs). cDNA synthesis was achieved with the NEBNext RNA First Strand Synthesis and NEBNext Ultra Directional RNA Second Strand Synthesis Modules (New England BioLabs). The remaining steps of library preparation were done using the NEBNext Ultra II DNA Library Prep Kit for Illumina (New England BioLabs). Adapters and PCR primers were purchased from New England BioLabs. Libraries were quantified using the Quant-iT™ PicoGreen® dsDNA Assay Kit (Life Technologies) and the Kapa Illumina GA with Revised Primers-SYBR Fast Universal kit (Kapa Biosystems). Average size fragment was determined using a LabChip GX (PerkinElmer) instrument.

The libraries were normalized, denatured in 0.05 N NaOH and then diluted to 200 pM and neutralized using HT1 buffer. ExAMP was added to the mix and the clustering was done on an Illumina cBot and the flowcell was run on a HiSeq 4000 for 2x100 cycles (paired-end mode) following the manufacturer's instructions. A phiX library was used as a control and mixed with libraries at 1% level. The Illumina control software was HCS HD 3.4.0.38 and the real-time analysis program was RTA v. 2.7.7. The program bcl2fastq2 v2.18 was then used to demultiplex samples and generate fastq reads.

2.6 Bioinformatics

2.6.1 Single-cell RNA Sequencing Analysis

Single cell RNA-Sequencing (RNA-Seq) analysis was originally performed by *Wu et al.* [179]. Raw UMI counts and cell metadata were acquired from ENA accession PRJEB35405. The data was processed using Seurat v4.0.0 [180]. Normalization and feature selection was performed using SCTransform [181] while regressing out the proportion of mitochondrial reads. Data was normalized and then processed with principal component analysis prior to generating UMAP embeddings base on the first PCs. Using FindNeightbors (dims=1:30) and FindClusters (resolution=0.2) functions implemented in Seurat. Cell type annotations from the original publication were used to define cluster labels for the data. All expression data shown in figures correspond to log-transformed counts per 10 000 UMIs.

2.6.2 RNA-Sequencing Processing and Differential Expression

Transcript quantification for each sample was performed using Kallisto (v0.45.0) [182] with the GRCm38 transcriptome reference and the -b 50 bootstrap option. The R package Sleuth (v0.30.0) [183] was then used to construct general linear models for the log-transformed expression of each gene across experimental conditions. Wald's test was used to test for significant variables for each gene and the resultant p-values were adjusted to q-values using the Benjamini-Hochberg false discovery rate method. Significant genes were defined as genes with a q-value < 0.05. An effect size (beta coefficient of the regression model) cut-off of $|b|>1$ was also used for each data set.

2.6.3 Gene Set Enrichment and Pathway Activity Inference

Enrichment of gene sets among differentially expressed genes was assess using the R package gProfileR. All gene sets discussed have a significant enrichment (Benjamini-

Hochberg adjust p-value <0.05) and relative enrichment between up- and down-regulated genes is reported. For pathway activity inference, we used the R package PROGENy (v1.9.6) [184]. Pathway activity was compared between experimental conditions using a simple linear model and p-values were adjusted using the Benjamini-Hochberg false detection rate method.

2.7 Statistical Analysis and Data Collection

In vitro experiments were all conducted in a minimum of three independent experiments and averaged. Error bars on all graphs represent Standard Error of the Mean (SEM). P-values were calculated between two groups using a two-tailed student's t-test analysis. For comparison between more than 2 groups, a one-way ANOVA approach was used along with a Tukey Post-hoc test. For Kaplan Meier survival analysis, a Mantel-Cox log-rank test was used to obtain a p value. Significance was determined by a p value under or equal to 0.05. In the figures, asterisks are used to represent different value for p (* = $p \leq 0.05$, ** = $p \leq 0.01$, *** = $p \leq 0.001$). For quantification of histology, multiple independent tissue samples were collected, and multiple sections of tissues were sectioned and stained. At least 10 field of views from random areas were used for the quantification, except for the lungs, which were assessed throughout for lesions.

Power calculations were performed early on to estimate that 15 mice were needed per genotype to detect a significant difference ($p \leq 0.05$) of 30 days in survival between Postn(+/+):NeuNDL, Postn (+/-):NeuNDL and Postn (-/-):NeuNDL with a power of 0.80. These calculations were performed using a mean survival of 210 days with a standard deviation of 31 days.

Table 2.1. List of primers

A list of primers, with their sequences and application used throughout this thesis is provided.

Primer	**Application**	**Sequence (5' to 3')**
Postn Forward	Cloning	TTAGGATCCATGGTTCCTCTCCTGC
Postn Reverse	Cloning	TGCGAATTCTCACTGAGAACGGCCT
Postn Forward WT (p01)	Genotyping	AGTGTGCAGATGTTTGCTTG
Postn Reverse WT (p02)	Genotyping	ACGAAATACAGTTTGGTAATCC
Postn Reverse KO (p03)	Genotyping	CAGCGCATCGCCTTCTATCG
NeuNDL Forward	Genotyping	TTCCGGAACCCACATCAGGCC
NeuNDL Reverse	Genotyping	GTTTCCTGCAGCAGCCTACGC
m18S Forward	qRT-PCR	GTCCCTGCCCTTTGTACACA
m18S Reverse	qRT-PCR	GATCCGAGGCCTCACTAAAC
mPostn Forward	qRT-PCR	AAGTTTGTTCGTGGCAGCAC
mPostn Reverse	qRT-PCR	TTCTGTCACCGTTTCGCCTT

Table 2.2 List of antibodies

A list of antibodies with supplier and catalog number used throughout this thesis are provided.

Antibody	Supplier	Catalog Number
Rat monoclonal anti-mouse CD45	BD Pharmingen	550539
Donkey anti-Mouse IgG (H&L), HRP	Bio-Rad	170-6516
Goat anti-Rabbit IgG (H&L), HRP	Bio-Rad	170-6515
Rabbit monoclonal anti-Phospho-ErbB2 (Tyr1221/1220)	Cell Signaling Technology	2243
Rabbit monoclonal anti-Phospho-Smad2 (Ser465/467)	Cell Signaling Technology	3108
Rabbit monoclonal anti-phospho-AKT (Ser473)	Cell Signaling Technology	4060
Rabbit monoclonal anti-α-Smooth Muscle Actin XP	Cell Signaling Technology	19245
Rabbit monoclonal anti-Smad2 XP	Cell Signaling Technology	5339
Rabbit monoclonal anti-PDGFRα XP	Cell Signaling Technology	3174
Rabbit monoclonal anti-Vimentin XP	Cell Signaling Technology	5741
Rabbit polyclonal anti-AKT	Cell Signaling Technology	9272
Rabbit polyclonal anti-PARP	Cell Signaling Technology	9542
Goat Polyclonal Mouse Periostin/OSF-2 Isoform 2	R&D Systems	AF2955
Goat Polyclonal Human Periostin/OSF-2	R&D Systems	AF3548
Mouse anti-Goat IgG-HRP	Santa Cruz Biotechnology	sc-2354

Mouse monoclonal anti-p-ERK (Y204)	Santa Cruz Biotechnology	sc-7383
Mouse monoclonal anti-PCNA	Santa Cruz Biotechnology	Sc-56
Mouse monoclonal anti-Smad4	Santa Cruz Biotechnology	sc-7966
Rabbit Polyclonal anti-ERK 1/2	Santa Cruz Biotechnology	Sc-154
Mouse monoclonal anti-beta-Actin	Sigma-Aldrich	A5316
Mouse monoclonal anti-ErbB2	Sigma-Aldrich	OP15
Rabbit polyclonal anti-Ki-67	Sigma-Aldrich	AB9260
Donkey anti-Goat IgG Alexa Fluor 488	Thermo Fisher/Invitrogen	A-11055
Donkey anti-Rabbit IgG Alexa Fluor 594	Thermo Fisher/Invitrogen	A-21207

Chapter 3

Deletion of *Postn* in *Neu*-driven mammary tumors delays tumor onset and increases overall survival

3.1 Introduction and Rationale

Our lab and other groups have previously shown that *POSTN* plays an important role in regulating critical processes of tumorigenesis in breast cancer and that its expression has been associated with the development of a more invasive and aggressive disease [143, 185-187]. It has been proposed that infiltrating tumor cells are dependent on *Postn* expression for lung colonization and that *Postn* recruits Wnt ligands to increase their signaling in cancer stem cells [143, 188]. It was also shown that acquired POSTN expression in human breast cancers results in a significant increase in tumor growth and angiogenesis involving VEGF through the activation of an integrin αvβ3-FAK signaling pathway [186]. Using DNA aptamer technology, disruption of Postn binding to its cell surface receptors and integrins shows a marked reduction in primary tumor growth and distant metastasis [189]. Multiple studies have observed a correlation between poor survival and the expression levels of *Postn* in both cancer tissue and serum [142, 187].

As *POSTN* has been shown to contribute to the processes of tumorigenesis and metastasis as well as being of poor prognostic value, we assessed the role of *Postn* in ErbB2-induced tumorigenesis and metastasis *in-vivo*. The observations that *Postn* expression promotes more aggressive phenotypes, led to the hypothesis that a global *Postn* deletion would result in a delay in tumor onset, an increase in overall survival and a reduction in lung metastasis in a murine model of HER2-induced mammary tumorigenesis.

3.2 Global deletion of *Postn* in *Neu*-driven tumorigenesis delays tumor onset and increase overall survival

To assess the effect of *Postn* in ErbB2-mediated tumor formation, we crossed MMTV-NeuNDL transgenic mice [58] into Postn-deficient mice bearing a knock-in a LacZ-Neo

cassette, deleting exons 1 to 3 [190] (Figure 3.1 A&B). PCR was used to genotype mouse DNA for the *Postn* allele and the NeuNDL positivity (Figure 3.1 C&D). The NeuNDL model expresses an activated *Neu* (HER2 rat homolog) in the mammary luminal epithelium that leads to mammary tumors that resemble human HER2-positive breast cancers [58].

To evaluate tumor formation in *Postn* (-/-):NeuNDL mice, females were palpated biweekly to assess mammary tumor onset, progression, and endpoint. Supporting our hypothesis, *Postn* (-/-):NeuNDL animals developed tumors on average 41.7 days later when compared to *Postn* (+/+):NeuNDL mice (Figure 3.2 A). An intermediate phenotype was observed for the heterozygous *Postn* (+/-):NeuNDL animals with a tumor onset that was about 28 days later than the wildtype control (Figure 3.2 A). Similarly, the control *Postn* (+/+):NeuNDL mice reached endpoint with a median survival of 201 days compared to 248 days for the *Postn* (-/-):NeuNDL, a significant increase in median survival. Heterozygous *Postn* (+/-):NeuNDL had a median survival time similar to the *Postn*-null counterpart with 242 days (Figure 3.2 B). The average time between onset and endpoint was assessed to estimate the effect of Postn on tumor growth. In a similar fashion, *Postn* (-/-):NeuNDL mice showed an average of 27.5 days from onset to endpoint compared to 17.9 days for control *Postn* (+/+):NeuNDL mice and 21.7 days for the heterozygous *Postn* (+/-):NeuNDL mice (Figure 3.2 C). Heterozygous animals showed a classical intermediate phenotype for all parameters analysed, suggesting a *Postn* dose-dependent effect on tumor initiation, tumor progression and median survival (Figure 3.2 A-C).

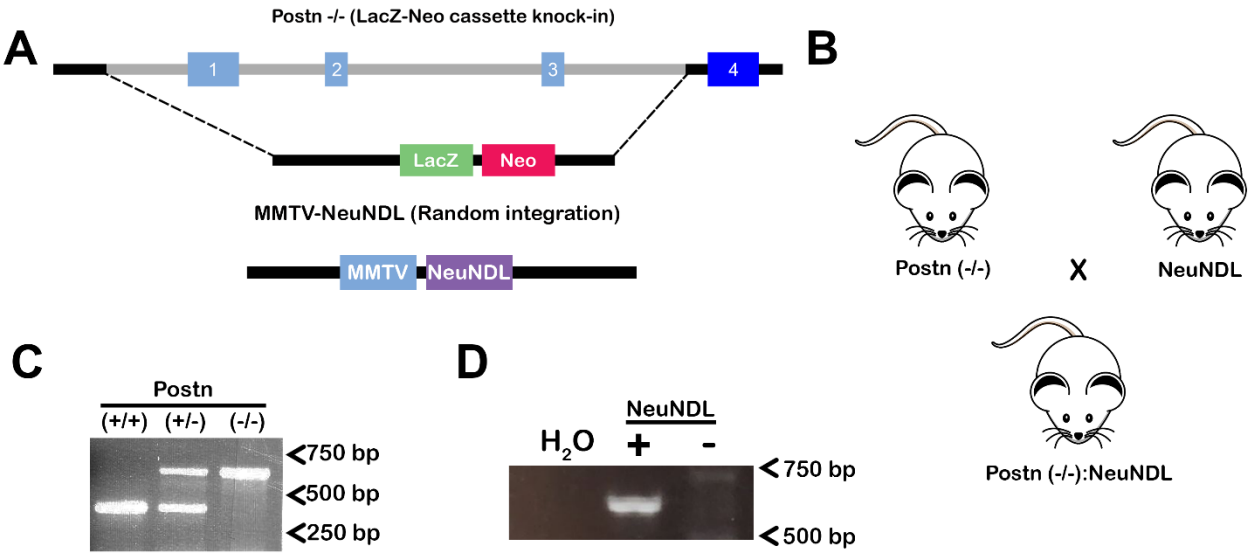

Figure 3.1: Schematic representation of the *Postn* (-/-):NeuNDL animal model.

(A) The *Postn* (-/-) animal model was generated by a targeted knock-in of a LacZ-Neo cassette replacing exons 1, 2 and 3 previously described in [190]. The gray area represents the deleted region in the knock-out allele. The MMTV-NeuNDL transgenic model was generated by zygote injection of an MMTV-Neu transgene as previously described in [58]. **(B)** Breeding scheme for *Postn* (-/-):NeuNDL animals is represented schematically. **(C)** Genotyping PCR is shown on a 2% agarose gel for *Postn* wildtype (+/+), heterozygous (+/-) and knockout alleles (-/-) using a 3-primer system. **(D)** Genotyping PCR is shown on a 2% agarose gel for NeuNDL positive and negative animals.

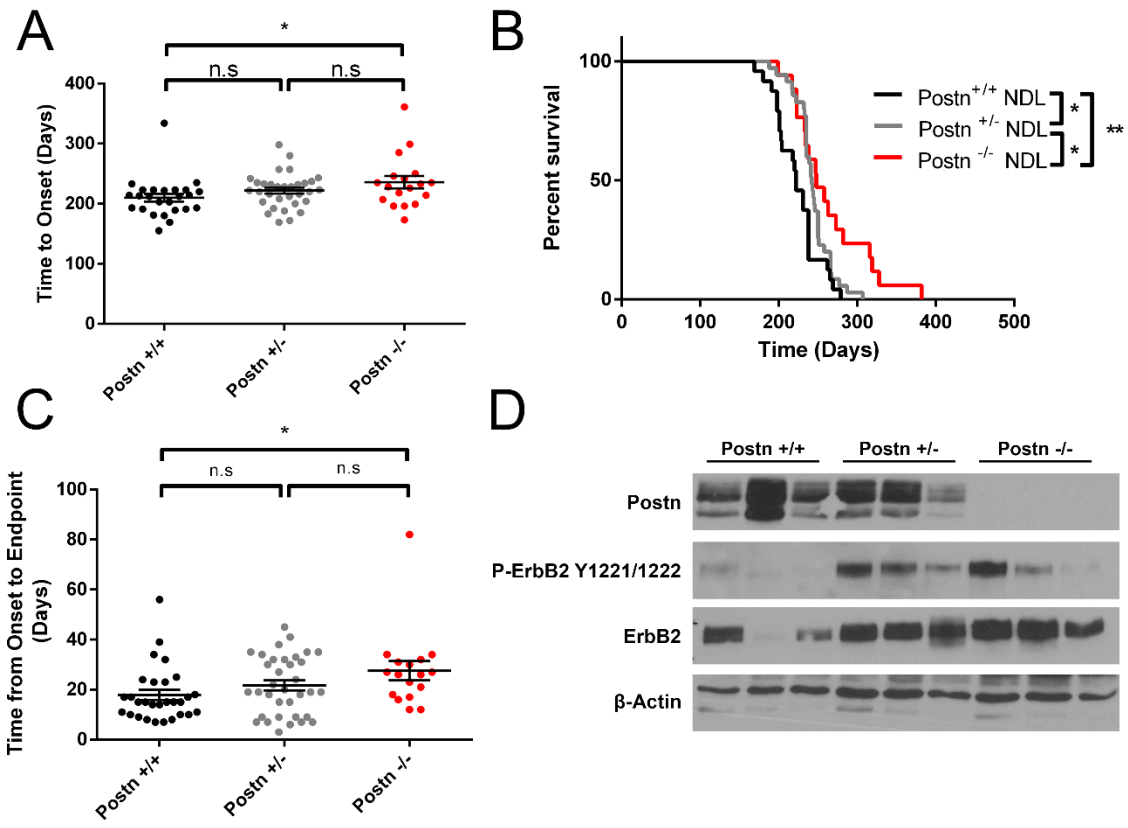

Figure 3.2: *Postn* deletion in a Neu+ model delays tumor initiation and progression.

(A) Biweekly palpation was performed to assess tumor onset in NeuNDL animals. Onset was defined by a mass greater or equal to 0,5cm^3. *Postn* (-/-) animals showed a delay in tumor onset compared to the wildtype control. **(B)** Tumor bearing animals of all genotypes were palpated biweekly to measure tumor size. A total tumor burden of 1.7cm^3 is set by the Animal Care Veterinary Services guidelines. A significant difference was observed between all genotypes. **(C)** Tumor progression was assessed by analyzing the time between onset and endpoint for each animal. *Postn* (-/-) animals showed a significant reduction in tumor progression compared to the wildtype control. **(D)** Tumor protein lysates were assessed for expression of Postn, active (phospho-specific Y1221/22) and total ErbB2, to validate the NeuNDL and Postn knockout model. For panel A-C, N= 25, 32, 28 for *Postn* (+/+), *Postn* (+/-) and *Postn* (-/-) respectively. ** = $P \leq 0.01$, * = $P \leq 0.05$.

Western blot analysis on endpoint tumors was performed to assess the expression of ErbB2 as well as Postn deletion in the *Postn* (-/-):NeuNDL tumors (Figure 3.2 D). Western analysis showed expression of ErbB2 and a complete absence of Postn in the *Postn* (-/-):NeuNDL samples (Figure 3.2 D). Taken together, these results demonstrate that *Postn* deletion in ErbB2-induced mammary tumorigenesis delays tumor initiation, tumor progression and overall endpoint of tumor-bearing mice.

3.3 Global deletion of *Postn* in *Neu*-driven tumorigenesis results in a reduced proliferation and apoptosis

As *POSTN* has been shown to affect pathways regulating proliferation and apoptosis, we investigated the levels of cell growth and cell death markers in the endpoint tumors. The proliferation marker Ki67 was used to assess the mitotic index of tumors by IHC staining on endpoint tumors (Figure 3.3 A). Quantification of Ki67-positive nuclei showed a significant decrease from 22.1% for control *Postn* (+/+):NeuNDL to 15.2% for *Postn* (-/-):NeuNDL (Figure 3.3 B).

Another proliferation marker, Proliferating Cell Nuclear Antigen (PCNA) was assessed by western blotting analysis but showed no significant difference between control and *Postn*-deficient tumors (Figure 3.3 C). This could be due to Western blot analysis performed on whole tumors which is less likely to pick up subtle differences at the single cell levels like Ki67 staining.

As higher apoptotic index tends to be correlated with tumor malignancy [191], we assessed apoptosis using western blot analysis on endpoint tumors for cleaved PARP.

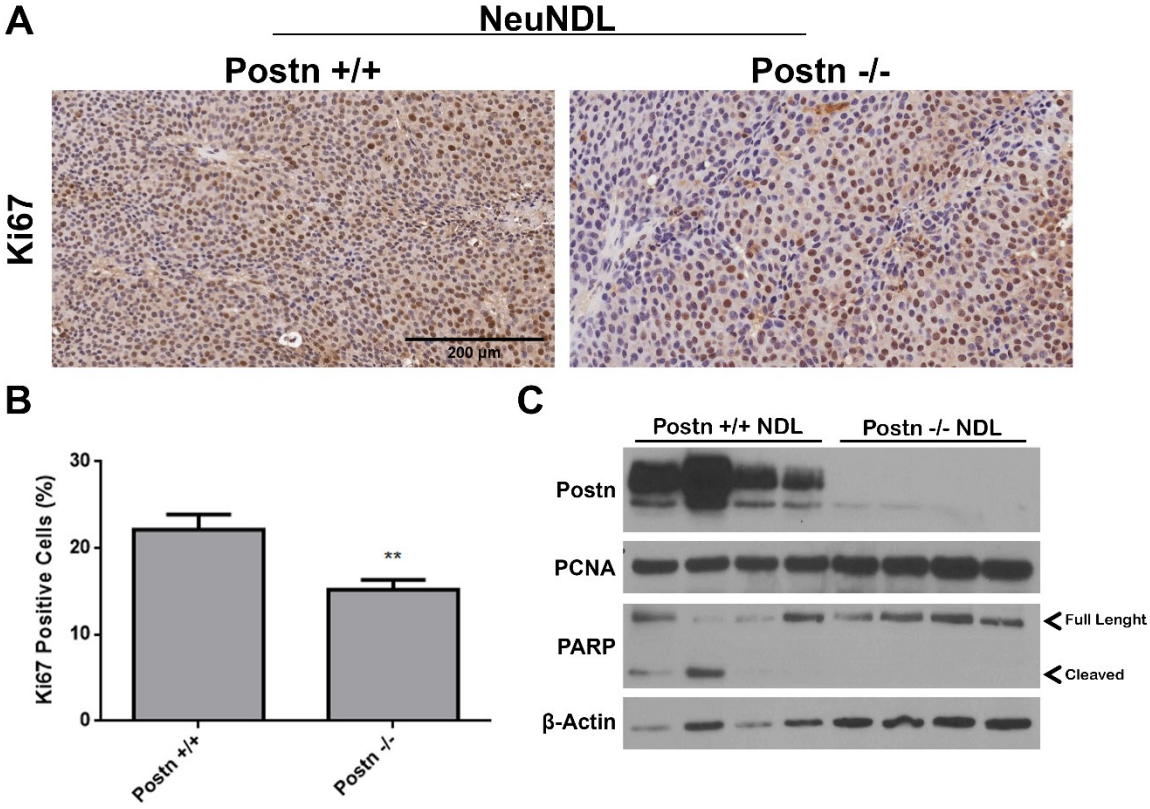

Figure 3.3: *Postn* deletion in NeuNDL mice reduces proliferation and apoptosis.

(A) Ki67 immunohistochemistry staining on endpoint tumors of both *Postn* (+/+):NeuNDL and *Postn* (-/-):NeuNDL animal models. Representative images are shown for both animal models. Scale bar = 200µm. **(B)** The percentage of Ki67 positive nuclei was enumerated using the ImageJ plug-in ImmunoRatio 1.0c. 5 random images from each tumor were analysed using the plug-in. N=10 tumors **(C)** Western blotting analysis showing the proliferation marker PCNA and the apoptosis marker PARP. Both full length and cleaved PARP are identified with arrowheads. Postn protein expression is also shown to validate the genotypes. N= 10 per genotype. ** = $P \leq 0.01$.

Interestingly, whereas 3 out of 4 wildtype tumors showed PARP cleavage, no *Postn* (-/-):NeuNDL tumors displayed cleaved PARP, suggesting a decrease in overall cell death in those tumors.

Together these results suggest that the lack of *Postn* in the tumor environment decreases proliferation and cell death. This is usually indicative of better prognosis and less aggressive tumors. The differences observed in tumor initiation, progression and overall survival could be explained by a decrease in proliferation and apoptosis in the *Postn*-deficient mice.

3.4 Global deletion of *Postn* in *Neu*-driven tumorigenesis does not alter the population of Cancer Associated Fibroblasts

Over the last few years, substantial evidence has shown that the microenvironment and more specifically cancer-associated fibroblasts (CAFs) are responsible for the aggressive characteristics of breast cancer (reviewed in [192]). The observation that *POSTN* has also been involved in processes of extracellular matrix remodelling led us to assess the population of CAFs. Using a panel of antibodies recognized as markers for CAFs, we immunostained endpoint tumors from the *Postn* (-/-):NeuNDL and *Postn* (+/+):NeuNDL control.

Alpha-smooth muscle actin (α-SMA), encoded by the ACTA2 gene, is a marker of cancer associated fibroblasts and also a predictor of tumor aggressiveness involving invasion and metastasis [193, 194]. Analysis of endpoint tumors revealed that α-SMA expression between *Postn* expressing and *Postn* depleted endpoint tumors was unchanged with around 1% of the cells staining positive in both genotypes (Figure 3.4 A, B).

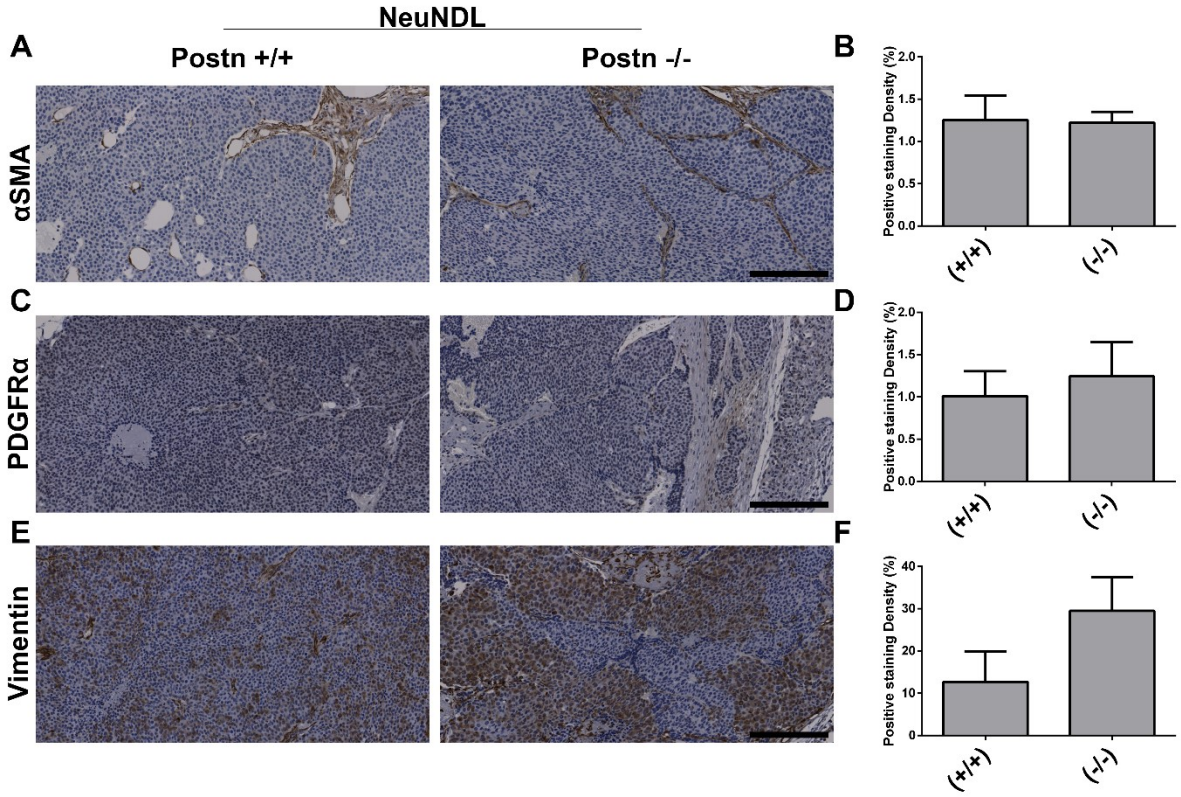

Figure 3.4: Cancer-associated fibroblasts markers are unchanged in *Postn*-null tumors. **(A)** alpha-SMA immunohistochemistry was performed on endpoint tumors from *Postn* (+/+):NeuNDL and *Postn* (-/-):NeuNDL animals. **(B)** Quantification of positive staining density of αSMA. Shown is the mean ± SEM. **(C)** PDGFRα immunohistochemistry for Wildtype and *Postn* deficient endpoint tumors was performed. Representative images are shown. **(D)** Quantification of positive staining density of αSMA. Shown is the mean ± SEM. **(E)** Vimentin immunohistochemistry was performed on endpoint tumors in animals from a *Postn* wildtype and *Postn*-deficient background. **(F)** Quantification of positive staining density of αSMA. Shown is the mean ± SEM. Error bars = 200μm. N=10 per genotype for each staining.

CAFs also express platelet derived growth factor receptor alpha (PDGFRα) which is also generally associated with aggressive tumors [195]. In a similar fashion, PDGFRα expression was unchanged when comparing *Postn* (+/+):NeuNDL and *Postn* (-/-):NeuNDL endpoint tumors (Figure 3.4 C, D). The staining density was similar to αSMA, independent of the genotypes. Finally, we assessed the number of vimentin-positive cells, another marker of progression and invasion in breast cancer [196, 197]. Although vimentin expression was higher than α-SMA and PDGFRα, no significant differences were observed between the two genotypes averaging 12.7% and 29.5% for the WT control and *Postn* (-/-) tumors, respectively (Figure 3.4 E, F). The expression of vimentin was highly heterogeneous throughout the tumors and between tumors. In addition, vimentin expression was also observed in tumor cells.

Although, many markers used for identifying CAFs are not exclusive to CAFs, the use of three independent markers showing no significant differences between genotypes strongly suggests that the population of CAFs is unchanged between the genotypes tested at endpoint.

3.5 Global deletion of *Postn* in *Neu*-driven tumors does not affect immune cell infiltration into the primary tumors

To gain further insights into the mechanisms of delayed tumor onset, progression, and prolonged overall survival in *Postn*-deficient mammary tumors, we assessed immune cells infiltration in the primary tumors of *Postn* (-/-):NeuNDL and *Postn* (+/+):NeuNDL animals. Multiple studies have shown that a higher immune infiltration correlates with improved clinical outcome and also a better response to treatment in breast cancers [198-200]. The classic marker to assess general immune cell infiltration is CD45, a marker of the hematopoietic lineage except for erythrocytes and platelets. Its wide usage as a marker for leukocytes provides a reliable estimation of immune infiltration in tumors.

Immunohistochemical staining for CD45 was used to assess the presence of infiltrating immune cells in endpoint tumors (Figure 3.5 A). Color deconvolution was used to facilitate the counting of the positive cells (Figure 3.5 B). Manual counts were used to quantify the number of infiltrating cells per mm^2 and revealed no significant differences in the number of infiltrating immune cells in endpoints tumors (Figure 3.5 C), suggesting that *Postn* deficiency does not affect the recruitment of immune cells to the primary tumors.

3.6 *Postn*-deficient *Neu*-positive tumors have decreased collagen deposition

POSTN has been shown to affect extracellular matrix remodeling by modulating a plethora of ECM related proteins and mainly by crosslinking collagen [118]. Furthermore, collagen deposition in breast cancer has been recently associated with metastasis and aggressive behavior [201, 202]. Due to the involvement of *POSTN* in collagen cross-linking and promoting aggressive phenotypes in breast cancer, we investigated the effect of *Postn* deletion on collagen deposition in endpoint tumors from the *Postn* (-/-):NeuNDL and *Postn* (+/+):NeuNDL animal models.

Using Masson's Trichrome staining, we assessed collagen deposition in those tumors (Figure 3.6 A). Using thresholding, a common digital image processing method, we were able to extract every blue area from the images and calculate collagen positive pixels as apercentage. A marked reduction of collagen deposition was seen in the *Postn* (-/-):NeuNDL compared to the control *Postn* (+/+):NeuNDL endpoint tumors, supporting the notion that *Postn* can promote the stability and fibrillogenesis of the collagen network. Collagen remodelling can transform the environment and subsequently facilitate the establishment of a metastatic niche and promote growth in the tumor.

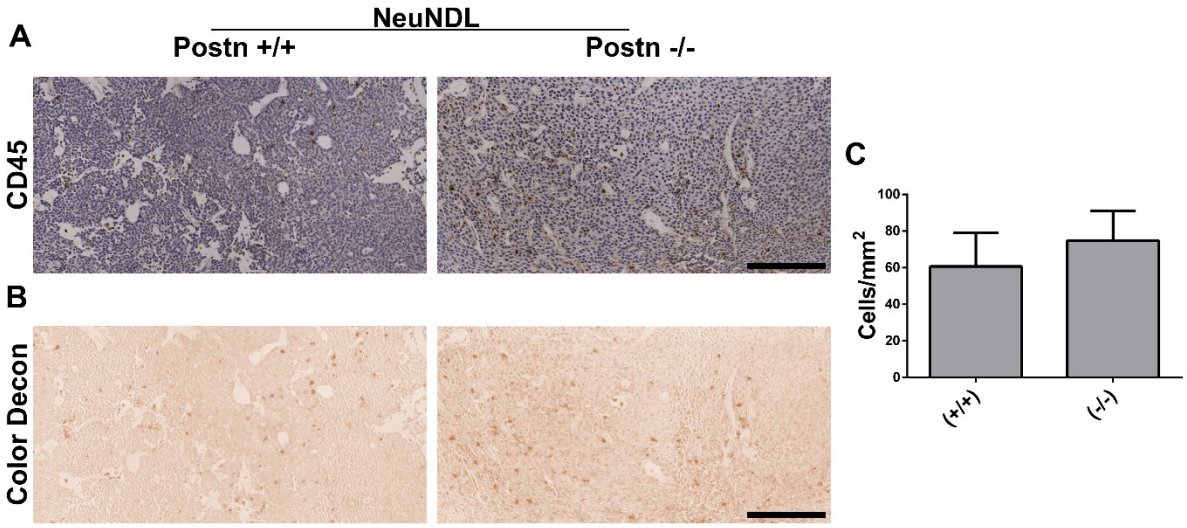

Figure 3.5: *Postn* deletion in *Neu*-induced tumors does not affect immune infiltration.

(A) Representative images of CD45 immunohistochemistry staining for endpoint tumors in the *Postn* (-/-):NeuNDL and *Postn* (+/+):NeuNDL animal models. **(B)** An example of color deconvolution is shown, virtually removing the blue staining from the hematoxylin counterstain leaving only brown specific staining of CD45 to facilitate the quantification. Scale bar = 200µm **(C)** Using the color deconvolution images, quantification was done by manual counting of CD45 positive cells per mm^2. Results are represented as the mean ± SEM. N= 10 per genotype.

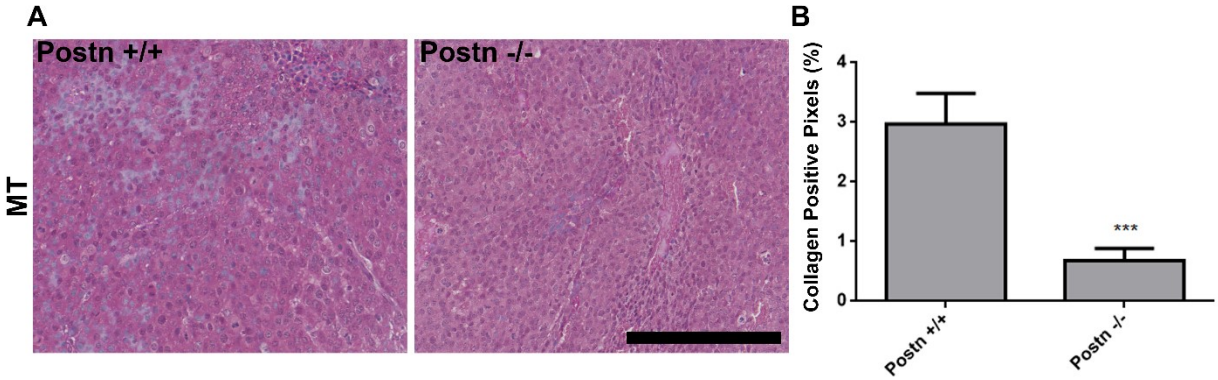

Figure 3.6 : Collagen deposition is reduced in *Postn*-deficient *Neu*-positive tumors.

(A) Masson's Trichrome (MT) staining was performed on *Postn* (-/-):NeuNDL and *Postn* (+/+):NeuNDL endpoint tumors. Collagen stains in blue while other components will stain red/purple. **(B)** Quantification using color thresholding was performed to calculate collagen positive pixels represented in percentage. The results are represented as the mean ± SEM. N = 10 per genotype. *** = $P \leq 0.001$.

3.7 Global deletion of *Postn* in *Neu*-driven tumorigenesis does not affect lung metastasis

POSTN expression has been correlated with metastasis in a panoply of studies in different types of cancers [143, 203, 204]. Its involvement in invasion and metastasis prompted us to investigate lung colonization in the *Postn* (-/-):NeuNDL model. The MMTV-NeuNDL tumor model is not optimal to study metastasis as only 67% of animals have been found to be positive for spontaneous lung metastases [82]. The number of animals that developed significant lung metastasis was much lower than the previously reported 67% for all animals studied. Nevertheless, we have harvested lungs at endpoint and performed Hematoxylin and Eosin (H&E) stains to detect tumor cells (Figure 3.7 A). The total tumor area in the lungs was calculated and represented as a percentage of the total lung area. Surprisingly, no change was observed in the overall lung coverage of cancer metastases and micro metastases (Figure 3.7 B), suggesting that *Postn* deletion did not significantly impair the ability of *Neu*-positive tumor cells to colonize the lungs.

3.8 *Postn* deletion *in vitro* does not alter cancer cell proliferation, migration and invasion

To better understand the mechanisms responsible for the delay in tumor initiation and growth, we investigated the effect of *Postn* deletion in tumor cells isolated from *Postn* (-/-): NeuNDL primary tumors. We have found that MEGS depletion results in *Postn* induction (see Chapter 4). Therefore, to confirm *Postn* deletion, we subjected *Postn* deficient cells to MEGS removal experiments (Figure 3.8 A). Removal of the MEGS supplement results in a robust *Postn* induction in the wildtype cells (Figure 3.8 A). However, Postn protein is undetectable in *Postn* (-/-) tumor cells, confirming the null alleles in three isolates. To overcome issues associated with tumor heterogeneity, we have re-expressed Postn (pMSCV-

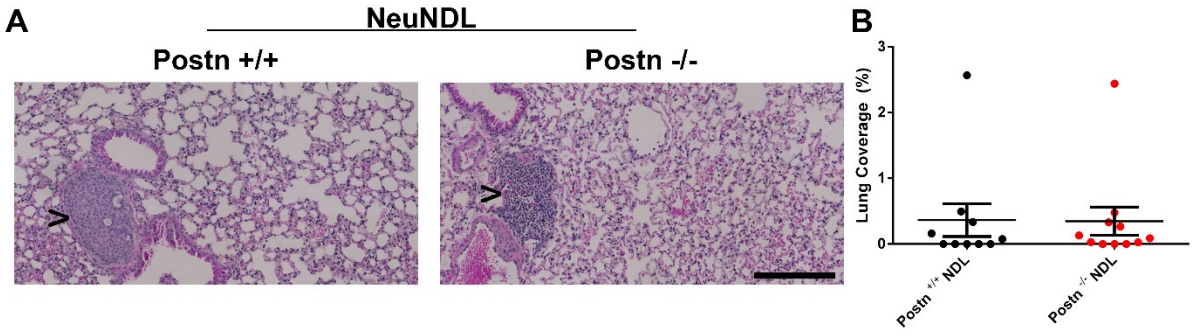

Figure 3.7: Postn deletion does not affect lung metastasis of Neu+ tumor cells.

(A) Hematoxylin and Eosin staining of lungs from endpoint animals from the *Postn* (+/+):NeuNDL and *Postn* (-/-):NeuNDL. Total lungs were sectioned, and sections were collected at every 100µm. Micro metastases or metastases are depicted with an arrowhead. **(B)** Quantification of lung coverage was performed using the measurement tool in ImageJ. Data are represented as mean ± SEM. N= 10 for *Postn* (+/+):NeuNDL, 11 for *Postn* (-/-):NeuNDL.

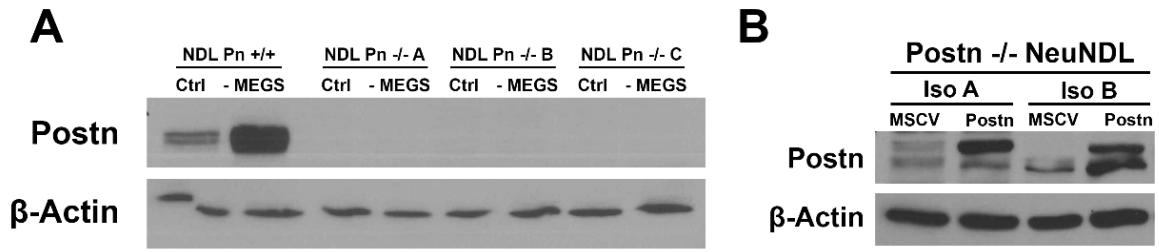

Figure 3.8: Characterisation of Postn-deficient cell lines.

(A) Three isolates of NeuNDL cancer cell lines from a *Postn*-deficient background were derived and grown in MEGS-depleted medium for 24 hours. Postn expression was assessed by Western blot. **(B)** Isolates A and B from a *Postn* (-/-):NeuNDL were infected using retroviral vectors to stably express pMSCV-Postn. The empty pMSCV vector was used as a control. Resulting cell lines were then assessed for Postn expression using Western Blot analysis.

Postn) in these *Postn*-deficient cells. Puromycin selection was used to obtain stably expressing cell lines for both *Postn* and the pMSCV control vector and two independent isolates were established, designated A and B (Figure 3.8 B).

As it was affected in the global deletion model *in vivo,* we first used these cell lines to assess proliferation. In contrast to our in vivo findings, the *in vitro* Postn re-expression model did not show any differences in proliferation when grown in a 2D model (Figure 3.9 A&B). This was observed for both isolates A and B.

Even though metastasis was not affected in our global deletion model, studies have shown that *POSTN* is involved in the process of cell migration in multiple models [205, 206]. We then assessed cell migration in our *Postn*-deficient cells. Interestingly, *Postn* deletion in *Neu* positive tumor cells did not induce any significant differences in cell migration as measured by collagen-coated Boyden Chamber haptotaxis migration assays (Figure 3.10 A&B). Isolate B showed an increase migration rate when compared to Isolate A, but no significant difference was seen between *Postn* expressing and non-expressing cells (Figure 3.10 B).

In a similar fashion, we assessed cell invasion through basement membrane extract (BME) -coated Boyden chambers. The membranes were then stained using crystal violet to assess the number of cells that invaded through the matrix (Figure 3.11). Surprisingly, a significant reduction in invasion potential is seen in Postn re-expressing isolate B while no significant difference was observed for isolate A. Although counterintuitive, it is unclear why isolate B shows a reduction in invasion potential upon Postn re-expression.

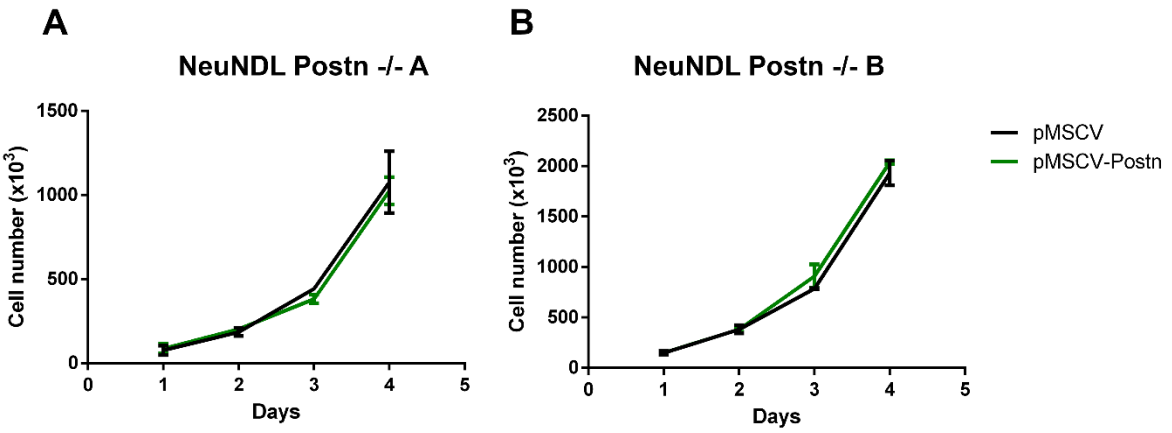

Figure 3.9: Postn re-expression in *Neu*+ tumor cells does not affect proliferation.

Postn-null cells re-expressing Postn (see Figure 3.8) were seeded, and live cell counts were obtained for up to 4-days post-seeding. Panels **(A)** and **(B)** represents the two independent isolates (A and B). Data is represented as the mean ± SEM. N=3.

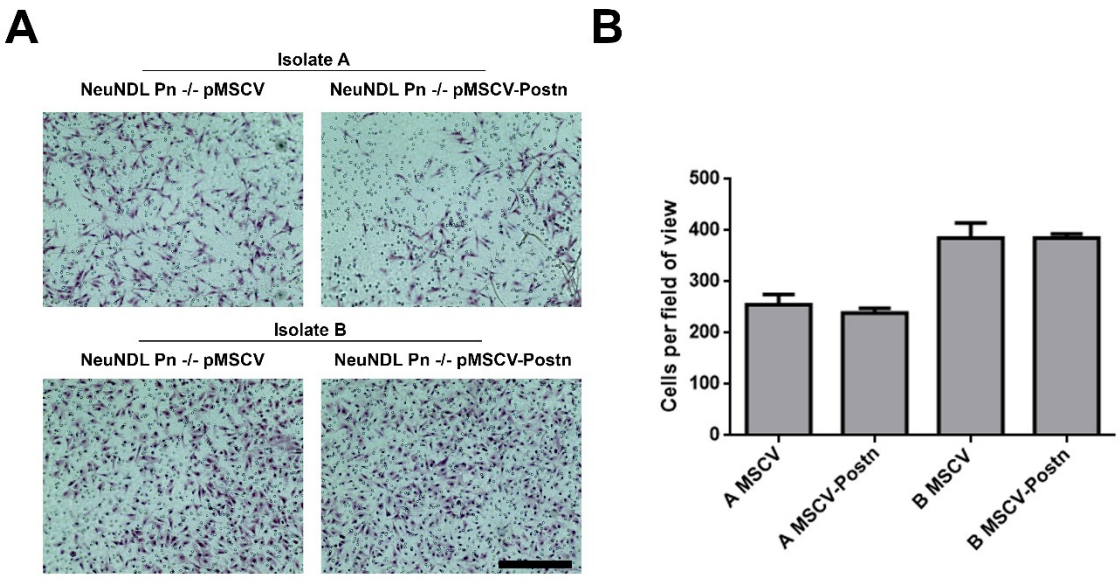

Figure 3.10: Migration rate is unaffected in *Postn*-null *Neu*-positive tumor cells.

(A) *Postn* (-/-):NeuNDL cells were subjected to boyden chamber migration assay. Haptotaxis was assessed between cells stably re-expressing Postn (pMSCV-*Postn*) or the empty vector (pMSCV). This was performed on two independent isolates of *Postn* (-/-) cells. Representative images of crystal violet-stained membranes are shown. Scale bar = 200µm. **(B)** Quantification by manual counting of 10 representative field of views per membrane are shown in the bar graph. Data is represented as mean ± SEM. N=3.

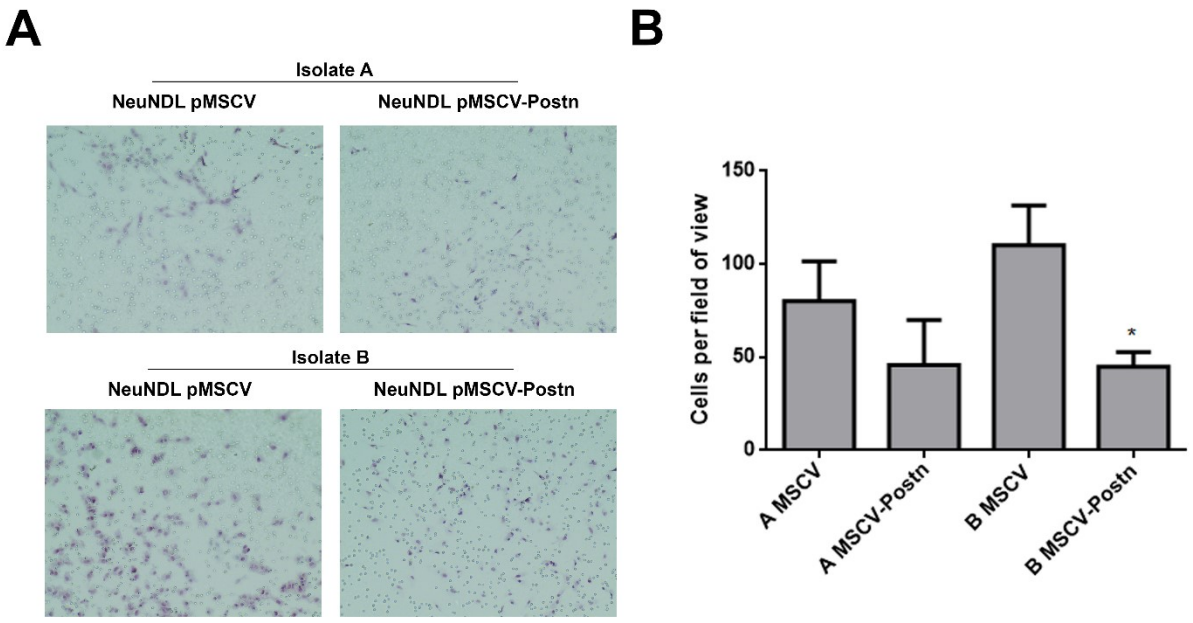

Figure 3.11: *Postn* deletion in cancer cells does not affect their invasive capacity *in vitro*. **(A)** Brightfield microscopy images of crystal violet-stained Boyden chamber membranes following basement membrane extract (BME) invasion for two independent isolates (A and B) of *Postn* (-/-):NeuNDL cells expressing either pMSCV or pMSCV-*Postn*. **(B)** Quantification of invasion by manual counting of cells per field of view. 10 representative images were counted per field of view. Data is represented as the mean ± SEM. N=3, * = $P \leq 0.05$

This might be due to the fact that isolate B has a higher "baseline" invasive potential when compared to isolate A, suggesting heterogeneous invasive properties between the isolates. Nevertheless, our data show that Postn re-expression did not increase invasion in vitro. One possibility is that Postn secretion from the epithelial compartments could affect other cell types or that a 3D environment is required to show any effects of Postn secretion.

3.9 *Postn* deletion in cancer cells does not alter tumor growth as 3D spheroids

As 2D culture did not show any differences in proliferation, we assessed growth as 3D spheroids by performing mammosphere formation assays using *Postn* (-/-):NeuNDL cancer cells stably expressing either pMSCV or pMSCV-*Postn*. Following seeding in suspension, the mammosphere forming efficiency was not significantly changed between the groups (Figure 3.12 B&D), suggesting that *Postn* deletion does not affect 3D spheroid growth. However, a drastic difference in mammosphere morphology was seen between isolate A and B, with A being much more spheroid and solid looking, while isolate B was much looser and monolayer-like (Figure 3.12 A&C). These differences in morphology were also seen in different breast cancer cell lines [207].

Although we used this technique to assess anchorage-independent 3D growth, it is also a measure of stem/progenitor cell activity *in vitro* when testing primary and secondary sphere formation. Interestingly, secondary sphere assays were unsuccessful using these cells. One possibility is that not enough mammospheres were formed in the primary passage to effectively seed secondary spheres. Alternatively, it is possible that the cells do not have enough self-renewal activity to form secondary spheres.

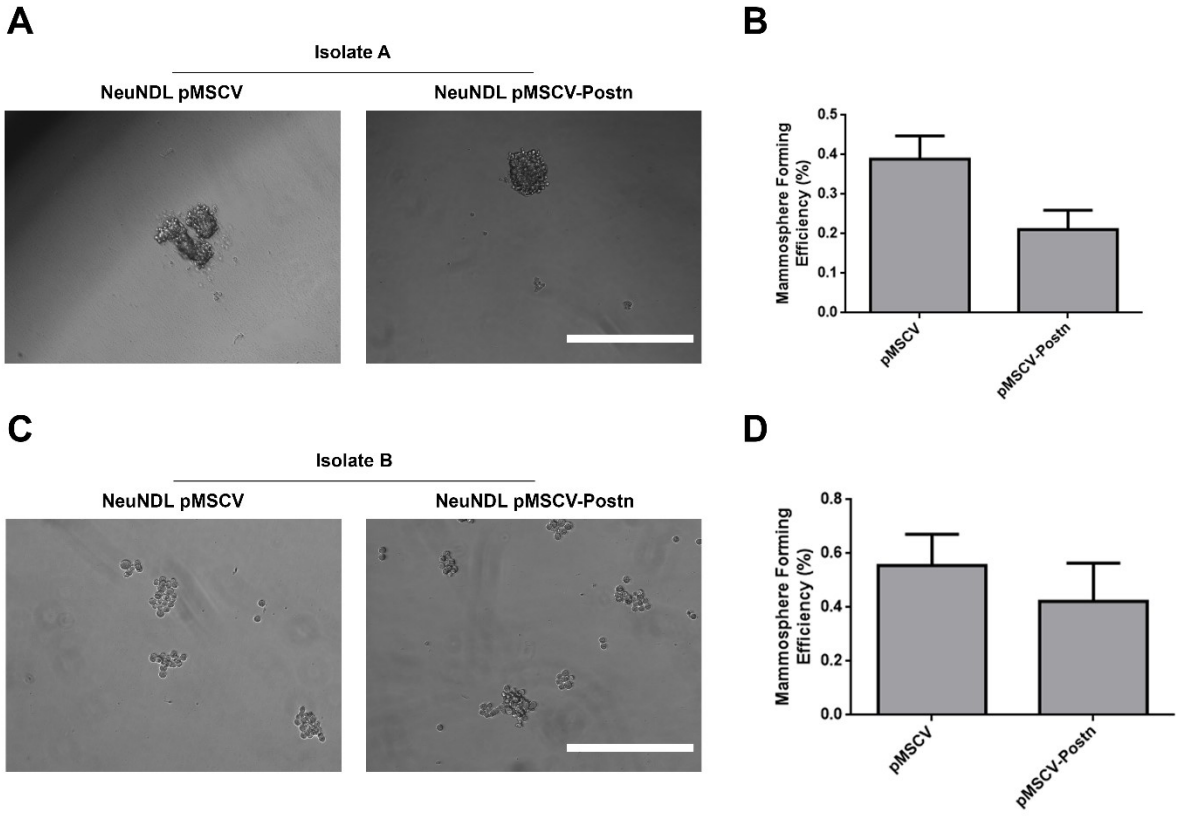

Figure 3.12: *Postn* deletion in cancer cells does not alter their sphere forming capacity. **(A, C)** Brightfield microscopy images of primary mammospheres from both isolates of *Postn* (-/-):NeuNDL cells stably expressing either pMSCV or pMSCV-*Postn* after 6 days of growth in 1x MEGS and 1X B27 supplement in low-attachment plates. Scale bar is equal to 400 µm. **(B, D)** Quantification of the respective Mammosphere Forming Efficiency was obtained by calculating the percentage of spheres per well with a diameter greater than 50 µm over the total number of cells seeded per well. Data represented as the mean ± SEM. N=3.

3.10 *Postn* deletion has no effect on subcutaneous tumor growth

To further our understanding on the role of *Postn* on tumorigenesis, we assessed the *in vivo* growth potential of *Postn* (-/-):NeuNDL cells stably expressing pMSCV or pMSCV-*Postn*. Cells from isolate A were injected subcutaneously in immune compromised mice (CD1 nude mouse) and tumor diameters and volumes were assessed every third day post-injection. Surprisingly, no significant changes were observed when comparing *Postn* (-/-):NeuNDL cells stably expressing pMSCV or pMSCV-*Postn* (Figure 3.13 A&B). At endpoint, tumors were extracted and weighed to estimate overall growth with no significant differences between the two groups (Figure 3.13 C). Images of the biggest and smallest extracted tumors were taken to highlight the variation in sizes within the same groups (Figure 3.13 D).

These data suggest that *Postn* deletion and reconstitution in *Neu*-positive tumor cells does not affect growth in immune compromised animals. The subcutaneous microenvironment expresses a basal level of Postn which could be sufficient to compensate for *Postn* deficiency in *Postn* (-/-):NeuNDL cells. Therefore, the injection site and tissue environment are likely to have an impact on tumor growth.

3.11 Summary

HER2-positive breast cancers accounts for 25-30% of all reported breast cancer cases and these tumors are generally more aggressive with poorer prognosis and clinical outcome [64]. It has been shown that *POSTN* promotes a more aggressive behavior in breast cancer by contributing to tumor growth, angiogenesis, and metastasis [186] [156]. Therefore, we hypothesized that deletion of *Postn* in both tumors and the microenvironment would significantly increase survival and outcome by delaying tumor onset and overall survival, making it a potential target for therapeutics.

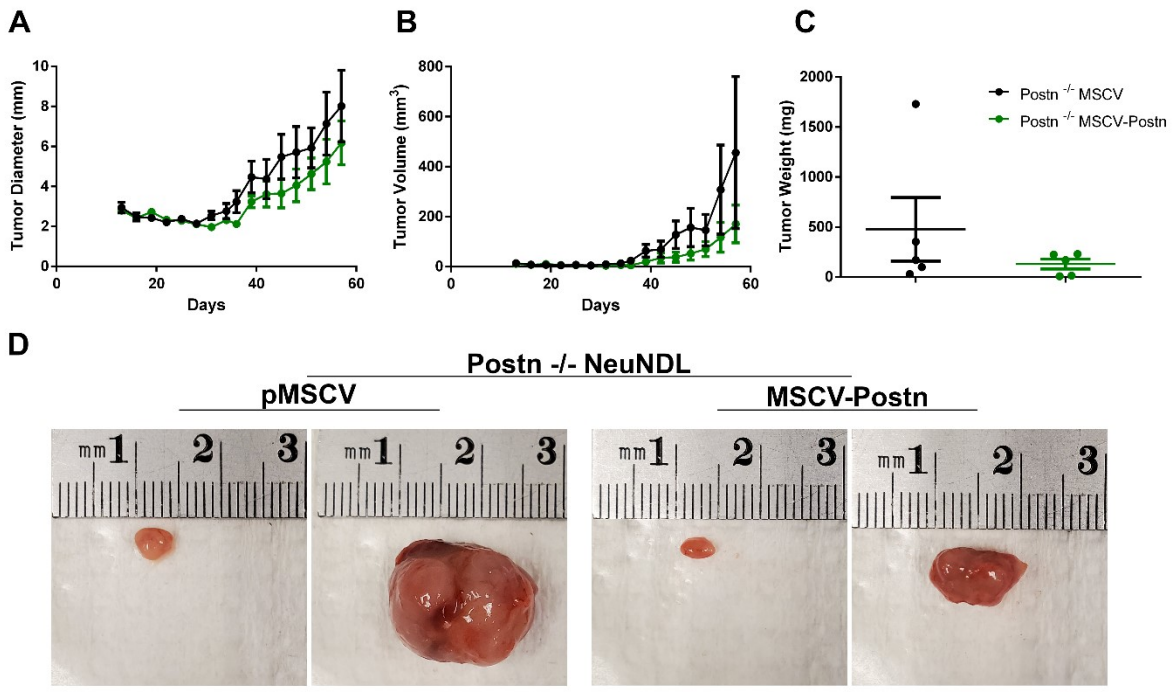

Figure 3.13: *Postn* re-expression in deficient cells does not alter subcutaneous growth. **(A)** *Postn*-deficient NeuNDL cells were stably transduced with either pMSCV or pMSCV-*Postn* and were injected subcutaneously in immunocompromised mice (5 mice per cell line). Tumors were measured every three days and mice were sacrificed when the tumor diameters reached 14 mm. Data are represented as the mean ± SEM. **(B)** Measured diameters were used to calculate the volume assuming tumors were spheroids ($V = \frac{3}{4} \pi r^3$). Data are presented as the mean ± SEM. N=5 **(C)** Once removed, the tumor mass was recorded and presented as the mean weight ± SEM. **(D)** The smallest and largest tumors from each group is shown next to a ruler to highlight the variance between the size of the tumors inside the same group.

In agreement with our initial hypothesis, the deletion of *Postn* lead to a delay in tumor onset and longer time to reach endpoint with better overall survival. Consistent with these observations, *Postn*-null tumors show reduced proliferation indices and lower levels of apoptosis markers. However, the loss of *Postn* in these animals did not affect the population of CAFs or the infiltration of immune cells as assayed by various specific markers. Interestingly, tumors from *Postn* knockout animals had decreased collagen deposition in the primary tumors which could play a role in the observed delayed onset and survival differences between genotypes. Furthermore, lung colonization was unaffected by the absence of Postn in this animal model. Lastly, our investigation of tumor cell cultures of *Postn* expressing and non-expressing lines *in* vitro revealed no significant changes in proliferation, migration, and invasion. Similarly, the growth of these cells as 3D spheroids or following injections *in vivo* was unaffected by the expression of *Postn*.

These results suggest that *Postn* plays an important role in the initiation and growth of the primary tumors in MMTV-NeuNDL mice. The effect seen *in vivo* is unlikely to be due to *Postn* directly affecting epithelial cells, since those cells overexpressing *Postn* do not gain any advantage in culture. It is more likely that the effect seen are due to *Postn* affecting the ECM or other cell types conferring growth advantage to the tumors. It is tempting to speculate that the loss of *Postn* may alter collagen crosslinking and extracellular matrix remodeling. This could result in a poor environment for tumor initiating cells and niche establishment. This also supports the use of *Postn* or collagen as biomarkers for aggressive tumor and overall outcome in breast cancer.

Chapter 4

Acquired *Postn* gene expression is regulated by a bovine pituitary extract in vitro

4.1 Introduction and Rationale

Global deletion of *Postn* leads to better overall outcome in *Neu*-driven mammary tumorigenesis. *Postn* deficiency leads to a delay in tumor onset and better overall survival (see Figure 3.2 A, B). Tumors lacking *Postn* display reduced rate of proliferation and apoptosis (Figure 3.4), accompanied with decreased collagen deposition (Figure 3.7).

Our observations stem from the global deletion of *Postn*. It has become apparent that the expression of *POSTN* in stromal compartments has a different effect than acquired expression in epithelial compartments [208]. In normal breast tissue, *Postn* expression is restricted to the stromal connective compartment whereas the epithelial component is always devoid of *Postn* [142]. The distribution of *Postn* expression in breast tumors is quite different from normal tissues. It was initially thought that Postn was exclusively expressed by fibroblasts and stromal compartments of the tumors. Interestingly, a subset of tumors also expresses *POSTN* in the epithelial compartments, which has been correlated with aggressiveness and poor overall survival [142, 208]. This suggests a deregulation of *POSTN* expression in a subset of epithelial cancer cells which could likely involve epithelial-specific regulatory mechanisms. We sought to investigate the signaling mechanisms that lead to acquired Postn expression in epithelial cancer cells.

4.2 Epithelial *Postn* expression is acquired in a subset of breast cancers

Prior to directly assessing the regulation of *Postn* in the epithelial compartment of *Neu*-positive tumors, we first assessed the epithelial expression of *Postn* in specific subtypes of breast cancers and in murine models of breast cancers. To test this, we established the proportion of tumors that acquired *Postn* expression in their epithelial compartments by immunohistochemistry using a panel of HER2 murine breast cancer models and comparing it

to a human tissue microarray (hTMA). The hTMA, containing a mix of subtypes (Biomax BR962), and endpoint tumors from MMTV-NeuNDL [58], MMTV-NIC [83] and MMTV-PyMT [79] models were subjected to IHC using an anti-Postn antibody (Figure 4.1 A).

Following the staining, tumors that had 30% or more positive pixels in the epithelial compartments were classified as "acquired" while those under the threshold were classified as "non-acquired". The rationale for the 30% threshold came from the observation that 90% of the tumors were either between 0-15% or 60-100%. Therefore, we arbitrarily selected a threshold between 15% and 60% to have an objective way of identifying acquired expression of Postn. Following quantification, 45% of human cores were positive for acquired expression independently of their breast cancer subtype (Figure 4.1 B). Interestingly, murine tumors from HER2-positive models also showed acquired *Postn* expression in 50-60% of the cases (Figure 4.1 B), suggesting that human tumors and murine models acquire Postn at a similar frequency.

To further analyze *POSTN* expression in various cell types present in breast tumors, we analyzed single-cell RNA-sequencing data generated by *Wu et al* [179] for 5 human triple negative breast cancers (TNBC). Using this data, we assessed *POSTN* expression levels across cell types and found that its expression is restricted to myoepithelial cells, fibroblasts, cancer cell populations and to a lesser extent to endothelial cells (Figure 4.2 A, B). Furthermore, comparing its expression between individual tumors shows that *POSTN* is consistently expressed in the fibroblast population but is expressed in cancer cells in only 2 of the 5 tumors (Figure 4.2 C).

Taken together, these results show that *Postn* epithelial expression is acquired in 40-50% of breast cancer irrespective of subtypes and species. It also demonstrates that Postn is

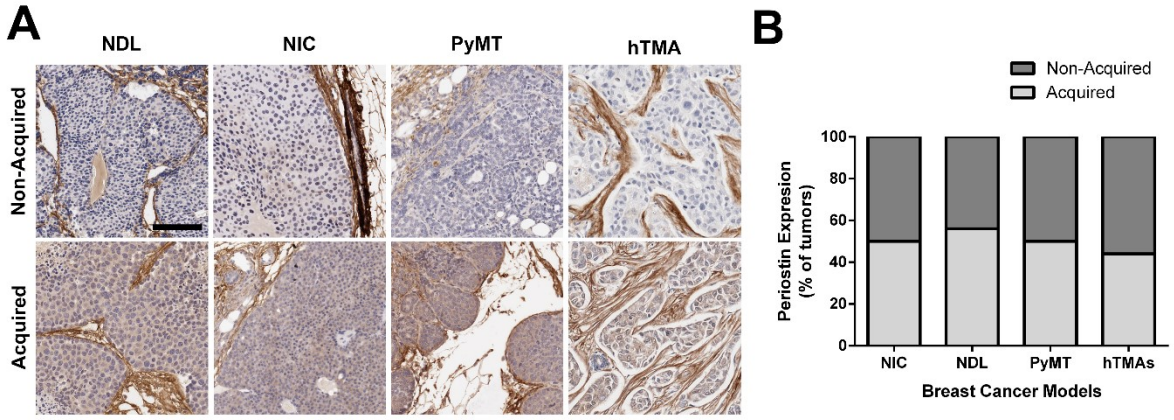

Figure 4.1: *Postn* distribution in tumors from murine cancer models and human TMAs. **(A)** Immunohistochemistry for the expression of *Postn* was performed on mammary gland tumors from a panel of MMTV-driven ErbB2-positive murine breast cancer models and on human Tissue Microarrays (TMAs). The models used were the MMTV-NeuNDL model (n=9), MMTV-NIC (n=10) and MMTV-PyMT (n=8). The human TMA contained 72 cores with various levels of HER2 expression and random breast cancer subtype. Error bar = 200µm **(B)** Tumors were classified as acquired or non-acquired according to their epithelial expression of Postn and were represented in a bar graph as a percentage of total cases.

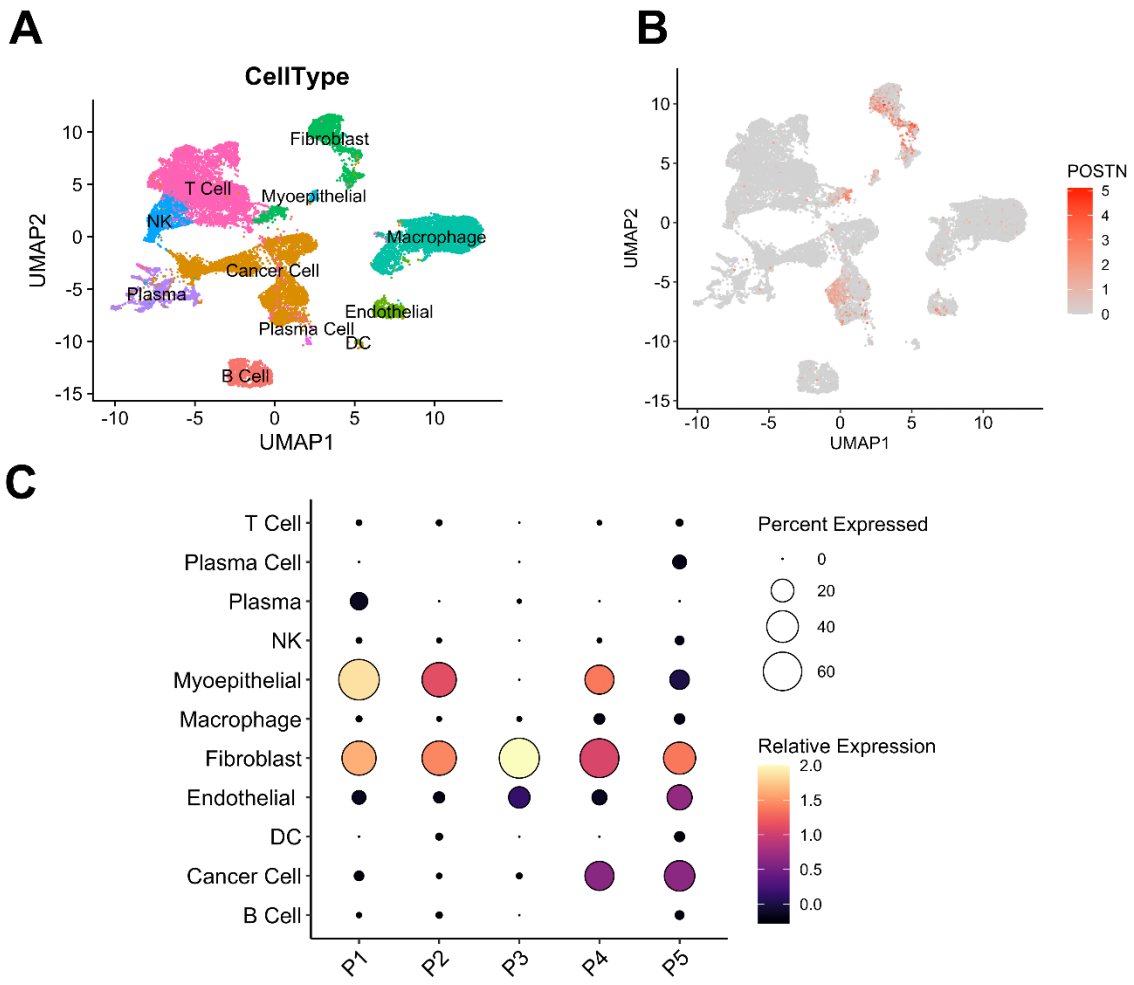

Figure 4.2: *POSTN* distribution in cell types from a single-cell RNA-Seq TNBC dataset. **(A)** Clustered UMAP embedding of scRNA-seq data of 24,271 cells from 5 triple-negative breast cancer tumors. Data and cell type annotations were acquired from Wu *et al.* [179]. **(B)** Identical UMAP to (A) showing the distribution of *POSTN* expression across the cell types comprising the tumor. Expression values correspond to log-transformed counters per 10k transcripts. **(C)** Summary of the average *POSTN* expression (Z-score) in each cell type and the percentage of cells with *POSTN* detection for each patient (P1-P5).

expressed in a small subset of cell types in breast cancer, such as endothelial cells, fibroblasts, myoepithelial cells, and cancer cells.

4.3 Mammary Epithelial Growth Supplement represses *Postn* expression *in vitro*

During the isolation and growth of MMTV-NeuNDL cells used in Chapter 3, we fortuitously discovered that cells grown for extended periods in culture without replenishing the growth medium, start to express *Postn* (Figure 4.3). The induction of *Postn* following prolonged growth suggests that short lived components in the growth medium could be repressing *Postn* and are being depleted over time. We then investigated the effect of the different components in the growth medium in an attempt to identify the repressive elements.

Surprisingly, the removal of MEGS from the growth medium was sufficient to markedly induce *Postn* mRNA expression (Figure 4.4 A). Although, in the presence of MEGS, removing the FBS from the growth media did not affect *Postn* mRNA expression (Figure 4.4 A), *Postn* induction by MEGS depletion was even more prominent under low serum conditions. Similarly, protein expression was assessed following MEGS removal, FBS removal and a combination of both. Western analysis showed that MEGS removal induced Postn protein expression and that low FBS conditions synergized to enhance the induction of *Postn* without any effect on its expression when MEGS is present (Figure 4.4 B).

To assess *Postn* expression at the single cell level, we performed immunofluorescence on cells growing in full medium or MEGS-depleted conditions for 24 hours using an anti-Postn antibody (Figure 4.4 C). Cells that were positive for Postn showed high perinuclear staining similar to a Golgi apparatus staining, which is a typical immunofluorescence pattern for secreted proteins (Figure 4.4 C). Quantification of Postn expressing cells from

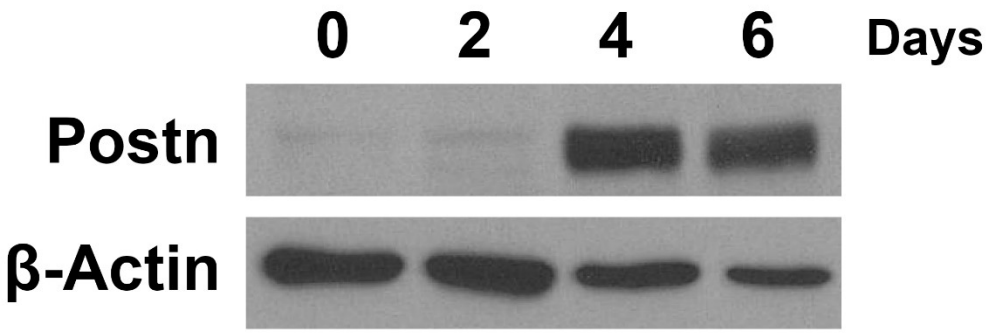

Figure 4.3: Long term culture of NeuNDL cells leads to *Postn* induction.
MMTV-NeuNDL cells were grown in full growth medium (10% FBS, 1X MEGS) for 0, 2 4 and 6 days without medium change. Postn protein expression was assessed by western blotting analysis to evaluate depletion of the medium components.

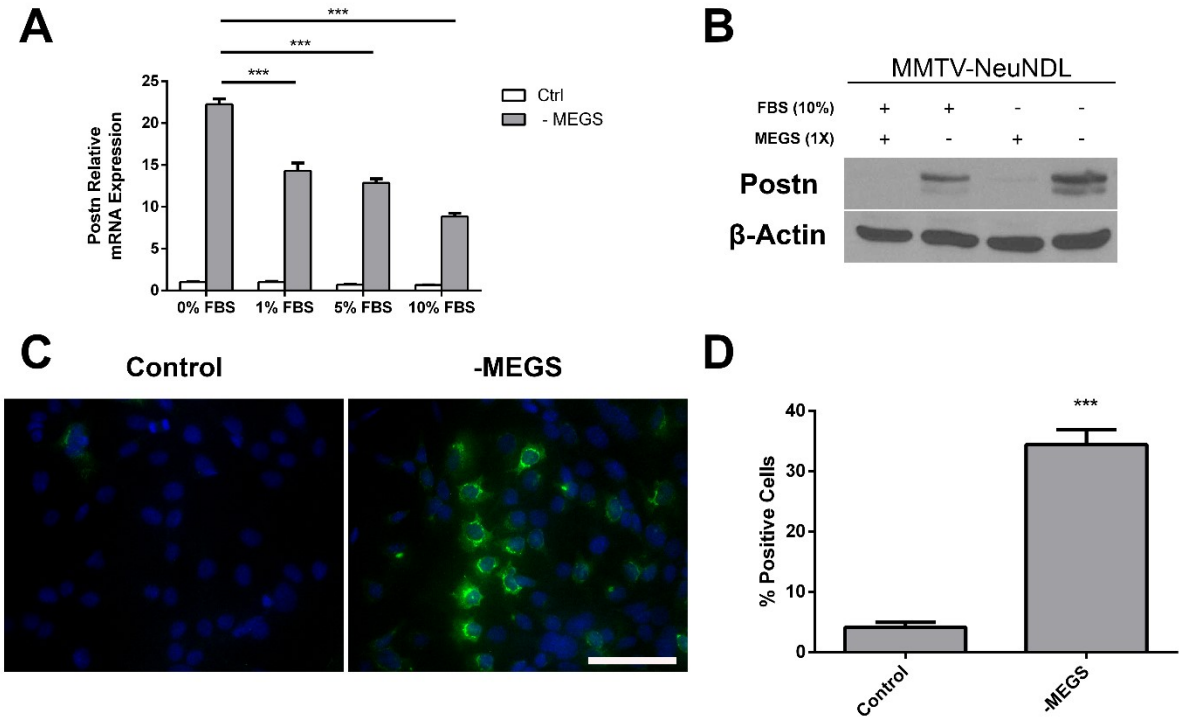

Figure 4.4: Mammary Epithelial Growth supplement represses Postn Expression *in vitro*. **(A**) NeuNDL cells were treated with or without MEGS in varying FBS concentrations from 0 to 10% and *Postn* mRNA expression was assessed 24 hours post-treatment. Data are represented as the mean ± SEM. N=3 for each treatment, *** = $P \leq 0.001$. **(B)** NeuNDL cells were grown in the presence or absence of FBS and MEGS for 24 hours. Postn levels were assessed by western blot analysis. **(C)** NeuNDL cells were seeded on coverslips, grown in the presence or absence of MEGS for 24 hours. Individual coverslips were immunostained for Postn and DAPI. Error bar = 100µm. **(D)** Stained coverslips were manually counted to assess the percentage of *Postn* expressing cells in both conditions. Data are represented as mean ± SEM. *** = $P \leq 0.001$

representative images showed a significant increase in the proportion of cells expressing *Postn* in MEGS-depleted cultures (Figure 4.4 D). The induction of *Postn* following MEGS-depletion was tested in additional cell lines to confirm that the induction was not isolate- or cell line-specific. Although the kinetics were different, the induction of *Postn* was observed in an independent isolate from both a MMTV-NeuNDL and a MMTV-NIC tumor (Figure 4.5 A, B).

Together our data suggest that components in the MEGS and serum can mediate the repressive effect on *Postn* gene expression. It also shows that the observed effect is likely due to increased transcription of the *Postn* gene, ruling out potential protein stability or secretion issues.

4.4 Bovine Pituitary Extract represses *Postn* expression *in vitro*

To further investigate the kinetics and mechanisms of MEGS-mediated repression, a time course experiment for the induction of *Postn* following MEGS removal from the growth medium was performed. *Postn* induction was first detected around 16 hours post-MEGS removal while maximal *Postn* expression occurred around 36 hours to reach a plateau maintained up to 48 hours (Figure 4.6 A). We then tested the individual components found in the MEGS. We subjected NeuNDL cells to a treatment with MEGS or its individual components (EGF, IGF1, Hydrocortisone, BPE) at their respective concentration found in the supplement. A 24-hour treatment with the individual components showed that only BPE and total MEGS had the same repressive effect on *Postn* expression (Figure 4.6 B). Similarly, BPE and MEGS were shown to significantly inhibit *Postn* mRNA induction (Figure 4.6 C), suggesting that BPE is necessary and sufficient to inhibit *Postn* gene induction.

BPE is a complex tissue extract produced by homogenizing bovine pituitary glands in PBS. Therefore, additional analyses were performed to further identify the repressive

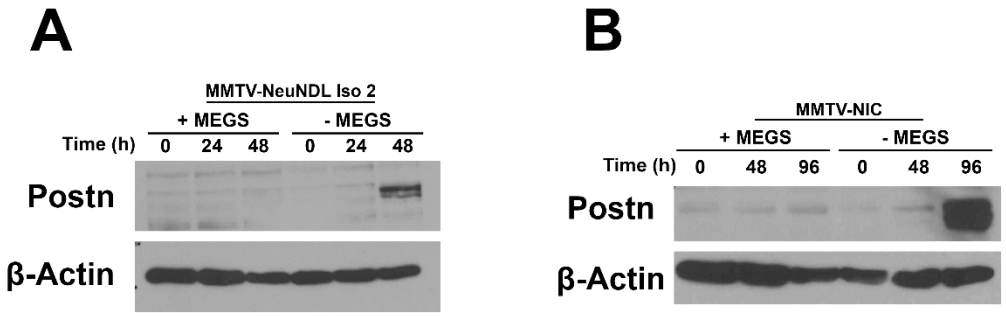

Figure 4.5: Removal of MEGS induces *Postn* in independent isolates and cell lines.

(A) A NeuNDL independent isolate was subjected to a MEGS-deficient medium and *Postn* expression was assessed up to 48 hours post-removal. **(B)** A MMTV-NIC cell line was subjected to a MEGS-depleted medium and Postn expression was assessed up to 96 hours post-medium change.

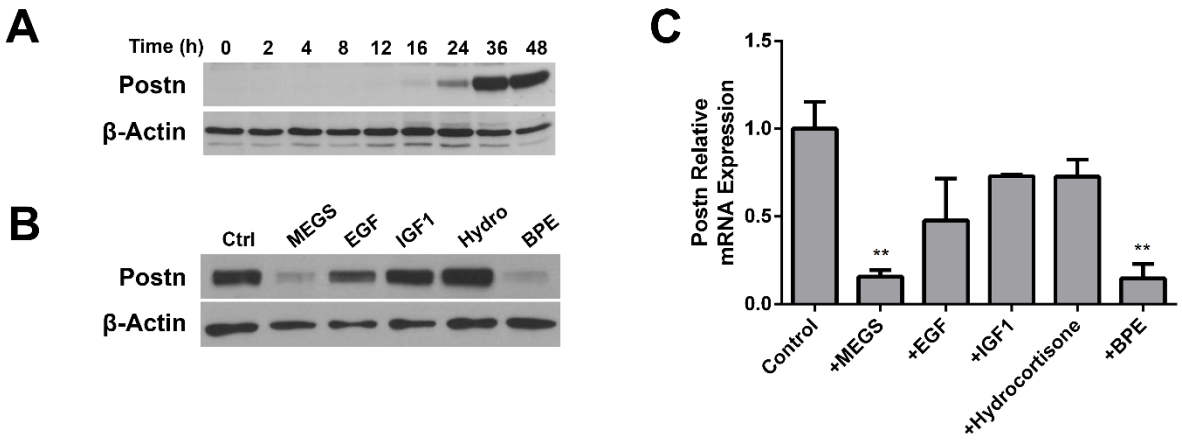

Figure 4.6: Bovine Pituitary Extract mediates *Postn* repression.

(A) NeuNDL cells were seeded and grown under MEGS-depleted conditions for up to 48 hours and Postn levels were assessed at multiple time points. **(B&C)** NeuNDL cells were seeded and then grown in either MEGS, or individual MEGS components (EGF 3ng/ml, IFG1 0.01 µg/mL, Hydrocortisone 0.5 µg/ml, BPE 0.4% v/v). Protein and mRNA expression were assessed by western blotting and Q-PCR analysis, respectively. mRNA expression data are represented as mean ± SEM. N=3, ** = $P \leq 0.01$.

component(s) found in BPE. We first assessed whether its effect on *Postn* expression was following a dose-dependency relationship.

To investigate this, a treatment with increasing concentrations of BPE (0%, 0.1%, 0.2% and 0.4%) was performed. Quantitative PCR analysis showed that a clear dose-dependency effect was observed on *Postn* mRNA levels. A 50% reduction was measured at 0.1% BPE while a 70% reduction occurred at 0.4% (Figure 4.7 A). Heating the extract at 100°C for 15 minutes prior to treatment completely abolished *Postn* mRNA induction, suggesting the denaturation of a protein-based repressive activity (Figure 4.7 B).

Taken together, these results show that BPE can strongly repress *Postn* expression in *in vitro*. The active component(s) in BPE are acting in a dose-dependent manner and are heat-labile, suggesting a proteinaceous component.

4.5 Fractionation of BPE to narrow down potential repressors of *Postn*

Due to the complexity of BPE, (abundance of proteins, hormones, amino acids, lipids and sugars), we attempted to fractionate BPE and ultimately use mass spectrometry to identify potential active components. We first performed an on-column size exclusion chromatography and obtained two absorption curves (Figure 4.8 A). Using a molecular standard curve allows for an estimation of the size of the proteins found in each of the peaks detected (Figure 4.8 A). Fractions were collected and pooled to reflect the 5 peaks identified with the chromatography absorption curve (Figure 4.8 B). Peaks were identified using mock colors and labeled P1 to P5 with Pc being the fractions that did not correspond to any peaks in the absorption curve (Figure 4.8 B). Silver stain analysis of the fractions (Figure 4.8 C), shows a significant overlap in the protein sizes present in multiple peaks, suggesting some leakiness in the fractionation.

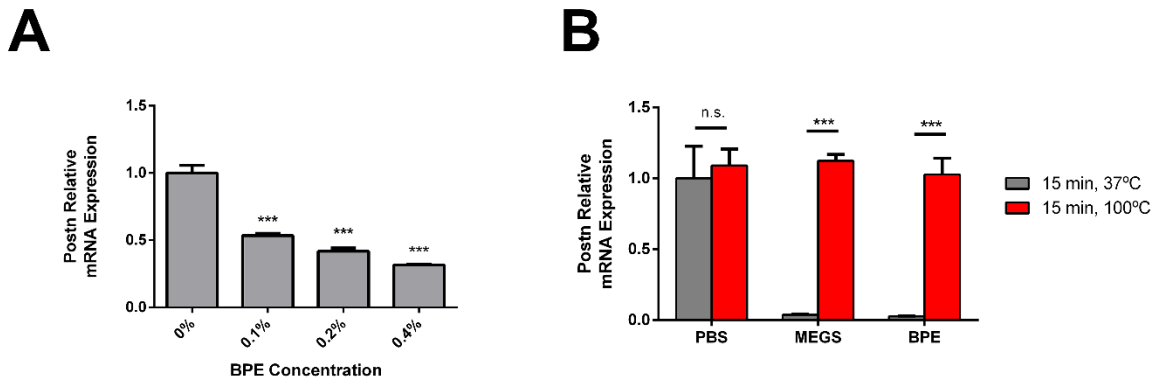

Figure 4.7: The BPE repressive activity is heat labile and dose dependent.

(A) NeuNDL cells were treated using 0%, 0.1%, 0.2% and 0.4% BPE to assess the dose-dependency relationship in the repression of *Postn*. **(B)** NeuNDL cells were treated with PBS, MEGS and BPE that were pre-incubated at 37°C or 100°C for 15 minutes to assess the heat sensitivity of the repressive components. *Postn* relative mRNA expression is shown in the bar graphs as mean ± SEM, *** = $P \leq 0.001$.

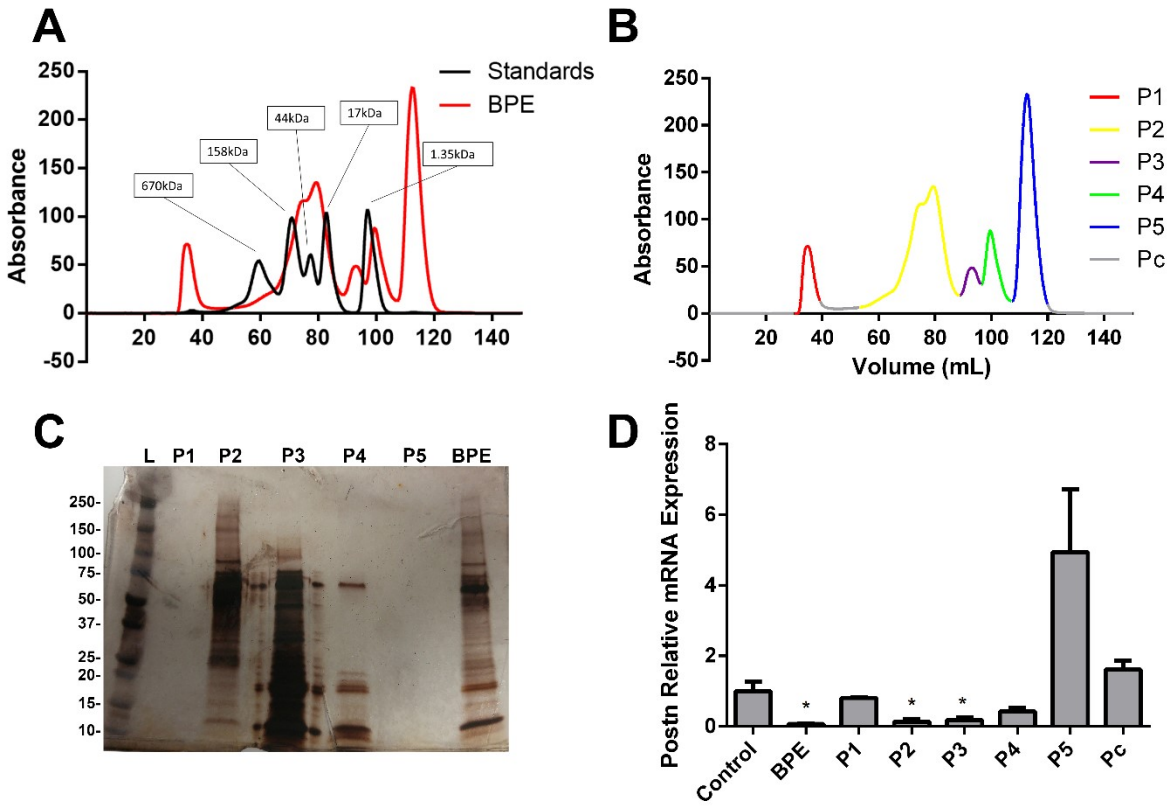

Figure 4.8: BPE size exclusion chromatography reveals repressive fractions.

(A) On-column molecular size exclusion chromatography was performed on molecular weight marker standards (black curve) and BPE (Red Curve). The molecular weight of the peaks in the standard curve are shown in the box indicating the corresponding peak. **(B)** Size-exclusion chromatography absorbance curve for BPE is assigned colors corresponding to their peaks. **(C)** Fractions corresponding to each peak were collected and pooled. They were then subjected to electrophoresis on a 4-20% polyacrylamide gel and silver stained. Ladder marks are seen to the left of the ladder. BPE was also used in the electrophoresis as a control. **(D)** The fractions corresponding to the assigned peaks were then used to treat NeuNDL cells along with a BPE treatment to assess the repressive ability of the individual peaks. N= 3, * = $P \leq 0.05$

Interestingly, peaks 1 and 5 had no proteins present on the silver stain which can be explained by the fact that they are well over 670kDa, and under 1.35kDa, respectively. Using the pooled fractions corresponding to each peak, we assessed the repressive ability of each peak by measuring *Postn* mRNA expression. Our PCR analysis revealed that peaks 2 and 3 had very strong repressive activity even though these fractions were markedly diluted compared to BPE alone (Figure 4.8 D). Together these results show that we can concentrate the repressive components from BPE using molecular size exclusion chromatography.

We next used on-column ion exchange chromatography to separate the proteins by their isoelectric points. To build from the size exclusion chromatography previously described, we combined peaks 2 and 3 together to form a combination designated P2-3. Following batch binding on Q Sepharose or SP Sepharose in low salt, the flow through (FT) was collected and the bound P2-3 mixture was then eluted with 1M NaCl. The "Bound" (B) and FT fractions of both types of Sepharose were used to treat NeuNDL cells and assess for *Postn* repression. The Q Sepharose FT and SP Sepharose B were shown to retain repressive activity following MEGS removal (Figure 4.9 A), suggesting that the repressive components found in P2-3 are positively charged.

We then set up large scale on-column ion exchange chromatography using SP Sepharose with the resulting absorption graph shown in Figure 4.9 B and C. Surprisingly, the area with small successive peaks, eluting at higher NaCl concentration, had a strong *Postn* repression activity shown by RT-PCR (Figure 4.9 D). In an attempt to narrow down our fraction selection even further, we tested the repressive ability of a subset of the P2-9 mixture by testing peaks 2 to 5 (P2-5) and peaks 6 to 9 (P6-9). Unexpectedly, neither P2-5 or P6-9 was able to repress *Postn* expression while P2-9 had a similarly strong repression as assessed by

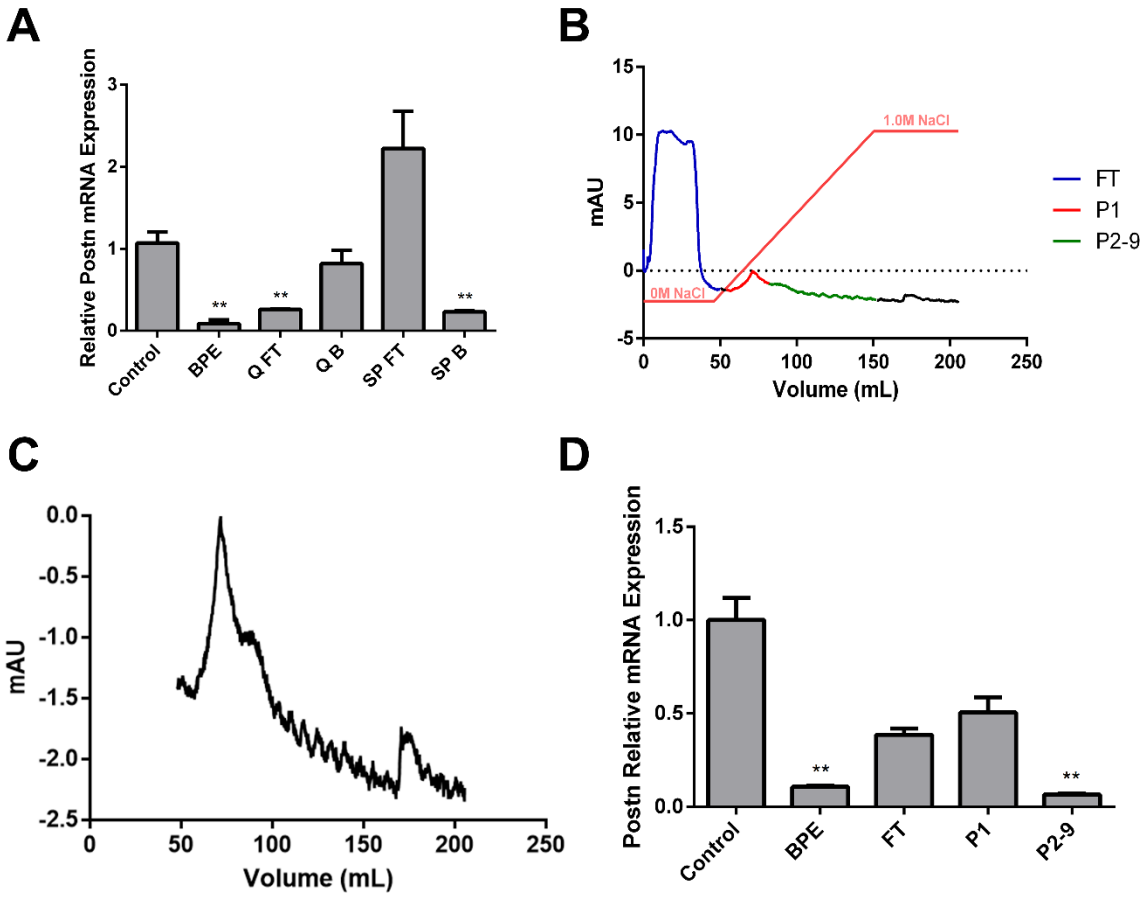

Figure 4.9: Ion exchange chromatography reveals repressive fractions.

(A) Fraction from peak 2 and 3 from the size exclusion chromatography were pooled and subjected to binding to Q and SP Sepharose. The fractions that bound are represented by a "B" while those that did not bind are represented by a "FT". These bound and unbound fractions were then used to treat NeuNDL cells and *Postn* mRNA was assessed by RT-PCR. Data are represented by mean ± SEM. N=3, ** = $P \leq 0.01$. **(B)** Absorption curve of P2-3 Q FT going through a column loaded with SP Sepharose. Salt gradient is shown in the pink curve from 0M to 1.0M NaCl. Colors were used to identify regions of interest such as flow through (FT), peak 1 (P1) and peaks 2-9 (P2-9). **(C)** Part of the graph in (B) is represented without the FT region (blue) to emphasize the peaks in P2-9. **(D)** Fraction corresponding to the 3 regions (FT, P1, P2-9) were used to treat NeuNDL cells and repressive ability was assessed by RT-PCR along with a control and BPE treatment to assess Postn repression. N = 3, ** = $P \leq 0.01$

the expression levels of both *Postn* mRNA (Figure 4.10 A) and protein (Figure 4.10 B). This suggests that P2-5 and P6-9 both contain independently important components that may synergize in the repression of *Postn* or that they both contain the same component but in concentration insufficient for an appropriate repression requiring the combination of all fractions to repress *Postn*. Taken together, these results show that the repressive activity is positively charged and mostly contained between 17-50 kDa.

4.6 Identifying potential repressive proteins by Mass Spectrometry

As we were unable to separate the fractions any further without losing the repressive effect on *Postn*, we used a mass spectrometry approach to identify the proteins present in the P2-9 repressive fractions, representing size exclusion chromatography P2-3 subjected to Sepharose ion exchange chromatography, resulting in the active peaks 2-9. This resulting extract has a significantly lower concentration of proteins than the original BPE which makes it an attractive sample to process for liquid-chromatography-mass spectrometry (LC-MS) and identify potential *Postn* repressive proteins.

Sample processing and mass spectrometry revealed 45 statistically significant proteins present in our fractionated extract. Out of those proteins, 12 were eliminated due to being uncharacterized and having no known associated genes, leaving a total 33 proteins with an associated gene. The results from the 33 proteins are summarized in Table 4.1. Although multiple proteins were identified following the mass spectrometry, none of these proteins seemed to have a relevant link to Postn. After reviewing the literature, we came to the same conclusion that no evident links to Postn were established. To further study the regulatory mechanisms of Postn in breast cancer epithelial cells, additional approaches were used to identify potential pathways involved in the regulation of Postn.

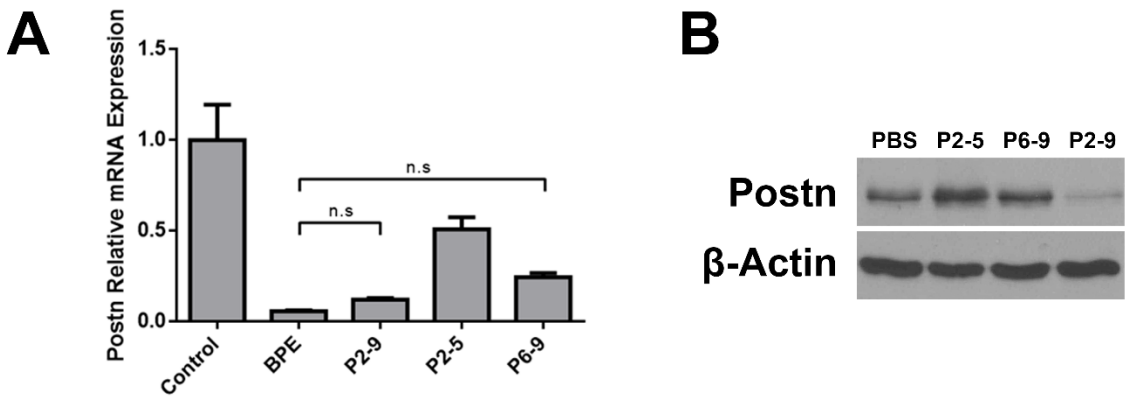

Figure 4.10: Smaller subset of P2-9 are unable to repress *Postn* expression.

(A) NeuNDL cells were treated with fractions containing peaks 2 to 9 (P2-9) as well as with fractions contained in peaks 2 to 5 and 6 to 9, P2-5 and P6-9, respectively. *Postn* relative mRNA expression was assessed by RT-PCR. Control and BPE treatment were used for comparison. Data are represented as mean ± SEM. N=3. **(B)** Western blotting analysis on NeuNDL cells treated with the same subsets of P2-9 (P2-5 and P6-9) to assess Postn protein expression.

Table 4.1 Validated protein identified in LC-MS.

Data is sorted by significance and confidence from the LC-MS PEP score. The Gene ID as well as the Gene name/description is shown.

Sum PEP Score	Gene ID	Description
53.38	ALB	Albumin
10.40	AHSG	Alpha-2-HS glycoprotein
7.32	KRT1	Keratin 1
6.83	SERPINA1	Serpin Family A Member 1
6.46	CHGA	Chromogranin-A
6.06	KRT5	Keratin 5
6.00	CGA	Glycoprotein hormone alpha subunit
4.88	CFB	Complement factor B
4.09	ORM1	Orosomucoid 1
3.85	POMC	Pro-opiomelanocortin
3.51	ITIH2	Inter-Alpha-Trypsin Inhibitor Heavy Chain 2
3.39	HBA1	Hemoglobin subunit alpha 1
3.39	TTR	Transthyretin
2.96	A1BG	Alpha-1B-glycoprotein
2.91	ITIH4	Inter-alpha-trypsin inhibitor heavy chain 4
2.49	SERPINF2	Serpin Family F Member 2
2.17	TF	Transferrin
2.14	KRT14	Keratin 14
1.84	KRT10	Keratin 10

1.56	RGS16	Regulator of G-protein signaling 16
1.56	H2AFX	H2A.X Variant Histone
1.55	MSN	Moesin
1.18	RPL19	Ribosomal Protein L19
1.13	ZC3H14	Zinc finger CCCH domain-containing protein 14
1.11	EEF1A2	Eukaryotic Translation Elongation factor 1-alpha 2
1.07	TXNL1	Thioredoxin Like 1
1.05	PDAP1	PDGFA Associated Protein 1
0.92	PPP2R5E	Protein Phosphatase 2 Regulatory Subunit B'Epsilon
0.78	PFN4	Profilin-4
0.72	CDR2L	Cerebellar Degeneration Related Protein 2 Like
0.68	ANXA2	Annexin A2
0.67	RPA2	Replication protein A2
0.67	TTLL5	Tubulin Tyrosine Ligase Like 5

4.7 BPE starvation triggers immune-like response and reduces mitotic processes

In parallel to the fractionation of BPE and LC-MS, we attempted to identify potential repressors of *Postn* expression following BPE treatment. We treated NeuNDL cells with either PBS or BPE in absence of MEGS and then performed RNA-sequencing to explore the expression pattern between the treatments and potentially identify an induced repressive activity.

The RNA sequencing revealed 1984 significantly upregulated genes (at least a 2-fold increase) and 6570 significantly downregulated genes (at least a 2-fold reduction) in the BPE treated cells when compared to PBS (*Postn* expressing) (Figure 4.11 A). Volcano plots showed that an impressive number of genes were significantly up- or downregulated following the treatments (Figure 4.11 B). Gene Ontology (GO) term enrichment analysis revealed an upregulation of genes involved in mitotic processes such as cell cycle, nuclear division, DNA metabolic processes, cell proliferation and development. Surprisingly, this was accompanied by a downregulation of immune response and viral infection genes such as innate immune response, herpes simplex infection, measles, influenza A, Human cytomegalovirus infection, human papillomavirus infection, human immunodeficiency virus 1 infection and phagosome (Figure 4.11 C). This supports the observation that cells growing in BPE are more proliferative due to the high levels of hormones and growth factors found in BPE. The downregulated GO terms suggests that cells that are BPE-starved and expressing *Postn* are behaving similarly to cells exposed to an inflammatory environment or viral infections. The full list of top scored GO terms is found in Figure 4.11.

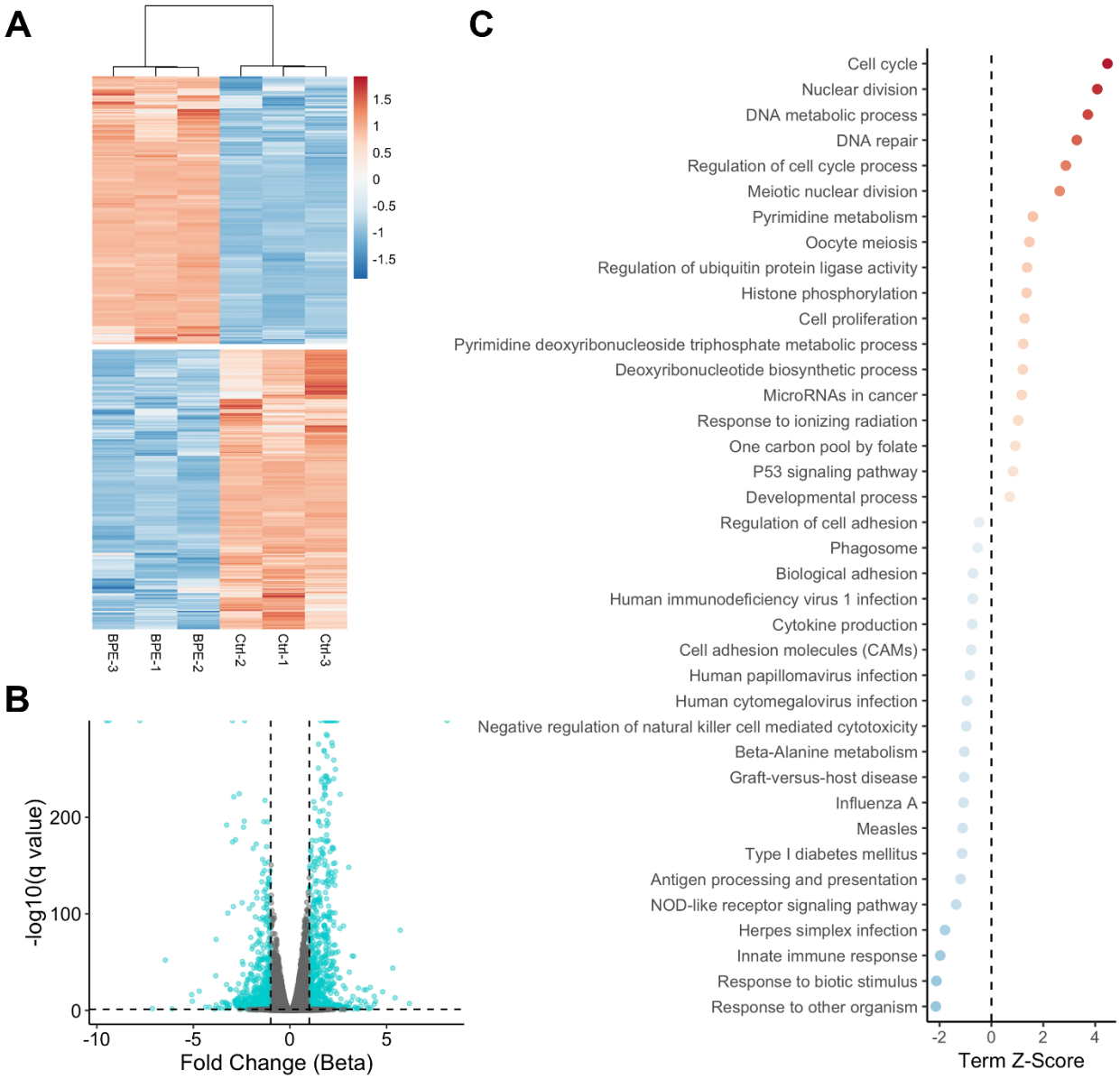

Figure 4.11 BPE starvation reduces proliferation and triggers immune-like responses. **(A)** RNA sequencing was performed on NeuNDL treated with either 0.4% BPE or PBS and the differentially expressed gene are shown in a heatmap. **(B)** A volcano plot showing fold change on the X axis and significance on the Y axis. The dots in blue represent genes that are significantly changed with a respectable fold change. While the grey dots represent either a low statistical significance or small fold change. **(C)** Heatmap of GO terms associated with differentially expressed genes. Term Z-score is computed based on the difference in term enrichment in upregulated and downregulated genes. Positive values correspond to terms associated with genes upregulated following BPE treatment.

4.8 Summary

Breast cancer cells have been shown to display deregulated signaling cascades that can have detrimental effects on cell functions. For example, metabolic deregulation can lead to increased proliferation and resistance to treatment [209] while cell cycle deregulation often promotes genomic instability which is directly correlated with increased mutation rates and heterogeneity [210].

Understanding how pro-tumorigenic genes are deregulated in cancer cells is critical to design new therapeutics and better treatments. We have shown that approximately 50% of breast cancer tumors, independent of the species and the subtype, acquire *Postn* expression in their epithelial compartments while the stromal compartment of all tumors shows *Postn* expression. To understand the regulation of *Postn* in the epithelial compartment of tumors we have established NeuNDL cancer cell lines from primary tumors to investigate the regulation of *Postn*. We found that the recommended growth medium contains components that repress *Postn* expression. The bovine pituitary extract (BPE) was identified as the major repressive activity for *Postn* expression.

Using commercial BPE and various chromatography methods, we attempted to fractionate BPE to identify the repressive components. The resulting repressive BPE fractions were then subjected to LC-MS to identify potential repressive proteins. The mass spectrometry results were unsuccessful at identifying direct modulator of Postn expression but revealed potential players. Concomitantly, we also performed RNA sequencing on cells grown in BPE -supplemented or -depleted medium to assess the differences in the cell state for both conditions. This revealed that cells growing in the presence of BPE showed an increase in

mitotic processes while cells grown in its absence resulted in an immune-like responses possibly related to virus infections, immune rejections, and autoimmune diseases.

Chapter 5

Postn gene expression in *Neu*-positive breast cancer cells is regulated by a FGFR signaling crosstalk with TGFβ/PI3K/AKT pathways

5.1 Introduction and Rationale

Several studies have implicated growth factors and hormones as regulators of *POSTN* expression [123]. *POSTN* has been shown to be implicated in a plethora of processes like EMT, ECM remodeling and development and multiple genes have been identified as potential regulators. Using the literature, the information found with the LC-MS following fractionation (Table 4.1) and RNA-sequencing data (Figure 4.11), we used a candidate molecule approach to identify critical signaling pathways involved in the regulation of *Postn*. Using a MEGS depletion assay on NeuNDL cells *in vitro*, we exposed the cultures to different pathway inhibitors and neutralizing antibodies and assessed *Postn* induction or repression.

Postn gene regulation has been extensively demonstrated to be context-dependent [124]. For example, the TGF-β-dependent EMT inducer Twist-1 and Snail have been correlated with *Postn* expression in lung and prostate cancer [162, 163] while growth factors and cytokines like bFGF, IL-4, IL-13, Oncostatin M, PDGF, and TNFα have all been shown to induce *POSTN* expression in various systems [126, 211-214]. This context-dependency led us to investigate the gene regulation mechanisms involved in *Postn* expression in ErbB2-mediated tumorigenesis.

5.2 Activation of TGFβ signaling leads to *Postn* induction *in vitro*

Postn upregulation during TGFβ-induced EMT has been extensively studied as a TGFβ-inducible gene in many cellular contexts [163, 215]. Therefore, we tested whether a treatment with TGFβ-1 would be sufficient to induce *Postn* expression in NeuNDL cells grown in MEGS. The induction of Postn was confirmed by western blot analysis following a 24-hour treatment with TGFβ-1 in MEGS supplemented medium (Figure 5.1 A). In a similar fashion, NeuNDL cells were unable to induce *Postn* expression following MEGS removal when a

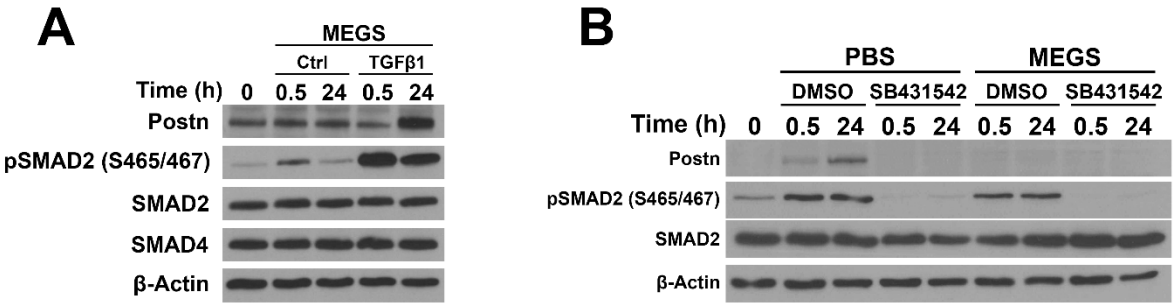

Figure 5.1 TGFβ signalling induces *Postn* expression in NeuNDL cells.

(A) NeuNDL cells were treated in the presence of MEGS with or without 10 ng/ml of TGFβ-1 for 0.5 and 24 hours. Phospho-SMAD2 antibody was used as a control for TGFβR activation. **(B)** NeuNDL cells were treated with 5µg/ml of TGFβR inhibitor SB431542 or DMSO control in either MEGS-deficient or MEGS-supplemented medium for 0.5 and 24 hours. Phospho-SMAD2 antibody was used as a control for TGFβR inhibition.

TGFβR inhibitor (SB431542) was added (Figure 5.1 B). This suggests that TGFβR signaling is essential for *Postn* induction in NeuNDL breast cancer cell lines and that overstimulation of this pathway can revert the MEGS/BPE repressive effects.

5.3 Activation of FGFR signaling by bFGF represses Postn expression *in vitro*

The FGFR signaling pathway is a highly complex system containing 23 signaling ligands and 4 receptors having a role in a wide range of cellular functions including migration, proliferation, and differentiation [216]. bFGF (FGF-2) has also been shown to induce *POSTN* in non-small-cell-lung cancer A549 cells [214]. Surprisingly, in contrast to A549 cells, we observed that bFGF treatment of NeuNDL cells following MEGS removal resulted in a complete repression of *Postn* expression (Figure 5.2 A). The addition of a pan-FGFR inhibitor (BGJ398) in combination with bFGF partially rescued the expression of *Postn* in NeuNDL cells (Figure 5.2 A).

To investigate whether bFGF could be one of the repressive components found in BPE and FBS, we pre-treated the BPE with a bFGF neutralizing antibody prior to treating NeuNDL cells. This revealed that neutralizing bFGF following MEGS removal (PBS treated) increased the levels of *Postn* significantly (Figure 5.2 B), suggesting that bFGF in the serum might also have a repressive effect. In addition, pre-treatment of the BPE with the neutralizing antibody lifted the repression on *Postn* expression (Figure 5.2 B), suggesting that neutralizing bFGF in the BPE also results in *Postn* induction in NeuNDL cells.

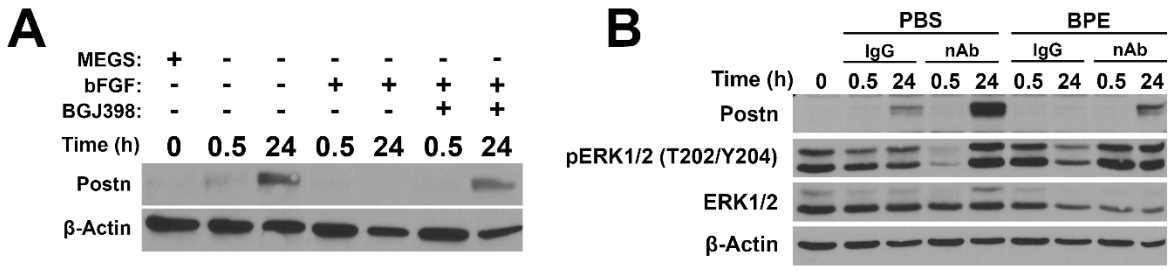

Figure 5.2: bFGF is a strong repressor of *Postn* expression.

(A) NeuNDL cells were treated in the absence of MEGS, with or without 10ng/ml of bFGF on its own or in combination with a FGFR pan-inhibitor BGJ398. Postn protein expression was assessed at 0.5- and 24-hours post-treatment. **(B)** MEGS-depleted (PBS) and BPE-supplemented media was pretreated with bFGF neutralizing antibody (nAb) or control IgG for 1 hour at 4°C. NeuNDL cells were then treated with anti-FGF pretreated media and Postn expression was assessed at 0.5 and 24 hours.

5.4 *Postn* regulation by bFGF and TGFβ is SMAD-independent and PKC-dependent

Both FGF and TGFβ signaling share extensive crosstalk to numerous signaling pathways. To gain further insights into the *Postn* repression and induction mechanisms, we attempted to identify the pathways through which both factors mediated their effects.

We then assessed whether the dependency on TGFβ signaling was due to canonical (SMAD-dependent) or non-canonical signaling (SMAD-independent). We tested SMAD activation by assessing nuclear import of SMAD2 following MEGS-removal. Immunofluorescence using an anti-SMAD2 antibody was performed following treatment with PBS (MEGS removal), bFGF and TGFβ and revealed that SMAD2 localization was unchanged after MEGS removal and bFGF treatment in NeuNDL cells (Figure 5.3). A control TGFβ-1 treatment was performed to assess a baseline activation of SMAD2 (Figure 5.3). These data suggest that *Postn* induction following MEGS removal does not involve canonical TGFβ signaling.

FGFR activation can also affect multiple intracellular signaling cascades. As bFGF represses *Postn* expression, we assessed the effect of phorbol 12-myristate 13-acetate (PMA), a strong activator of protein kinase C (PKC). The use of PMA was as efficient as bFGF in preventing *Postn* induction following MEGS-removal (Figure 5.4). Furthermore, the use of bFGF and PMA in combination has a synergistic effect on the repression of Postn rendering it completely undetectable by western blot analysis (Figure 5.4). This suggests that bFGF-mediated repression of *Postn* is at least in part due to the activation of PKC downstream of FGFRs.

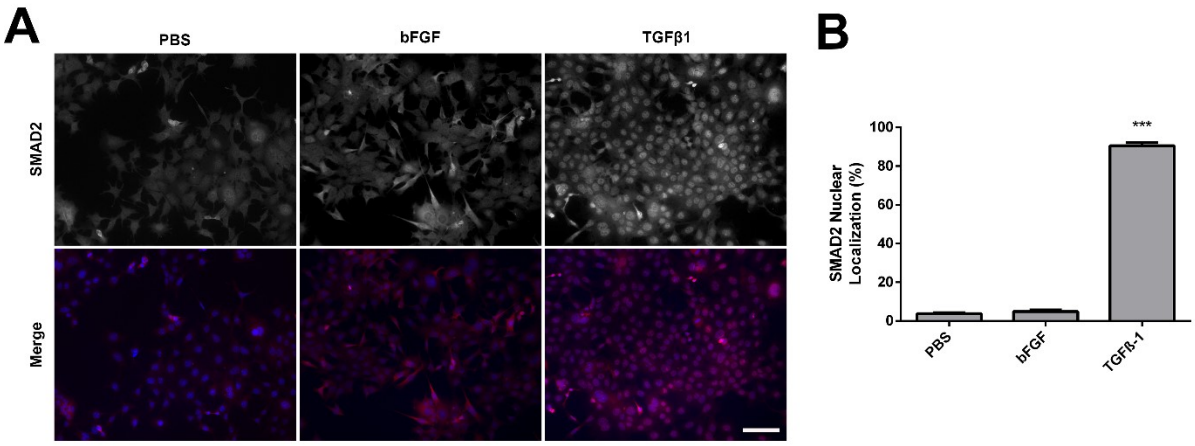

Figure 5.3: SMAD2 nuclear import is unaffected by *Postn* induction and repression.

(A) SMAD2 localization was assessed by immunofluorescence following a 24-hour treatment with PBS (MEGS-removal), 10ng/ml bFGF or 10ng/ml of TGFβ-1. Representative images are shown for SMAD2 as a single channel and merged with DAPI. TGFβ-1 treatment was used as a control for elevated SMAD2 nuclear import. Scale bar = 100µm **(B)** Manual counting of DAPI and SMAD2-positive nuclei for 10 representative images per group was performed to represent data as a percentage of nuclear SMAD2-positive cells. Data are represented as mean ± SEM.N = 3, *** = $P \leq 0.001$

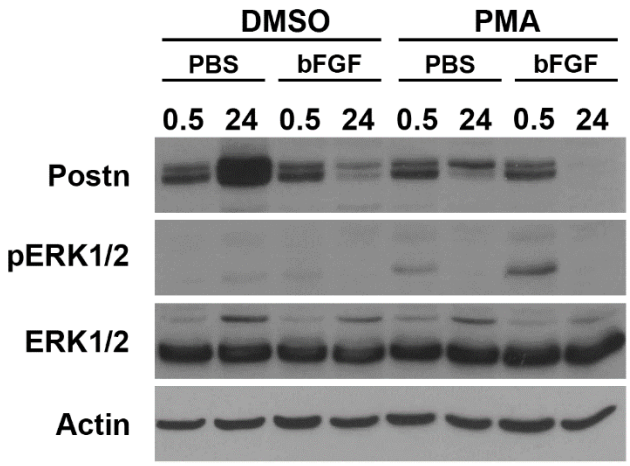

Figure 5.4: PKC activator represses *Postn* expression and enhances bFGF repression. NeuNDL cells were grown in the absence of MEGS, using 1µg/ml of PMA or DMSO, in combination with either PBS or 10ng/ml of bFGF. Postn expression was assessed by western blot at 0.5- and 24-hours post-treatment. Phosphor-ERK1/2 is used as a control for PKC activation by PMA.

5.5 PI3K/AKT is required for *Postn* induction following MEGS removal

The PI3K/AKT system has been shown to be activated downstream of TGFβ and is a main pathway activated by receptor tyrosine kinases, implicated in cell survival and proliferation [217]. Interestingly, *Postn* signaling has been shown to be PI3K/AKT-dependent in multiple development and disease models [206, 218, 219]. Therefore, we tested the potential involvement of PI3K/AKT in the regulation of *Postn* expression.

To test this, we used a panel of inhibitors specific to critical components of the signaling cascade. The use of a PI3K inhibitor, LY294004, revealed a complete blockade of *Postn* induction following MEGS-removal accompanied by a reduction in Phosho-Akt S473 (Figure 5.5 A). In a similar fashion, the use of a PDK1 inhibitor (PDK1 inhibitor II) resulted in the complete block of *Postn* induction (Figure 5.5 B). To further validate the requirement of this pathway in *Postn* induction, the pan-AKT inhibitor MK-2206 was tested. As for PI3K and PDK1 inhibition, MK-2206 also prevented the induction of *Postn* following MEGS removal from the growth medium (Figure 5.5 C).

These results suggest that inhibition of the PI3K/AKT pathway at multiple levels is sufficient to completely block the MEGS starvation-mediated *Postn* induction (Figure 5.5 D) Although kinase inhibitors are notorious to have off-target effects, the use of three different inhibitors strongly support a major role for the PI3K/AKT pathway for the induction of *Postn*.

5.6 FGFR activation by bFGF prevents TGFβ-mediated induction of *Postn*

Our results show that TGFβ treatment can induce *Postn* expression in the presence of MEGS and that inhibition of the TGFβR blocks *Postn* induction upon MEGS removal.

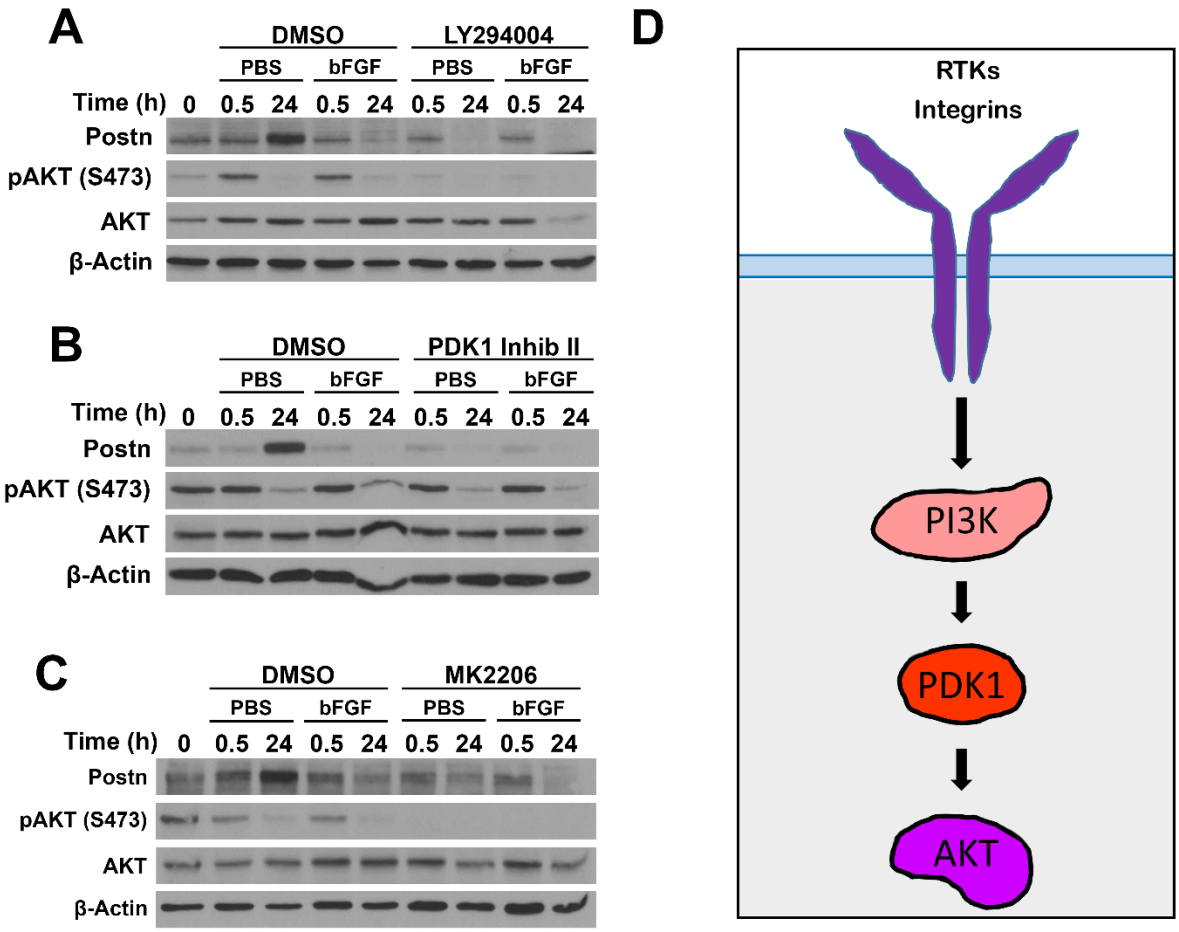

Figure 5.5: PI3K/AKT pathway is essential for the induction of *Postn*.

(A) NeuNDL cells were treated with 25 µM of PI3K inhibitor LY294004 or DMSO control in both PBS and bFGF (10ng/ml) supplemented medium in the absence of MEGS. Postn protein expression was assessed after 0.5 and 24 hours. Phospho-specific AKT (S473) was used as a control for inhibition of PI3K. **(B)** NeuNDL cells were treated with a PDK1 inhibitor at 10µM or DMSO control in in MEGS-depleted medium containing PBS or bFGF (10ng/ml). **(C)** NeuNDL cells were treated using 10µM of pan-AKT inhibitor MK-2206 or DMSO control in both PBS and bFGF (10 ng/ml) supplemented medium in absence of MEGS. Phospho-specific AKT (S473) was used as a control for the inhibition of AKT. **(D)** A simplified PI3K/AKT signaling pathway showing the order of PI3K, PDK1, and AKT as the central intracellular axis for activation of *Postn*. Receptor tyrosine kinases (RTKs) and integrins are shown as potential activator the PI3K/AKT intracellular pathway.

We next addressed whether bFGF treatment could suppress the effect of TGFβ on *Postn* induction. Therefore, a combination of bFGF and TGFβ was used in a MEGS-deficient environment and *Postn* expression was monitored. This revealed that bFGF was indeed capable of repressing *Postn* expression even in the presence of TGFβ-1 (Figure 5.6), suggesting that FGFR activation likely represses TGFβ downstream signaling either in part or completely.

To investigate the role of the PI3K/AKT pathway in the crosstalk between bFGF and TGFβ, we assessed the repressive effect of combinations of bFGF neutralizing antibodies with the pan-AKT inhibitor MK-2206. Our data show that, treatment with both bFGF neutralizing antibodies and MK2206 results in a repression of *Postn* (Figure 5.7), suggesting that the induction of Postn following bFGF neutralization cannot proceed when AKT activity is inhibited. Similarly, TGFβ-1 treatment in the presence of MK-2206 failed to induce *Postn* expression (Figure 5.8), further supporting the notion that TGFβ-mediated induction of *Postn* is dependent on AKT activity.

Together, these results suggest that the PI3K/AKT signaling pathway is a potential link between the TGFβ and FGFR signaling. Furthermore, activation of FGFR may result in an inhibitory crosstalk to PI3K/AKT downstream of TGFβ. Evidence of crosstalk between PKC and PI3K has been shown where PKCα is a strong inactivator of AKT signaling even in instances of hyperactive PI3K/AKT in endometrial cancer [220, 221]. This suggests that some PKC isoforms are negatively regulating the PI3K/AKT pathway potentially directly in the context of cancer.

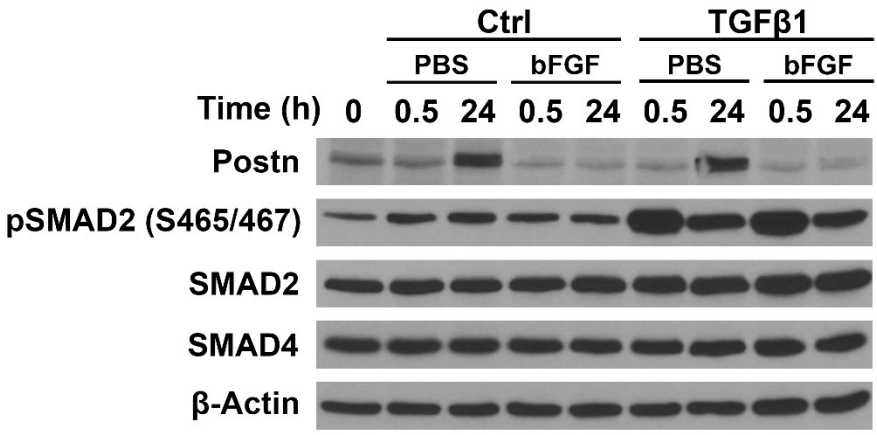

Figure 5.6: TGFβ-mediated induction of *Postn* is abrogated by bFGF supplementation. NeuNDL cells were treated in the absence of MEGS, with 10ng/ml of TGFβ-1 in combination with 10ng/ml of bFGF or their respective controls. Postn protein expression was assessed 0.5- and 24-hours post treatment by western blotting analysis. Phospho-specific SMAD2 antibody is shown as a control for the activation of TGFβRs.

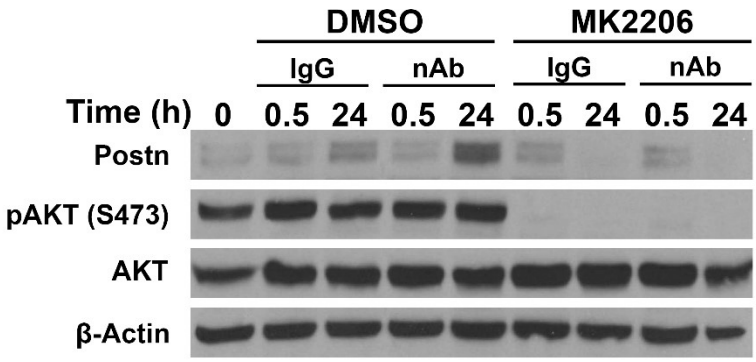

Figure 5.7: AKT inhibition following bFGF neutralization prevents *Postn* induction. NeuNDL cells were treated with either 10μM of a pan-AKT inhibitor, MK2206 or DMSO control in medium pre-treated with either non targeting IgG or bFGF neutralizing antibodies (nAb). Postn protein expression was assessed 0.5- and 24-hour post-treatment for each condition. Phospho-specific AKT (S473) was used as a readout the inhibition AKT by MK2206.

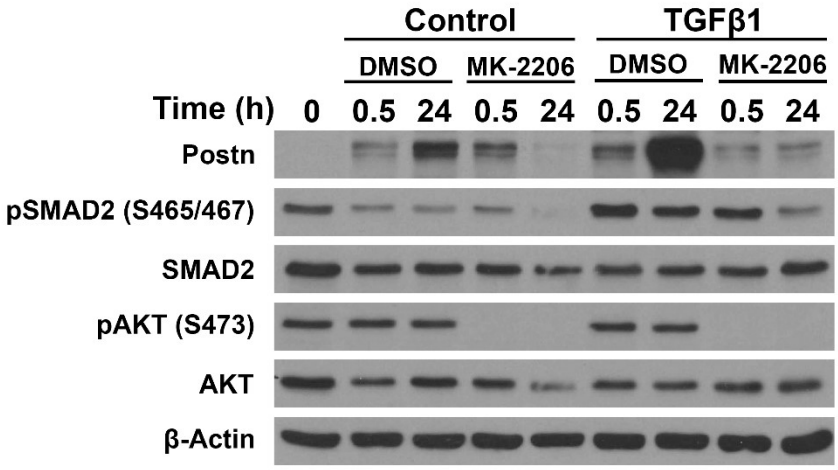

Figure 5.8: AKT inhibition prevents TGFβ-mediated induction of *Postn*.

NeuNDL cells were treated with or without 10ng/ml of TGFβ-1 in combination with either 10μM pan-AKT inhibitor MK2206 or DMSO control. Phospho-specific SMAD2 and AKT levels were used as control for TGFβR activation and AKT inhibition, respectively.

Together, these results suggest that the PI3K/AKT signaling pathway is a potential link between the TGFβ and FGFR signaling. It appears that PI3K/AKT is a common downstream target of both pathways in the context of *Postn* regulation.

5.7 Summary

A number of signaling pathways have been identified as critical for breast cancer progression. These systems contain countless crosstalk between each other, often sharing similar effectors or inducing the same target genes. These highly regulated and complex networks have been highlighted in a multitude of studies, uncovering new cross-talks and novel regulators.

Here, we reveal a major crosstalk between two extensively studied pathways that converge to regulate *Postn* expression in our model of HER2-postivive breast cancer. Firstly, the TGFβ pathway which promotes *Postn* expression through activation of the TGFβRs, acting in a non-canonical manner (SMAD-independent). The second one is the FGFR signaling pathway, which leads to a repression of *Postn* expression in a PKC-dependent manner. The last pathway identified is the PI3K/AKT for which the activity was found to be essential for the induction of *Postn* expression. Interestingly, FGFR activation was able to prevent TGFβ-mediated induction of *Postn*. Importantly, the PI3K/AKT pathway is critical as its inhibition blocked the *Postn* induction upon FGF removal or TGFβ treatment.

Taken together, these data suggest that *Postn* expression is induced through a TGFβ/PI3K/AKT axis while activation of FGFR by bFGF can repress this induction. It is still unclear where along the TGFβ/PI3K/AKT pathway this negative regulation occurs.

Chapter 6

General Discussion

6.1 Summary of Findings

HER2-positive breast cancer is a heterogeneous disease that represents 20-30% of all human breast cancers and is usually characterized by genetic alterations leading to overexpression and amplification of HER2 [64]. Tumors that are classified as HER2-positive are generally more aggressive, leading to a highly metastatic disease and a poor prognosis in patients [64]. Even though targeted therapies exist against HER2, a high proportion of patients develop resistance and relapses over time and such treatment are deemed unsuccessful [222]. Metastatic breast cancer also remains generally incurable regardless of the subtype. Identifying pathways regulating tumor-promoting phenotypes is required to develop novel therapeutics and increase the drug arsenal available to treat such tumors. In this study we investigated the effect of *Postn* deletion on *Neu*-driven mammary tumorigenesis as well as the regulation mechanisms involved in controlling *Postn* expression in epithelial breast cancer cells.

We have shown that *Postn* deletion delays tumor onset and overall survival accompanied with a decrease in proliferation and apoptosis in *Neu*-driven tumors. We have also shown a reduction in collagen deposition in the resulting *Postn*-deficient tumors. Furthermore, we have uncovered a novel *Postn* regulation mechanism in epithelial breast cancer cells involving a signaling interplay between *FGFR* and the *TGFβ/PI3K/AKT* signaling pathways. Herein, we discuss the relevance and implications of these findings and propose future directions to further assess the role of *Postn* in breast oncopathologies.

6.2 *Postn*-deletion delays *Neu*-driven tumor onset and survival

Tumor growth and progression are incredibly complex processes which include multiple deregulation steps and interplay between various pathways to promote tumor growth. Cancer cells can undergo continuous proliferative signaling using multiple mechanisms such

as the production of growth factors as well as their specific receptors, leading to autocrine loop stimulation. They can also produce signals for normal cells within the stroma to induce responses that are conducive to cancer cell growth and survival [223, 224]. Alternatively, deregulation of receptor signaling by increasing the number of surface receptors as well as mutations leading to activation in the absence of ligands can also increase proliferation signaling pathways [225].

POSTN expression in cancer has been extensively studied in term of its pattern of expression and clinical outcome. However, very few studies investigated its role directly in tumor progression. *Postn* has been shown to be essential for cancer stem cell maintenance and metastasis in a murine breast cancer model (MMTV-PyMT) [143]. Here, we demonstrate that *Postn*-deletion results in a delay in tumor initiation and survival (Figure 3.2). Furthermore, we also have shown a decrease in the proportion of proliferation and apoptosis markers in *Postn*-deficient tumors (Figure 3.3). We speculate that *Postn* remodeling of the ECM and its implication in integrin signaling could explain such a change in tumor progression and marker expression patterns for proliferation and apoptosis.

Additionally, changes in the ECM can completely modify the environment in which the tumor is growing. The balance between ECM degradation and remodeling is an essential aspect of homeostasis and disease development. POSTN has been shown to induce matrix metalloproteinases (MMPs) levels, more specifically MMP-2 and MMP-9 [226, 227]. This family of proteins is responsible for ECM degradation. One possibility is that that a deregulation of the ECM degradation could result in an aberrant composition which could promote a proliferative environment. Although their clinical relevance in breast cancer is controversial, MMPs have been shown to be implicated in multiple pro-carcinogenic processes

such as cell proliferation, angiogenesis, cancer progression and metastasis [228]. Therefore, the lack of *Postn* in tumors would reduce the levels of those MMPs and potentially reduce proliferation rate and tumor initiation.

Another possible explanation for these changes in tumor dynamics might be due to the ability for POSTN to bind and activate integrin signaling [219]. More specifically Postn has been shown to bind to integrin $\alpha_V\beta_1$, $\alpha_V\beta_3$ $\alpha_V\beta_5$, $\alpha_6\beta_4$ and $\alpha_M\beta_2$ and activate the receptor and induce signal transduction [229]. These specific integrins, when activated by *Postn* can in turn activate signaling pathways such as FAK, PI3K, AKT, ERK, NF-κB and STAT3 (reviewed in [229]). All these pathways are involved in multiple processes of tumor initiation, progression, therapy-resistance, and metastasis. It is tempting to speculate that if a subset of these pathways are activated by *Postn* in our model, tumor onset and progression would be significantly delayed by the deletion of *Postn*. For example, *Postn*, through integrin signaling can activate PI3K, AKT and/or ERK, which are all survival and growth pathways. *Postn* deletion could explain the decrease in proliferation markers observed in our tumor study. Integrin $\alpha_V\beta_5$-mediated activation of TNFα has been shown to induce apoptosis in multiple tumor cell lines [230]. This induction of apoptosis by TNFα usually requires that specific anti-apoptosis pathways are blocked or inactivated, such as NF-κB [230]. It is possible that TNFα is downregulated in *Postn* (-/-): NeuNDL tumors leading to a reduction of apoptosis marked by a reduction in PARP cleavage.

The reduction in apoptosis markers observed in *Postn* (-/-) endpoint tumor would suggest that *Postn* is critical for oncogene-induced apoptosis. In a few cancer models, *Postn* has been shown to induce apoptosis and inhibit cell growth. For example, a study used a *Postn* (-/-) mouse model along with an inflammation-related colon carcinogenesis model to show

that *Postn* promoted apoptosis and growth inhibition [231]. Furthermore, using *Postn* (-/-) CAFs conditioned medium, they showed that growth rate was increased in the *Postn*-deficient medium when compared to its control [231]. A similar observation was shown in Dupuytren's disease regarding *Postn*-related induction of apoptosis [232]. In contrast, multiple other studies showed an opposite role for *Postn* during apoptosis in colorectal cancer cells. Recombinant and fibroblastic *Postn* was shown to promote proliferation of colorectal cancer cells and *Postn* overexpression was also found to be a poor prognostic indicator in colorectal cancer [145, 233]. These opposing roles for *Postn* in cell growth and apoptosis indicate a highly context dependent function for *Postn*. This can be explained by the difference in integrin expression patterns between cell types, suggesting that the biological effect of *Postn* can be modulated by the complement of integrins at the cell surface. Another possibility to explain the dual implications of *Postn* is the fact that specific variants can promote different pathways. For example, if a specific variant is preferentially expressed in a particular context, it can potentially promote cell growth or apoptosis.

6.3 *Postn*-deletion alters *Neu*-driven breast cancer collagen deposition

Another striking difference in our animal tumor model is the observation that collagen deposition was significantly reduced in *Postn* (-/-):NeuNDL tumors (Figure 3.6). This change in collagen could alter the entire ECM landscape and have major effects on the behaviour of the tumors. Multiple studies have implicated ECM composition and more specifically collagen deposition in the development, progression, and metastasis of breast cancers. Dense breast tissues, evaluated by mammography, is one of the greatest independent risk factors in breast cancer [234, 235]. Furthermore, higher breast density areas are associated with an increase in

fibrillar collagen deposition [236, 237], which has been shown to promote tumor formation and progression in a murine model of mammary carcinogenesis [238].

Although these observations were made decades ago, the molecular mechanisms responsible for tumor promotion and progression in dense tissue are still unclear. Collagen deposition has also been shown to contribute to overall ECM stiffness which in turn also promotes cancer progression and resistance to chemotherapy [239].

ECM stiffness, also known as ECM rigidity, ECM tension and interstitial hypertension, has been correlated with tumor growth and increased rate of metastasis along with poor clinical outcome [240, 241]. LOX, the enzyme responsible for collagen cross-linking, is often upregulated in cancers, which correlates with a stiffer matrix and cancer malignancy by enhancing integrin signaling [242]. The increase in cancer incidence due to aging is explained partly by the fact that tissues in older population are generally stiffer and contain a higher level of aberrant collagen cross-linking [242].

A pivotal study investigated the effects of *Postn* deletion in the MMTV-PyMT model of breast cancer using *Postn* (-/-) mice; more specifically they studied its effect on metastasis [143]. The major conclusion was that infiltrating tumor cells must induce stromal *Postn* expression at the secondary site (lungs) to initiate colonization. In addition, the authors claim that POSTN is essential for the maintenance of cancer stem cells and that blocking POSTN functions prevents metastasis altogether. It was suggested that infiltrating tumor cells need to educate stromal cells at distant sites for them to start producing POSTN, subsequently establishing a metastatic niche. That study also showed that POSTN could recruit Wnt ligands and induce signaling in CSCs. In stark contrast, we have observed that *Postn* deletion does not

affect lung colonization in *Postn*-deficient tumor bearing animals (Figure 3.7) or the sphere forming potential of tumor cells in culture.

Multiple studies have shown similarities between the PyMT and NeuNDL breast cancer models [243]. The main difference between PyMT and NeuNDL is the accelerated tumor onset and increased rate of metastasis in the PyMT model [79, 244]. It is possible that the PyMT model increased metastasis rate depends on *Postn* due to potential differences in downstream targets and modulators. This would suggest that some important ECM differences exist between the PyMT and NeuNDL model. Such a change in ECM composition and stiffness can lead to an increase in Wnt expression through integrin signaling [245]. Another possibility is that, due to the long latency of the NeuNDL model, cellular mechanisms can be activated to compensate for the absence of *Postn*. More in-depth side by side studies will have to be conducted to address these discrepancies.

6.4 *Postn* is acquired in a subset of breast cancer epithelial compartments

We have shown that *Postn* expression can be acquired in the epithelial compartment of mammary breast tumors in our *in vitro* models (Figure 4.1). Multiple studies have also shown POSTN expression in human and murine mammary cancer cells [208, 246]. *Postn* expression has also been shown to be elevated in high-grade tumors and correlated with the histological grade [247]. As histological grades are an indication of tumor differentiation, it is possible that less differentiated tumors acquire *POSTN*. Another possibility is that *POSTN* is induced through an unrelated mechanism and its expression drives cells to dedifferentiate.

Interestingly, EMT also correlates significantly with the histological grade of tumors. As *Postn* as been shown to promote EMT in multiple cancer types [163, 248], it is also possible that elevated levels of *Postn* induces EMT events that are in turn responsible for a more

migratory and invasive disease resulting in an elevated histological grade. The opposite is also possible, whereby *Postn* is induced as a result of cells undergoing EMT.

Our analysis of *Postn* re-expression in deficient breast cancer cells revealed no consistent or significant differences in their ability to proliferate, migrate, invade, and grow in 3D spheroids (Figure 3.9, 3.10, 3.11, 3.12). Although the acquired expression of *Postn* is associated with an aggressive phenotype in tumor progression and metastasis, the expression of *Postn* in cultured cells did not affect their invasive properties *in vitro* and subcutaneously. It is likely that the *Postn* effects are dependent on a complex ECM network to modulate that invasive behaviour.

Recently, studies have investigated the involvement *Postn* in the development and maintenance of cancer stem-like cells. Although controversial, some studies debate that the origin of breast tumors arise from cells that acquired self-renewal capabilities and intrinsic resistance to therapy designated cancer stem cells (CSCs) [249]. Furthermore CSCs, characterized by $CD44^{+}/CD24^{-}$ and aldehyde dehydrogenase-1 (ALDH1) have been shown to promote cancer initiation, angiogenesis, and metastasis in breast cancer [250]. It has been demonstrated that POSTN contributes to the acquisition of stem-like features in breast cancer [251]. Therefore, one possibility is that the loss of *Postn* results in a reduction of CSCs, leading to decreased proliferation and delayed onset.

6.5 Regulation of Epithelial *Postn* expression in vitro

In this study, we have shown that a Bovine Pituitary Extract is a potent repressor of *Postn* expression in *Neu*-driven mammary cancer cells (Figure 4.6 B&D). The use of bovine pituitary extract as a hormone-rich growth-promoting supplement dates back to 1934 when a group used it as a growth supplement *in vivo* to study its effect on albino rat early growth

[252]. Later, it was common to use embryonic and brain extract to promote the proliferation of chicken periosteal fibroblasts [253]. The fact that this highly mitogenic extract can completely repress *Postn* expression is not overly surprising. Epithelial cancer cells growing in the presence of this extract are more likely to remain in a proliferative state and display a classical epithelial gene expression pattern. It is likely that BPE depletion in those cultures induce an adaptation response. This could be compared to cells going through a crisis when lacking nutrients. This is apparent when comparing the two conditions using RNA-Sequencing analyses (Figure 4.11).

Indeed, response to biotic stimulus, virus infections and immune related terms are markedly down regulated in BPE-treated samples (Figure 4.11 C), suggesting that they are highly expressed in BPE-lacking conditions. In a similar fashion, terms related to proliferation are upregulated in BPE-treated cells. These data suggest that the cells are in a highly proliferative state when subjected to BPE, while cells lacking BPE are not proliferative and are perhaps trying to recruit the immune system, mimicking a response to virus infections. The upregulation of *Postn* could either cause this response or be as a result of that same response. The causality relationship between *Postn* and this response is yet to be established.

We have shown that neutralizing bFGF from BPE by using an antibody is sufficient to lift the BPE-mediated repression on *Postn* expression in breast cancer cells (Figure 5.2 B). Interestingly, a study showed that a protein-based "Fibroblast Growth Factor" activity was first identified in an extract from bovine pituitary glands [254]. This specific "activity" was found to be thermolabile and protease sensitive, and was able to promote the proliferation of 3T3 fibroblast at low concentrations [255]. The activity was then purified and would later be referred to as basic FGF (bFGF or FGF2) due to mostly a basic overall composition of amino

acids and its high isoelectric molecular point [256]. This strongly supports our observations that both BPE and bFGF have a similar repressive effect on *Postn* expression.

6.6 Epithelial *Postn* is induced by TGFβ signaling

In this study, we show that TGFβ1 is sufficient to induce *Postn* expression in MEGS-supplemented medium and that TGFβR inhibitor prevents *Postn* induction following the removal of MEGS (Figure 5.1 A&B). TGFβ is an interesting pathway since it has a dual role in breast cancer, both promoting and preventing tumor progression. In the context of transformation, TGFβ signaling has been shown to promote EMT which facilitates migration and metastasis of cancer cells [257]. However, TGFβ has also been shown to have tumor suppressor activity by promoting cell cycle arrest and apoptosis [258]. To this day, it is still unclear how this switch from tumor suppressor to promoter of metastasis occurs.[259]

TGFβ is a well-established inducer of POSTN expression in multiple models and processes such as EMT, invasion and metastasis [128, 163]. We have also shown that *Postn* induction following BPE removal from the culture medium did not affect the localization of SMAD2 to the nucleus (Figure 5.3), indicating that the effect of TGFβ is not dependent on SMAD signaling and potentially involves non-canonical features of TGFβ signaling. There seems to be some context dependency in the mechanism of action by which TGFβ signaling can induce *POSTN* expression. In contrast to our findings, other studies have shown that SMAD2/3-dependent TGFβ signaling could induce *POSTN* expression [260-262].

Interestingly, Fetuin-A, also known as Alpha-2-HS glycoprotein (AHSG), has been identified as one of the top hits in our mass spectrometry analysis (Table 4.1). This specific gene has been identified as a TGFβ antagonist by preventing TGFβ1 from binding to its cell surface receptors, suppressing signal transduction and subsequently EMT in intestinal tumors

[263]. This could explain how BPE is repressing *Postn* expression in our *in vitro* expression model (Figure 4.6 B&C). Fetuin-A that is present in the BPE could potentially block TGFβ in a manner that is like a TGFβR inhibitor (Figure 5.1 B) and subsequently prevent *Postn* expression that is dependent on an active TGFβ signaling pathway.

6.7 Epithelial *Postn* repression by FGFR signaling

Our data show that bFGF treatment of the cultures with neutralizing antibodies targeting bFGF can promote *Postn* expression, validating the repressive effect of bFGF (Figure 5.2). Surprisingly, bFGF downregulation has been identified as a marker of poor prognosis in breast cancer using data to assess differentially expressed and aberrantly methylated genes with a novel bioinformatic approach [264].

An interesting relationship between bFGF and *POSTN* is the fact that germline and conditional loss-of-function for both genes revealed some phenotypic overlap. *FGF2*-null and *Postn*-null animals exerted muscle and skeletal development issues [190, 265, 266]. Likewise, conditional deletion of bFGF resulted in decreased cardiac hypertrophy induced by ischemic injury, delayed wound healing, and increased bone mineralization while *Postn* has been linked to cardiac issues, wound healing, and bone regeneration [267-271]. This overlap in processes suggest that their expression could be modulated by similar factors.

Furthermore, Fetuin-A, a protein found in our mass spectrometry analysis following fractionation of BPE, has been shown to cause a significant increase in mRNA levels of multiple angiogenic and proinflammatory proteins, including bFGF [272]. This could also be a possible explanation for the repressive effects of BPE and active fractions following

chromatography. Fetuin-A could increase the production of bFGF by cancer cells, activate FGFR signaling and *Postn* repression in an autocrine loop.

Another interesting observation is the fact that bFGF has an isometric point of 9.6, meaning a positive charge at physiological conditions and a molecular weight between 17 and 23 kDa. These characteristics strongly suggest that bFGF could be in the fraction analyzed by mass spectrometry since the molecular size range and isoelectric point matched the eluted fraction characteristics. As our final fractions were extremely dilute, it is possible that the detection threshold did not identify bFGF.

6.8 AKT activity is required for *Postn* induction in epithelial breast cancer cells

The PI3K/AKT pathway has been extensively studied in a panoply of cancers. Alterations of this pathway is common and it is estimated that up to 60% of tumors have an hyperactivation of this system [273]. The catalytic domain of PI3K, coded by the PIK3CA gene, is commonly mutated or amplified in breast cancer and therapeutic inhibition of this pathway has shown some promising results in some types of breast cancers [274, 275]. We have shown that inhibition of the PI3K/AKT pathway, using three different inhibitors, completely blocked *Postn* induction following the removal of BPE (Figure 5.5).

Studies have shown that *Postn* activity is often modulated through the PI3K/AKT signaling pathway, whether it is to facilitate EMT or invasion [219, 276]. Although we have shown that *Postn* induction requires AKT signaling, it is still unclear which downstream target is responsible for this repression/induction mechanism. AKT can activate and deactivate a wide range of substrate to modulate different processes such as mTOR, FOXOs, GSK3b and several others (reviewed in [277]). The critical DNA elements or active chromatin regions that drive *Postn* expression in this context remain to be identified. This would pave the way for the

identification of specific transcriptional regulators implicated in the control of *Postn* expression.

6.9 Signaling interplay modulating *Postn* expression in breast cancer cells

Our results show that the regulation of *Postn* is quite complex, involving multiple signaling pathways. The control of its expression is showcased by a modulation of the FGFR, TGFβ and PI3K/AKT pathways. Our data show that the removal of bFGF from the culture medium is sufficient to induce *Postn* gene expression. This specific induction of *Postn* is however dependent on the activity of TGFβ/PI3K/AKT signaling. Furthermore, *Postn* upregulation through activation of this signaling axis appears to be SMAD-independent. In addition, the repression through activation of FGFR appears to be PKC-dependent.

These individual pathways have been extensively studied as modulators of breast cancer progression. Interestingly, our data show that expression of *Postn* appears to proceed through a TGFβ/AKT pathway in this context. Along with the loss of bFGF expression, activation of the TGFβ/AKT axis could lead to *Postn* induction in tumor cells, contributing to an increase in invasion and subsequently, worse outcomes [264].

Interesting crosstalk between the aforementioned pathways have been identified in different disease and cancer models. TGFβ signaling has been shown to crosstalk to the PI3K/AKT [217, 278]. More specifically, binding and activation of p85, the regulatory subunit of PI3K, by TGFβRI and TGFβRII has been demonstrated in mammary epithelial cells [279]. Whether this is the mechanism responsible for *Postn* modulation in MEGS-depleted cells remains to be investigated. PI3K/AKT signaling has been shown to directly interact with SMAD3 to antagonize TGFβ-induced growth arrest and apoptosis [280, 281]. Furthermore, it

has been proposed that PI3K/AKT activation leads to TGFβ-dependent pro-oncogenic responses in breast cancer [282].

Contrary to our observations, a study using A549 cells, a non-small-cell lung cancer cell line, showed that bFGF induced *Postn* expression in a PI3K/AKT-dependent manner [214]. It is more than likely that *Postn* expression is subject to tissue- as well as tumor-specific regulation. However, it is interesting to note that *Postn* induction proceeds through PI3K/AKT signaling pathway in both cancer models.

Although we have shown that the PI3K/AKT pathway modulates *Postn* expression downstream of both FGFR and TGFβ, it is not clear what the AKT effectors are. We have shown that blocking the PI3K/AKT or TGFβ pathway leads to a complete repression of *Postn*, while bFGF is also repressing its expression. Our data suggest that a PKC-dependent FGFR signaling is repressing the PI3K/AKT pathway. One possibility is that FGFR activation prevents TGFβR from signaling to PI3K. Alternatively, the bFGF signal could prevent AKT from signaling to its downstream effector or components of the transcriptional complex. FGFR signaling could also be competing with the TGFβ/PI3K/AKT axis. This could imply that FGFR signaling promotes a proliferative state while the TGFβ/PI3K/AKT axis could promote a more mesenchymal and invasive state through the induction of *Postn* expression. Supporting this, TGFβ signaling has been shown to promote EMT through PI3K activation [283]. Furthermore, PKCα can suppress AKT activity through a Protein Phosphatase 2A (PP2A)-dependent mechanism [220]. Given the number of PKC isoforms and targets, it is possible that some PKC substrates are acting through this TGFβ/PI3K/AKT axis (reviewed in [284]). For instance, the SKI protein, a potential PKC substrate, is a negative regulator of TGFβ acting

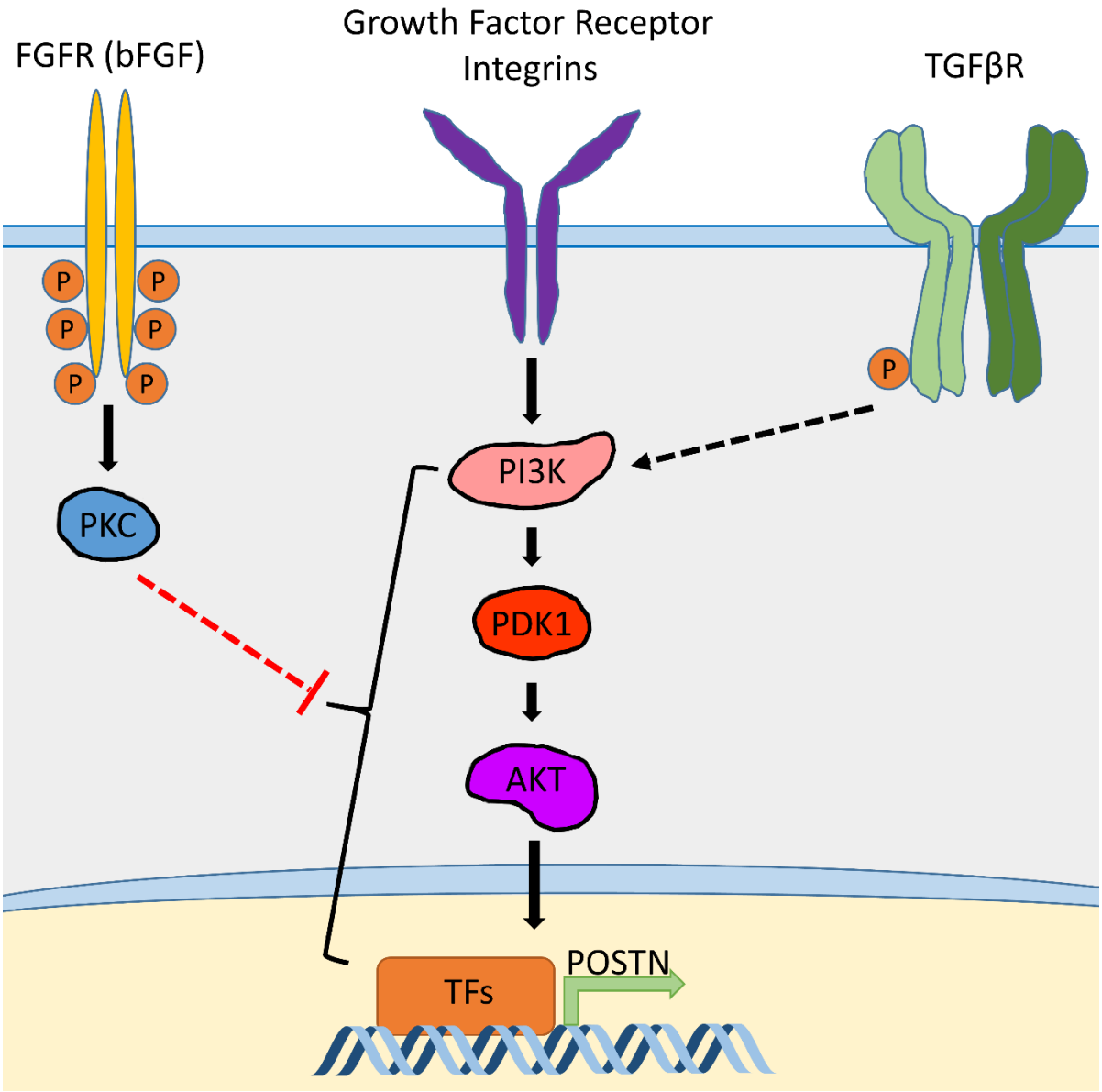

Figure 6.1 Schematic representation of *Postn* expression control.

Summary model showcasing PI3K/AKT as the central modulator of *Postn* expression. FGFR signaling can repress *Postn* expression by acting somewhere in the PI3K/AKT pathway to prevent expression of *Postn*. TGFβ signaling is shown to activate PI3K to promote activation of this pathway, and eventually the expression of *Postn*.

through the SMAD family [285]. A brief summary of *Postn* gene expression modulation is shown in Figure 6.1.

6.10 Perspectives and Considerations

Genetic variation in patients influences susceptibility, progression, and response to therapy. In addition, genetic variability, other genes as well as the environment can influence the disease penetrance and progression. It becomes challenging to evaluate the contribution of a specific gene to breast cancer because of the high genetic variability found in the population.

A way to study the contribution of a specific gene in breast cancer is to use inbred murine strains in controlled environments to obtain uniform tumor histology and decrease the complexity of genetic backgrounds [188]. This can be accomplished by using knockout models from identical backgrounds except for a specific locus where a gene mutation or deletion has been introduced. This uniformity in their genetic background permits the investigation of a genetic deletion in virtually identical mice.

The use of such models also comes with disadvantages when comparing results from genetically identical murine models back to the human population. Extrapolation will provide a potentially limited correlation due to the exclusion of genetic variation. It is also possible to use outbred murine strain to study the effect of genetic variation on transgene expression and phenotypes observed. Interestingly, not all inbred mouse strains respond the same to transgene expression. The C57BL/6 genetic background was shown to be resistant to MMTV infections and tumorigenesis using the MMTV promoter was found to increase tumor latency significantly [84]. These specific observations led to the universal use of inbred FVB/N genetic backgrounds due to its high propensity to develop breast cancer.

It is then important to understand those limitations in terms of murine models of breast cancer before conclusions can be drawn from the results. In this study, we have used inbred FVB/N mice to evaluate the effect of *Postn* on *Neu*-driven mammary tumors.

6.11 Future Studies

Our understanding of the role of *Postn* in breast cancer is constantly evolving. This study, in addition to resolving important research questions, also unravels multiple open-ended issues and potential future directions. Using ATAC-seq (Assay for Transposase-Accessible Chromatin-Sequencing), it would be interesting to assess the differences in accessible or open chromatin between breast cancer cells grown in MEGS-supplemented medium to determine key regulatory factors that could be involved in the regulation of *Postn*. This could also be done on *Postn*-deficient cells in which *Postn* was re-introduced to see the effect of *Postn* expression on the availability of chromatin which could identify new signaling targets and functions for *Postn* in breast cancer.

Another interesting avenue that has been briefly mentioned previously is the analysis of breast CSCs. This assessment is made by evaluating surface markers. Evaluating the percentage of $CD44^{+}/CD24^{-}$ by flow cytometry in our *Postn* (-/-):NeuNDL would be a starting point to investigate the role of *Postn* in the establishment, maintenance, or self-renewal of breast cancer stem cells.

An intriguing question which is quite technically challenging would be to assess whether *Postn* (+/+):NeuNDL cells are able to invade and colonize distant sites in a *Postn* (-/-) environment. The difficult problem with this is the fact that *Postn* (-/-) animals would most likely reject cells expressing *Postn*. In recent years, multiple novel ways to induce immune tolerance to specific genes has been made available. For example, through a DNA vaccine, we

can train the murine immune system to accept foreign vectors and their encoded protein. A similar approach can most likely be optimized to build tolerance in *Postn* (-/-):NeuNDL animals and then injecting tumor cells orthotopically and assess metastasis.

The use of *Postn* conditional knockout or drug-inducible systems would greatly help eliminate early embryonic compensation effects, often seen with global knockout animals [286]. The use of such models gives a much better control over when and where your gene is deleted or expressed. The use of such animals would have been greatly beneficial to understand the *Postn* effects and dynamics in breast cancer. Conditional studies are currently limited as those animals have not yet been engineered or are not commercially available.

6.12 Conclusion

In this study, we explored the role of *Postn* in *Neu*-driven tumorigenesis using a global genetic knockout model. Our results show a major role for *Postn* in promoting tumor progression and aggressive features of breast cancer. Furthermore, we explained this phenotype to the relationship between collagen deposition and ECM composition. Finally, we unraveled a novel *Postn* gene regulation mechanism in *Neu*-driven epithelial breast cancer cells involving FGFR, TGFβ, PI3K and AKT signaling pathways (Figure 6.1). Taken together, these findings suggest that *Postn* expression in breast cancer may be used for therapeutic approaches to prevent tumors from acquiring aggressive and invasive characteristics.

References

1. Bray F, Ferlay J, Soerjomataram I, Siegel RL, Torre LA and Jemal A (2018) Global cancer statistics 2018: GLOBOCAN estimates of incidence and mortality worldwide for 36 cancers in 185 countries. CA Cancer J Clin 68:394-424. doi: 10.3322/caac.21492
2. Curtis C, Shah SP, Chin SF, Turashvili G, Rueda OM, Dunning MJ, Speed D, Lynch AG, Samarajiwa S, Yuan Y, Graf S, Ha G, Haffari G, Bashashati A, Russell R, McKinney S, Group M, Langerod A, Green A, Provenzano E, Wishart G, Pinder S, Watson P, Markowetz F, Murphy L, Ellis I, Purushotham A, Borresen-Dale AL, Brenton JD, Tavare S, Caldas C and Aparicio S (2012) The genomic and transcriptomic architecture of 2,000 breast tumours reveals novel subgroups. Nature 486:346-52. doi: 10.1038/nature10983
3. Marusyk A, Almendro V and Polyak K (2012) Intra-tumour heterogeneity: a looking glass for cancer? Nat Rev Cancer 12:323-34. doi: 10.1038/nrc3261
4. Perou CM, Sorlie T, Eisen MB, van de Rijn M, Jeffrey SS, Rees CA, Pollack JR, Ross DT, Johnsen H, Akslen LA, Fluge O, Pergamenschikov A, Williams C, Zhu SX, Lonning PE, Borresen-Dale AL, Brown PO and Botstein D (2000) Molecular portraits of human breast tumours. Nature 406:747-52. doi: 10.1038/35021093
5. Hu Z, Fan C, Oh DS, Marron JS, He X, Qaqish BF, Livasy C, Carey LA, Reynolds E, Dressler L, Nobel A, Parker J, Ewend MG, Sawyer LR, Wu J, Liu Y, Nanda R, Tretiakova M, Ruiz Orrico A, Dreher D, Palazzo JP, Perreard L, Nelson E, Mone M, Hansen H, Mullins M, Quackenbush JF, Ellis MJ, Olopade OI, Bernard PS and Perou CM (2006) The molecular portraits of breast tumors are conserved across microarray platforms. BMC Genomics 7:96. doi: 10.1186/1471-2164-7-96
6. Perou CM, Jeffrey SS, van de Rijn M, Rees CA, Eisen MB, Ross DT, Pergamenschikov A, Williams CF, Zhu SX, Lee JC, Lashkari D, Shalon D, Brown PO and Botstein D (1999) Distinctive gene expression patterns in human mammary epithelial cells and breast cancers. Proc Natl Acad Sci U S A 96:9212-7. doi: 10.1073/pnas.96.16.9212
7. Brenton JD, Carey LA, Ahmed AA and Caldas C (2005) Molecular classification and molecular forecasting of breast cancer: ready for clinical application? J Clin Oncol 23:7350-60. doi: 10.1200/JCO.2005.03.3845
8. Sorlie T, Tibshirani R, Parker J, Hastie T, Marron JS, Nobel A, Deng S, Johnsen H, Pesich R, Geisler S, Demeter J, Perou CM, Lonning PE, Brown PO, Borresen-Dale AL and Botstein D (2003) Repeated observation of breast tumor subtypes in independent gene expression data sets. Proc Natl Acad Sci U S A 100:8418-23. doi: 10.1073/pnas.0932692100
9. Schechter AL, Stern DF, Vaidyanathan L, Decker SJ, Drebin JA, Greene MI and Weinberg RA (1984) The neu oncogene: an erb-B-related gene encoding a 185,000-Mr tumour antigen. Nature 312:513-6.
10. Yang W, Klos KS, Zhou X, Yao J, Yang Y, Smith TL, Shi D and Yu D (2003) ErbB2 overexpression in human breast carcinoma is correlated with p21Cip1 up-regulation and tyrosine-15 hyperphosphorylation of p34Cdc2: poor responsiveness to chemotherapy with cyclophoshamide methotrexate, and 5-fluorouracil is associated with Erb2 overexpression and with p21Cip1 overexpression. Cancer 98:1123-30. doi: 10.1002/cncr.11625
11. Marone R, Hess D, Dankort D, Muller WJ, Hynes NE and Badache A (2004) Memo mediates ErbB2-driven cell motility. Nat Cell Biol 6:515-22. doi: 10.1038/ncb1134
12. Denkert C, Liedtke C, Tutt A and von Minckwitz G (2017) Molecular alterations in triple-negative breast cancer-the road to new treatment strategies. Lancet 389:2430-2442. doi: 10.1016/S0140-6736(16)32454-0
13. Goldhirsch A, Wood WC, Coates AS, Gelber RD, Thurlimann B, Senn HJ and Panel m (2011) Strategies for subtypes--dealing with the diversity of breast cancer: highlights of the St. Gallen International Expert Consensus on the Primary Therapy of Early Breast Cancer 2011. Ann Oncol 22:1736-47. doi: 10.1093/annonc/mdr304

14. Avagliano A, Ruocco MR, Aliotta F, Belviso I, Accurso A, Masone S, Montagnani S and Arcucci A (2019) Mitochondrial Flexibility of Breast Cancers: A Growth Advantage and a Therapeutic Opportunity. Cells 8. doi: 10.3390/cells8050401
15. Amin MB, American Joint Committee on Cancer. and American Cancer Society. (2017) AJCC cancer staging manual. American Joint Committee on Cancer, Springer, Chicago IL.
16. Patanaphan V, Salazar OM and Risco R (1988) Breast cancer: metastatic patterns and their prognosis. South Med J 81:1109-12.
17. Dillon D, Guidi A and Schnitt S (2010) Pathology of invasive breast cancer. Diseases of the Breast. Philadelphia: Wolters Kluwer/Lippincott Williams&Wilkins.
18. DeVita VT, Lawrence TS and Rosenberg SA (2019) DeVita, Hellman, and Rosenberg's cancer : principles & practice of oncology. Wolters Kluwer, Philadelphia.
19. Waks AG and Winer EP (2019) Breast Cancer Treatment: A Review. JAMA 321:288-300. doi: 10.1001/jama.2018.19323
20. Miller E, Lee HJ, Lulla A, Hernandez L, Gokare P and Lim B (2014) Current treatment of early breast cancer: adjuvant and neoadjuvant therapy. F1000Res 3:198. doi: 10.12688/f1000research.4340.1
21. Citri A and Yarden Y (2006) EGF-ERBB signalling: towards the systems level. Nat Rev Mol Cell Biol 7:505-16. doi: 10.1038/nrm1962
22. Yarden Y and Sliwkowski MX (2001) Untangling the ErbB signalling network. Nat Rev Mol Cell Biol 2:127-37. doi: 10.1038/35052073
23. Heldin CH (1995) Dimerization of cell surface receptors in signal transduction. Cell 80:213-23. doi: 10.1016/0092-8674(95)90404-2
24. Marmor MD, Skaria KB and Yarden Y (2004) Signal transduction and oncogenesis by ErbB/HER receptors. Int J Radiat Oncol Biol Phys 58:903-13. doi: 10.1016/j.ijrobp.2003.06.002
25. Kovacs E, Zorn JA, Huang Y, Barros T and Kuriyan J (2015) A structural perspective on the regulation of the epidermal growth factor receptor. Annu Rev Biochem 84:739-64. doi: 10.1146/annurev-biochem-060614-034402
26. Carraway KL, 3rd and Cantley LC (1994) A neu acquaintance for erbB3 and erbB4: a role for receptor heterodimerization in growth signaling. Cell 78:5-8. doi: 10.1016/0092-8674(94)90564-9
27. Hynes NE and Lane HA (2005) ERBB receptors and cancer: the complexity of targeted inhibitors. Nat Rev Cancer 5:341-54. doi: 10.1038/nrc1609
28. Sardi SP, Murtie J, Koirala S, Patten BA and Corfas G (2006) Presenilin-dependent ErbB4 nuclear signaling regulates the timing of astrogenesis in the developing brain. Cell 127:185-97. doi: 10.1016/j.cell.2006.07.037
29. Pinkas-Kramarski R, Soussan L, Waterman H, Levkowitz G, Alroy I, Klapper L, Lavi S, Seger R, Ratzkin BJ, Sela M and Yarden Y (1996) Diversification of Neu differentiation factor and epidermal growth factor signaling by combinatorial receptor interactions. EMBO J 15:2452-67.
30. Cohen S (1964) Isolation and Biological Effects of an Epidermal Growth-Stimulating Protein. Natl Cancer Inst Monogr 13:13-37.
31. Derynck R, Roberts AB, Winkler ME, Chen EY and Goeddel DV (1984) Human transforming growth factor-alpha: precursor structure and expression in E. coli. Cell 38:287-97. doi: 10.1016/0092-8674(84)90550-6
32. Shoyab M, Plowman GD, McDonald VL, Bradley JG and Todaro GJ (1989) Structure and function of human amphiregulin: a member of the epidermal growth factor family. Science 243:1074-6. doi: 10.1126/science.2466334
33. Strachan L, Murison JG, Prestidge RL, Sleeman MA, Watson JD and Kumble KD (2001) Cloning and biological activity of epigen, a novel member of the epidermal growth factor superfamily. J Biol Chem 276:18265-71. doi: 10.1074/jbc.M006935200
34. Toyoda H, Komurasaki T, Uchida D, Takayama Y, Isobe T, Okuyama T and Hanada K (1995) Epiregulin. A novel epidermal growth factor with mitogenic activity for rat primary hepatocytes. J Biol Chem 270:7495-500. doi: 10.1074/jbc.270.13.7495

35. Shing Y, Christofori G, Hanahan D, Ono Y, Sasada R, Igarashi K and Folkman J (1993) Betacellulin: a mitogen from pancreatic beta cell tumors. Science 259:1604-7. doi: 10.1126/science.8456283
36. Higashiyama S, Abraham JA, Miller J, Fiddes JC and Klagsbrun M (1991) A heparin-binding growth factor secreted by macrophage-like cells that is related to EGF. Science 251:936-9. doi: 10.1126/science.1840698
37. Chang H, Riese DJ, 2nd, Gilbert W, Stern DF and McMahan UJ (1997) Ligands for ErbB-family receptors encoded by a neuregulin-like gene. Nature 387:509-12. doi: 10.1038/387509a0
38. Carraway KL, 3rd, Weber JL, Unger MJ, Ledesma J, Yu N, Gassmann M and Lai C (1997) Neuregulin-2, a new ligand of ErbB3/ErbB4-receptor tyrosine kinases. Nature 387:512-6. doi: 10.1038/387512a0
39. Zhang D, Sliwkowski MX, Mark M, Frantz G, Akita R, Sun Y, Hillan K, Crowley C, Brush J and Godowski PJ (1997) Neuregulin-3 (NRG3): a novel neural tissue-enriched protein that binds and activates ErbB4. Proc Natl Acad Sci U S A 94:9562-7. doi: 10.1073/pnas.94.18.9562
40. Harari D, Tzahar E, Romano J, Shelly M, Pierce JH, Andrews GC and Yarden Y (1999) Neuregulin-4: a novel growth factor that acts through the ErbB-4 receptor tyrosine kinase. Oncogene 18:2681-9. doi: 10.1038/sj.onc.1202631
41. Uchida T, Wada K, Akamatsu T, Yonezawa M, Noguchi H, Mizoguchi A, Kasuga M and Sakamoto C (1999) A novel epidermal growth factor-like molecule containing two follistatin modules stimulates tyrosine phosphorylation of erbB-4 in MKN28 gastric cancer cells. Biochem Biophys Res Commun 266:593-602. doi: 10.1006/bbrc.1999.1873
42. Kinugasa Y, Ishiguro H, Tokita Y, Oohira A, Ohmoto H and Higashiyama S (2004) Neuroglycan C, a novel member of the neuregulin family. Biochem Biophys Res Commun 321:1045-9. doi: 10.1016/j.bbrc.2004.07.066
43. Lemmon MA (2009) Ligand-induced ErbB receptor dimerization. Exp Cell Res 315:638-48. doi: 10.1016/j.yexcr.2008.10.024
44. Garrett TP, McKern NM, Lou M, Elleman TC, Adams TE, Lovrecz GO, Kofler M, Jorissen RN, Nice EC, Burgess AW and Ward CW (2003) The crystal structure of a truncated ErbB2 ectodomain reveals an active conformation, poised to interact with other ErbB receptors. Mol Cell 11:495-505. doi: 10.1016/s1097-2765(03)00048-0
45. Graus-Porta D, Beerli RR, Daly JM and Hynes NE (1997) ErbB-2, the preferred heterodimerization partner of all ErbB receptors, is a mediator of lateral signaling. EMBO J 16:1647-55. doi: 10.1093/emboj/16.7.1647
46. Real FX, Rettig WJ, Chesa PG, Melamed MR, Old LJ and Mendelsohn J (1986) Expression of epidermal growth factor receptor in human cultured cells and tissues: relationship to cell lineage and stage of differentiation. Cancer Res 46:4726-31.
47. Press MF, Cordon-Cardo C and Slamon DJ (1990) Expression of the HER-2/neu proto-oncogene in normal human adult and fetal tissues. Oncogene 5:953-62.
48. Miettinen PJ, Berger JE, Meneses J, Phung Y, Pedersen RA, Werb Z and Derynck R (1995) Epithelial immaturity and multiorgan failure in mice lacking epidermal growth factor receptor. Nature 376:337-41. doi: 10.1038/376337a0
49. Morris JK, Lin W, Hauser C, Marchuk Y, Getman D and Lee KF (1999) Rescue of the cardiac defect in ErbB2 mutant mice reveals essential roles of ErbB2 in peripheral nervous system development. Neuron 23:273-83. doi: 10.1016/s0896-6273(00)80779-5
50. Threadgill DW, Dlugosz AA, Hansen LA, Tennenbaum T, Lichti U, Yee D, LaMantia C, Mourton T, Herrup K, Harris RC and et al. (1995) Targeted disruption of mouse EGF receptor: effect of genetic background on mutant phenotype. Science 269:230-4. doi: 10.1126/science.7618084
51. Xie W, Paterson AJ, Chin E, Nabell LM and Kudlow JE (1997) Targeted expression of a dominant negative epidermal growth factor receptor in the mammary gland of transgenic mice inhibits pubertal mammary duct development. Mol Endocrinol 11:1766-81. doi: 10.1210/mend.11.12.0019

52. Andrechek ER, White D and Muller WJ (2005) Targeted disruption of ErbB2/Neu in the mammary epithelium results in impaired ductal outgrowth. Oncogene 24:932-7. doi: 10.1038/sj.onc.1208230
53. Shih C, Padhy LC, Murray M and Weinberg RA (1981) Transforming genes of carcinomas and neuroblastomas introduced into mouse fibroblasts. Nature 290:261-4. doi: 10.1038/290261a0
54. Brandt R, Wong AM and Hynes NE (2001) Mammary glands reconstituted with Neu/ErbB2 transformed HC11 cells provide a novel orthotopic tumor model for testing anti-cancer agents. Oncogene 20:5459-65. doi: 10.1038/sj.onc.1204709
55. Bargmann CI, Hung MC and Weinberg RA (1986) Multiple independent activations of the neu oncogene by a point mutation altering the transmembrane domain of p185. Cell 45:649-57. doi: 10.1016/0092-8674(86)90779-8
56. Weiner DB, Liu J, Cohen JA, Williams WV and Greene MI (1989) A point mutation in the neu oncogene mimics ligand induction of receptor aggregation. Nature 339:230-1. doi: 10.1038/339230a0
57. Siegel PM and Muller WJ (1996) Mutations affecting conserved cysteine residues within the extracellular domain of Neu promote receptor dimerization and activation. Proc Natl Acad Sci U S A 93:8878-83. doi: 10.1073/pnas.93.17.8878
58. Siegel PM, Dankort DL, Hardy WR and Muller WJ (1994) Novel activating mutations in the neu proto-oncogene involved in induction of mammary tumors. Mol Cell Biol 14:7068-77. doi: 10.1128/mcb.14.11.7068
59. Segatto O, King CR, Pierce JH, Di Fiore PP and Aaronson SA (1988) Different structural alterations upregulate in vitro tyrosine kinase activity and transforming potency of the erbB-2 gene. Mol Cell Biol 8:5570-4. doi: 10.1128/mcb.8.12.5570
60. Di Fiore PP, Pierce JH, Kraus MH, Segatto O, King CR and Aaronson SA (1987) erbB-2 is a potent oncogene when overexpressed in NIH/3T3 cells. Science 237:178-182.
61. Chazin VR, Kaleko M, Miller AD and Slamon DJ (1992) Transformation mediated by the human HER-2 gene independent of the epidermal growth factor receptor. Oncogene 7:1859-66.
62. Benz CC, Scott GK, Sarup JC, Johnson RM, Tripathy D, Coronado E, Shepard HM and Osborne CK (1992) Estrogen-dependent, tamoxifen-resistant tumorigenic growth of MCF-7 cells transfected with HER2/neu. Breast Cancer Res Treat 24:85-95. doi: 10.1007/BF01961241
63. Muthuswamy SK, Gilman M and Brugge JS (1999) Controlled dimerization of ErbB receptors provides evidence for differential signaling by homo- and heterodimers. Mol Cell Biol 19:6845-57. doi: 10.1128/mcb.19.10.6845
64. Slamon DJ, Godolphin W, Jones LA, Holt JA, Wong SG, Keith DE, Levin WJ, Stuart SG, Udove J, Ullrich A and et al. (1989) Studies of the HER-2/neu proto-oncogene in human breast and ovarian cancer. Science 244:707-12. doi: 10.1126/science.2470152
65. Kallioniemi OP, Kallioniemi A, Kurisu W, Thor A, Chen LC, Smith HS, Waldman FM, Pinkel D and Gray JW (1992) ERBB2 amplification in breast cancer analyzed by fluorescence in situ hybridization. Proc Natl Acad Sci U S A 89:5321-5. doi: 10.1073/pnas.89.12.5321
66. Venter DJ, Tuzi NL, Kumar S and Gullick WJ (1987) Overexpression of the c-erbB-2 oncoprotein in human breast carcinomas: immunohistological assessment correlates with gene amplification. Lancet 2:69-72. doi: 10.1016/s0140-6736(87)92736-x
67. Park K, Han S, Kim HJ, Kim J and Shin E (2006) HER2 status in pure ductal carcinoma in situ and in the intraductal and invasive components of invasive ductal carcinoma determined by fluorescence in situ hybridization and immunohistochemistry. Histopathology 48:702-7. doi: 10.1111/j.1365-2559.2006.02403.x
68. Latta EK, Tjan S, Parkes RK and O'Malley FP (2002) The role of HER2/neu overexpression/amplification in the progression of ductal carcinoma in situ to invasive carcinoma of the breast. Mod Pathol 15:1318-25. doi: 10.1097/01.MP.0000038462.62634.B1

69. Weigelt B, Hu Z, He X, Livasy C, Carey LA, Ewend MG, Glas AM, Perou CM and Van't Veer LJ (2005) Molecular portraits and 70-gene prognosis signature are preserved throughout the metastatic process of breast cancer. Cancer Res 65:9155-8. doi: 10.1158/0008-5472.CAN-05-2553
70. Dowsett M (2001) Overexpression of HER-2 as a resistance mechanism to hormonal therapy for breast cancer. Endocr Relat Cancer 8:191-5. doi: 10.1677/erc.0.0080191
71. Schmid P, Wischnewsky MB, Sezer O, Bohm R and Possinger K (2002) Prediction of response to hormonal treatment in metastatic breast cancer. Oncology 63:309-16. doi: 10.1159/000066224
72. Pegram MD, Finn RS, Arzoo K, Beryt M, Pietras RJ and Slamon DJ (1997) The effect of HER-2/neu overexpression on chemotherapeutic drug sensitivity in human breast and ovarian cancer cells. Oncogene 15:537-47. doi: 10.1038/sj.onc.1201222
73. Gabos Z, Sinha R, Hanson J, Chauhan N, Hugh J, Mackey JR and Abdulkarim B (2006) Prognostic significance of human epidermal growth factor receptor positivity for the development of brain metastasis after newly diagnosed breast cancer. J Clin Oncol 24:5658-63. doi: 10.1200/JCO.2006.07.0250
74. Muller WJ, Sinn E, Pattengale PK, Wallace R and Leder P (1988) Single-step induction of mammary adenocarcinoma in transgenic mice bearing the activated c-neu oncogene. Cell 54:105-15. doi: 10.1016/0092-8674(88)90184-5
75. Bouchard L, Lamarre L, Tremblay PJ and Jolicoeur P (1989) Stochastic appearance of mammary tumors in transgenic mice carrying the MMTV/c-neu oncogene. Cell 57:931-6. doi: 10.1016/0092-8674(89)90331-0
76. Cardiff RD and Muller WJ (1993) Transgenic mouse models of mammary tumorigenesis. Cancer Surv 16:97-113.
77. Sakamoto K, Schmidt JW and Wagner KU (2012) Generation of a novel MMTV-tTA transgenic mouse strain for the targeted expression of genes in the embryonic and postnatal mammary gland. PLoS One 7:e43778. doi: 10.1371/journal.pone.0043778
78. Lee JW, Soung YH, Seo SH, Kim SY, Park CH, Wang YP, Park K, Nam SW, Park WS, Kim SH, Lee JY, Yoo NJ and Lee SH (2006) Somatic mutations of ERBB2 kinase domain in gastric, colorectal, and breast carcinomas. Clin Cancer Res 12:57-61. doi: 10.1158/1078-0432.CCR-05-0976
79. Guy CT, Cardiff RD and Muller WJ (1992) Induction of mammary tumors by expression of polyomavirus middle T oncogene: a transgenic mouse model for metastatic disease. Mol Cell Biol 12:954-61. doi: 10.1128/mcb.12.3.954-961.1992
80. Maglione JE, Moghanaki D, Young LJ, Manner CK, Ellies LG, Joseph SO, Nicholson B, Cardiff RD and MacLeod CL (2001) Transgenic Polyoma middle-T mice model premalignant mammary disease. Cancer Res 61:8298-305.
81. Guy CT, Webster MA, Schaller M, Parsons TJ, Cardiff RD and Muller WJ (1992) Expression of the neu protooncogene in the mammary epithelium of transgenic mice induces metastatic disease. Proc Natl Acad Sci U S A 89:10578-82.
82. Siegel PM, Ryan ED, Cardiff RD and Muller WJ (1999) Elevated expression of activated forms of Neu/ErbB-2 and ErbB-3 are involved in the induction of mammary tumors in transgenic mice: implications for human breast cancer. Embo j 18:2149-64. doi: 10.1093/emboj/18.8.2149
83. Ursini-Siegel J, Hardy WR, Zuo D, Lam SH, Sanguin-Gendreau V, Cardiff RD, Pawson T and Muller WJ (2008) ShcA signalling is essential for tumour progression in mouse models of human breast cancer. Embo j 27:910-20. doi: 10.1038/emboj.2008.22
84. Rowse GJ, Ritland SR and Gendler SJ (1998) Genetic modulation of neu proto-oncogene-induced mammary tumorigenesis. Cancer Res 58:2675-9.
85. Davie SA, Maglione JE, Manner CK, Young D, Cardiff RD, MacLeod CL and Ellies LG (2007) Effects of FVB/NJ and C57Bl/6J strain backgrounds on mammary tumor phenotype in inducible nitric oxide synthase deficient mice. Transgenic Res 16:193-201. doi: 10.1007/s11248-006-9056-9
86. Takeshita S, Kikuno R, Tezuka K and Amann E (1993) Osteoblast-specific factor 2: cloning of a putative bone adhesion protein with homology with the insect protein fasciclin I. Biochem J 294 (Pt 1):271-8.

87. Horiuchi K, Amizuka N, Takeshita S, Takamatsu H, Katsuura M, Ozawa H, Toyama Y, Bonewald LF and Kudo A (1999) Identification and characterization of a novel protein, periostin, with restricted expression to periosteum and periodontal ligament and increased expression by transforming growth factor beta. J Bone Miner Res 14:1239-49. doi: 10.1359/jbmr.1999.14.7.1239
88. Hoersch S and Andrade-Navarro MA (2010) Periostin shows increased evolutionary plasticity in its alternatively spliced region. BMC Evolutionary Biology 10:30. doi: 10.1186/1471-2148-10-30
89. Litvin J, Selim AH, Montgomery MO, Lehmann K, Rico MC, Devlin H, Bednarik DP and Safadi FF (2004) Expression and function of periostin-isoforms in bone. J Cell Biochem 92:1044-61. doi: 10.1002/jcb.20115
90. Bao S, Ouyang G, Bai X, Huang Z, Ma C, Liu M, Shao R, Anderson RM, Rich JN and Wang XF (2004) Periostin potently promotes metastatic growth of colon cancer by augmenting cell survival via the Akt/PKB pathway. Cancer Cell 5:329-39.
91. Li G, Jin R, Norris RA, Zhang L, Yu S, Wu F, Markwald RR, Nanda A, Conway SJ, Smyth SS and Granger DN (2010) Periostin mediates vascular smooth muscle cell migration through the integrins alphavbeta3 and alphavbeta5 and focal adhesion kinase (FAK) pathway. Atherosclerosis 208:358-65. doi: 10.1016/j.atherosclerosis.2009.07.046
92. Baril P, Gangeswaran R, Mahon PC, Caulee K, Kocher HM, Harada T, Zhu M, Kalthoff H, Crnogorac-Jurcevic T and Lemoine NR (2007) Periostin promotes invasiveness and resistance of pancreatic cancer cells to hypoxia-induced cell death: role of the beta4 integrin and the PI3k pathway. Oncogene 26:2082-94. doi: 10.1038/sj.onc.1210009
93. Elliott C and Hamilton D (2011) Deconstructing fibrosis research: Do pro-fibrotic signals point the way for chronic dermal wound regeneration? Journal of cell communication and signaling 5:301-15. doi: 10.1007/s12079-011-0131-5
94. Walma DAC and Yamada KM (2020) The extracellular matrix in development. Development 147. doi: 10.1242/dev.175596
95. Kudo A and Kii I (2018) Periostin function in communication with extracellular matrices. J Cell Commun Signal 12:301-308. doi: 10.1007/s12079-017-0422-6
96. Zhu S, Barbe MF, Amin N, Rani S, Popoff SN, Safadi FF and Litvin J (2008) Immunolocalization of Periostin-like factor and Periostin during embryogenesis. J Histochem Cytochem 56:329-45. doi: 10.1369/jhc.7A7321.2007
97. Cai L, Brophy RH, Tycksen ED, Duan X, Nunley RM and Rai MF (2019) Distinct expression pattern of periostin splice variants in chondrocytes and ligament progenitor cells. Faseb j 33:8386-8405. doi: 10.1096/fj.201802281R
98. Dwek JR (2010) The periosteum: what is it, where is it, and what mimics it in its absence? Skeletal Radiol 39:319-23. doi: 10.1007/s00256-009-0849-9
99. Bonnet N, Garnero P and Ferrari S (2016) Periostin action in bone. Mol Cell Endocrinol 432:75-82. doi: 10.1016/j.mce.2015.12.014
100. Bonnet N, Standley KN, Bianchi EN, Stadelmann V, Foti M, Conway SJ and Ferrari SL (2009) The matricellular protein periostin is required for sost inhibition and the anabolic response to mechanical loading and physical activity. J Biol Chem 284:35939-50. doi: 10.1074/jbc.M109.060335
101. Bonnet N, Conway SJ and Ferrari SL (2012) Regulation of beta catenin signaling and parathyroid hormone anabolic effects in bone by the matricellular protein periostin. Proc Natl Acad Sci U S A 109:15048-53. doi: 10.1073/pnas.1203085109
102. Gerbaix M, Vico L, Ferrari SL and Bonnet N (2015) Periostin expression contributes to cortical bone loss during unloading. Bone 71:94-100. doi: 10.1016/j.bone.2014.10.011
103. Zhou HM, Wang J, Elliott C, Wen W, Hamilton DW and Conway SJ (2010) Spatiotemporal expression of periostin during skin development and incisional wound healing: lessons for human fibrotic scar formation. J Cell Commun Signal 4:99-107. doi: 10.1007/s12079-010-0090-2
104. Greiling D and Clark RA (1997) Fibronectin provides a conduit for fibroblast transmigration from collagenous stroma into fibrin clot provisional matrix. J Cell Sci 110 (Pt 7):861-70.

105. Assoian RK, Fleurdelys BE, Stevenson HC, Miller PJ, Madtes DK, Raines EW, Ross R and Sporn MB (1987) Expression and secretion of type beta transforming growth factor by activated human macrophages. Proc Natl Acad Sci U S A 84:6020-4. doi: 10.1073/pnas.84.17.6020
106. Walker JT, Kim SS, Michelsons S, Creber K, Elliott CG, Leask A, Hamilton DWJR and Biochemistry Ri (2015) Cell–matrix interactions governing skin repair: matricellular proteins as diverse modulators of cell function. 5:73-88.
107. Jackson-Boeters L, Wen W and Hamilton DW (2009) Periostin localizes to cells in normal skin, but is associated with the extracellular matrix during wound repair. J Cell Commun Signal 3:125-33. doi: 10.1007/s12079-009-0057-3
108. Elliott CG, Wang J, Guo X, Xu SW, Eastwood M, Guan J, Leask A, Conway SJ and Hamilton DW (2012) Periostin modulates myofibroblast differentiation during full-thickness cutaneous wound repair. J Cell Sci 125:121-32. doi: 10.1242/jcs.087841
109. Nishiyama T, Kii I, Kashima TG, Kikuchi Y, Ohazama A, Shimazaki M, Fukayama M and Kudo A (2011) Delayed re-epithelialization in periostin-deficient mice during cutaneous wound healing. PLoS One 6:e18410. doi: 10.1371/journal.pone.0018410
110. Stanton LW, Garrard LJ, Damm D, Garrick BL, Lam A, Kapoun AM, Zheng Q, Protter AA, Schreiner GF and White RT (2000) Altered patterns of gene expression in response to myocardial infarction. Circ Res 86:939-45. doi: 10.1161/01.res.86.9.939
111. Ieda M, Tsuchihashi T, Ivey KN, Ross RS, Hong TT, Shaw RM and Srivastava D (2009) Cardiac fibroblasts regulate myocardial proliferation through beta1 integrin signaling. Dev Cell 16:233-44. doi: 10.1016/j.devcel.2008.12.007
112. Snider P, Hinton RB, Moreno-Rodriguez RA, Wang J, Rogers R, Lindsley A, Li F, Ingram DA, Menick D, Field L, Firulli AB, Molkentin JD, Markwald R and Conway SJ (2008) Periostin is required for maturation and extracellular matrix stabilization of noncardiomyocyte lineages of the heart. Circ Res 102:752-60. doi: 10.1161/circresaha.107.159517
113. Norris RA, Moreno-Rodriguez RA, Sugi Y, Hoffman S, Amos J, Hart MM, Potts JD, Goodwin RL and Markwald RR (2008) Periostin regulates atrioventricular valve maturation. Dev Biol 316:200-13. doi: 10.1016/j.ydbio.2008.01.003
114. Norris RA, Potts JD, Yost MJ, Junor L, Brooks T, Tan H, Hoffman S, Hart MM, Kern MJ, Damon B, Markwald RR and Goodwin RL (2009) Periostin promotes a fibroblastic lineage pathway in atrioventricular valve progenitor cells. Dev Dyn 238:1052-63. doi: 10.1002/dvdy.21933
115. Uzel MI, Scott IC, Babakhanlou-Chase H, Palamakumbura AH, Pappano WN, Hong HH, Greenspan DS and Trackman PC (2001) Multiple bone morphogenetic protein 1-related mammalian metalloproteinases process pro-lysyl oxidase at the correct physiological site and control lysyl oxidase activation in mouse embryo fibroblast cultures. J Biol Chem 276:22537-43. doi: 10.1074/jbc.M102352200
116. Maruhashi T, Kii I, Saito M and Kudo A (2010) Interaction between periostin and BMP-1 promotes proteolytic activation of lysyl oxidase. J Biol Chem 285:13294-303. doi: 10.1074/jbc.M109.088864
117. Christiansen DL, Huang EK and Silver FH (2000) Assembly of type I collagen: fusion of fibril subunits and the influence of fibril diameter on mechanical properties. Matrix Biol 19:409-20. doi: 10.1016/s0945-053x(00)00089-5
118. Norris RA, Damon B, Mironov V, Kasyanov V, Ramamurthi A, Moreno-Rodriguez R, Trusk T, Potts JD, Goodwin RL, Davis J, Hoffman S, Wen X, Sugi Y, Kern CB, Mjaatvedt CH, Turner DK, Oka T, Conway SJ, Molkentin JD, Forgacs G and Markwald RR (2007) Periostin regulates collagen fibrillogenesis and the biomechanical properties of connective tissues. J Cell Biochem 101:695-711. doi: 10.1002/jcb.21224
119. Yoshida S, Umeno Y and Haruta M (2019) Periostin in Eye Diseases. Adv Exp Med Biol 1132:113-124. doi: 10.1007/978-981-13-6657-4_12
120. Kuwatsuka Y and Murota H (2019) Involvement of Periostin in Skin Function and the Pathogenesis of Skin Diseases. Adv Exp Med Biol 1132:89-98. doi: 10.1007/978-981-13-6657-4_10

121. O'Dwyer DN and Moore BB (2017) The role of periostin in lung fibrosis and airway remodeling. Cell Mol Life Sci 74:4305-4314. doi: 10.1007/s00018-017-2649-z
122. Ishida A, Ohta N, Suzuki Y, Kakehata S, Okubo K, Ikeda H, Shiraishi H and Izuhara K (2012) Expression of pendrin and periostin in allergic rhinitis and chronic rhinosinusitis. Allergol Int 61:589-95. doi: 10.2332/allergolint.11-OA-0370
123. González-González L and Alonso J (2018) Periostin: A Matricellular Protein With Multiple Functions in Cancer Development and Progression. Front Oncol 8:225. doi: 10.3389/fonc.2018.00225
124. Kudo A (2017) Introductory review: periostin—gene and protein structure. Cellular and Molecular Life Sciences 74:4259-4268. doi: 10.1007/s00018-017-2643-5
125. Qu Y, Chi W, Hua X, Deng R, Li J, Liu Z, Pflugfelder SC and Li DQ (2015) Unique expression pattern and functional role of periostin in human limbal stem cells. PLoS One 10:e0117139. doi: 10.1371/journal.pone.0117139
126. Takayama G, Arima K, Kanaji T, Toda S, Tanaka H, Shoji S, McKenzie AN, Nagai H, Hotokebuchi T and Izuhara K (2006) Periostin: a novel component of subepithelial fibrosis of bronchial asthma downstream of IL-4 and IL-13 signals. J Allergy Clin Immunol 118:98-104. doi: 10.1016/j.jaci.2006.02.046
127. Woodruff PG, Boushey HA, Dolganov GM, Barker CS, Yang YH, Donnelly S, Ellwanger A, Sidhu SS, Dao-Pick TP, Pantoja C, Erle DJ, Yamamoto KR and Fahy JV (2007) Genome-wide profiling identifies epithelial cell genes associated with asthma and with treatment response to corticosteroids. Proc Natl Acad Sci U S A 104:15858-63. doi: 10.1073/pnas.0707413104
128. Woodruff PG, Modrek B, Choy DF, Jia G, Abbas AR, Ellwanger A, Koth LL, Arron JR and Fahy JV (2009) T-helper type 2-driven inflammation defines major subphenotypes of asthma. Am J Respir Crit Care Med 180:388-95. doi: 10.1164/rccm.200903-0392OC
129. Sidhu SS, Yuan S, Innes AL, Kerr S, Woodruff PG, Hou L, Muller SJ and Fahy JV (2010) Roles of epithelial cell-derived periostin in TGF-beta activation, collagen production, and collagen gel elasticity in asthma. Proc Natl Acad Sci U S A 107:14170-5. doi: 10.1073/pnas.1009426107
130. Shimazaki M, Nakamura K, Kii I, Kashima T, Amizuka N, Li M, Saito M, Fukuda K, Nishiyama T, Kitajima S, Saga Y, Fukayama M, Sata M and Kudo A (2008) Periostin is essential for cardiac healing after acute myocardial infarction. J Exp Med 205:295-303. doi: 10.1084/jem.20071297
131. Lindner V, Wang Q, Conley BA, Friesel RE and Vary CP (2005) Vascular injury induces expression of periostin: implications for vascular cell differentiation and migration. Arterioscler Thromb Vasc Biol 25:77-83. doi: 10.1161/01.ATV.0000149141.81230.c6
132. Goetsch SC, Hawke TJ, Gallardo TD, Richardson JA and Garry DJ (2003) Transcriptional profiling and regulation of the extracellular matrix during muscle regeneration. Physiol Genomics 14:261-71. doi: 10.1152/physiolgenomics.00056.2003
133. Hinshaw DC and Shevde LA (2019) The Tumor Microenvironment Innately Modulates Cancer Progression. Cancer Res 79:4557-4566. doi: 10.1158/0008-5472.Can-18-3962
134. Henke E, Nandigama R and Ergün S (2019) Extracellular Matrix in the Tumor Microenvironment and Its Impact on Cancer Therapy. Front Mol Biosci 6:160. doi: 10.3389/fmolb.2019.00160
135. Nuzzo PV, Rubagotti A, Zinoli L, Ricci F, Salvi S, Boccardo S and Boccardo F (2012) Prognostic value of stromal and epithelial periostin expression in human prostate cancer: correlation with clinical pathological features and the risk of biochemical relapse or death. BMC Cancer 12:625. doi: 10.1186/1471-2407-12-625
136. Tischler V, Fritzsche FR, Wild PJ, Stephan C, Seifert HH, Riener MO, Hermanns T, Mortezavi A, Gerhardt J, Schraml P, Jung K, Moch H, Soltermann A and Kristiansen G (2010) Periostin is up-regulated in high grade and high stage prostate cancer. BMC Cancer 10:273. doi: 10.1186/1471-2407-10-273
137. Hong LZ, Wei XW, Chen JF and Shi Y (2013) Overexpression of periostin predicts poor prognosis in non-small cell lung cancer. Oncol Lett 6:1595-1603. doi: 10.3892/ol.2013.1590

138. Ben QW, Jin XL, Liu J, Cai X, Yuan F and Yuan YZ (2011) Periostin, a matrix specific protein, is associated with proliferation and invasion of pancreatic cancer. Oncol Rep 25:709-16. doi: 10.3892/or.2011.1140
139. Liu Y and Du L (2015) Role of pancreatic stellate cells and periostin in pancreatic cancer progression. Tumour Biol 36:3171-7. doi: 10.1007/s13277-015-3386-2
140. Sung PL, Jan YH, Lin SC, Huang CC, Lin H, Wen KC, Chao KC, Lai CR, Wang PH, Chuang CM, Wu HH, Twu NF, Yen MS, Hsiao M and Huang CY (2016) Periostin in tumor microenvironment is associated with poor prognosis and platinum resistance in epithelial ovarian carcinoma. Oncotarget 7:4036-47. doi: 10.18632/oncotarget.6700
141. Zhu M, Fejzo MS, Anderson L, Dering J, Ginther C, Ramos L, Gasson JC, Karlan BY and Slamon DJ (2010) Periostin promotes ovarian cancer angiogenesis and metastasis. Gynecol Oncol 119:337-44. doi: 10.1016/j.ygyno.2010.07.008
142. Kim GE, Lee JS, Park MH and Yoon JH (2017) Epithelial periostin expression is correlated with poor survival in patients with invasive breast carcinoma. PLoS One 12:e0187635. doi: 10.1371/journal.pone.0187635
143. Malanchi I, Santamaria-Martinez A, Susanto E, Peng H, Lehr HA, Delaloye JF and Huelsken J (2012) Interactions between cancer stem cells and their niche govern metastatic colonization. Nature 481:85-9. doi: 10.1038/nature10694
144. Ratajczak-Wielgomas K, Grzegrzolka J, Piotrowska A, Gomulkiewicz A, Witkiewicz W and Dziegiel P (2016) Periostin expression in cancer-associated fibroblasts of invasive ductal breast carcinoma. Oncol Rep 36:2745-2754. doi: 10.3892/or.2016.5095
145. Oh HJ, Bae JM, Wen XY, Cho NY, Kim JH and Kang GH (2017) Overexpression of POSTN in Tumor Stroma Is a Poor Prognostic Indicator of Colorectal Cancer. J Pathol Transl Med 51:306-313. doi: 10.4132/jptm.2017.01.19
146. Wu G, Wang X and Zhang X (2013) Clinical implications of periostin in the liver metastasis of colorectal cancer. Cancer Biother Radiopharm 28:298-302. doi: 10.1089/cbr.2012.1374
147. Li Z, Zhang X, Yang Y, Yang S, Dong Z, Du L, Wang L and Wang C (2015) Periostin expression and its prognostic value for colorectal cancer. Int J Mol Sci 16:12108-18. doi: 10.3390/ijms160612108
148. Riener MO, Fritzsche FR, Soll C, Pestalozzi BC, Probst-Hensch N, Clavien PA, Jochum W, Soltermann A, Moch H and Kristiansen G (2010) Expression of the extracellular matrix protein periostin in liver tumours and bile duct carcinomas. Histopathology 56:600-6. doi: 10.1111/j.1365-2559.2010.03527.x
149. Lv Y, Wang W, Jia WD, Sun QK, Li JS, Ma JL, Liu WB, Zhou HC, Ge YS, Yu JH, Xia HH and Xu GL (2013) High-level expression of periostin is closely related to metastatic potential and poor prognosis of hepatocellular carcinoma. Med Oncol 30:385. doi: 10.1007/s12032-012-0385-7
150. Jang SY, Park SY, Lee HW, Choi YK, Park KG, Yoon GS, Tak WY, Kweon YO, Hur K and Lee WK (2016) The Combination of Periostin Overexpression and Microvascular Invasion Is Related to a Poor Prognosis for Hepatocellular Carcinoma. Gut Liver 10:948-954. doi: 10.5009/gnl15481
151. Hu F, Shang XF, Wang W, Jiang W, Fang C, Tan D and Zhou HC (2016) High-level expression of periostin is significantly correlated with tumour angiogenesis and poor prognosis in osteosarcoma. Int J Exp Pathol 97:86-92. doi: 10.1111/iep.12171
152. Wang W, Sun QK, He YF, Ma DC, Xie MR, Ji CS and Hu B (2014) Overexpression of periostin is significantly correlated to the tumor angiogenesis and poor prognosis in patients with esophageal squamous cell carcinoma. Int J Clin Exp Pathol 7:593-601.
153. Morra L, Rechsteiner M, Casagrande S, Duc Luu V, Santimaria R, Diener PA, Sulser T, Kristiansen G, Schraml P, Moch H and Soltermann A (2011) Relevance of periostin splice variants in renal cell carcinoma. Am J Pathol 179:1513-21. doi: 10.1016/j.ajpath.2011.05.035
154. Kim CJ, Yoshioka N, Tambe Y, Kushima R, Okada Y and Inoue H (2005) Periostin is down-regulated in high grade human bladder cancers and suppresses in vitro cell invasiveness and in vivo metastasis of cancer cells. Int J Cancer 117:51-8. doi: 10.1002/ijc.21120

155. Zhang Y, Yuan D, Yao Y, Sun W, Shi Y and Su X (2017) Predictive and prognostic value of serum periostin in advanced non-small cell lung cancer patients receiving chemotherapy. Tumour Biol 39:1010428317698367. doi: 10.1177/1010428317698367
156. Sasaki H, Yu CY, Dai M, Tam C, Loda M, Auclair D, Chen LB and Elias A (2003) Elevated serum periostin levels in patients with bone metastases from breast but not lung cancer. Breast Cancer Res Treat 77:245-52. doi: 10.1023/a:1021899904332
157. Xu CH, Wang W, Lin Y, Qian LH, Zhang XW, Wang QB and Yu LK (2017) Diagnostic and prognostic value of serum periostin in patients with non-small cell lung cancer. Oncotarget 8:18746-18753. doi: 10.18632/oncotarget.13004
158. Nuzzo PV, Rubagotti A, Argellati F, Di Meglio A, Zanardi E, Zinoli L, Comite P, Mussap M and Boccardo F (2015) Prognostic Value of Preoperative Serum Levels of Periostin (PN) in Early Breast Cancer (BCa). Int J Mol Sci 16:17181-92. doi: 10.3390/ijms160817181
159. Ben QW, Zhao Z, Ge SF, Zhou J, Yuan F and Yuan YZ (2009) Circulating levels of periostin may help identify patients with more aggressive colorectal cancer. Int J Oncol 34:821-8. doi: 10.3892/ijo_00000208
160. Lv Y, Wang W, Jia WD, Sun QK, Huang M, Zhou HC, Xia HH, Liu WB, Chen H, Sun SN and Xu GL (2013) High preoparative levels of serum periostin are associated with poor prognosis in patients with hepatocellular carcinoma after hepatectomy. Eur J Surg Oncol 39:1129-35. doi: 10.1016/j.ejso.2013.06.023
161. Thuwajit C, Thuwajit P, Jamjantra P, Pairojkul C, Wongkham S, Bhudhisawasdi V, Ono J, Ohta S, Fujimoto K and Izuhara K (2017) Clustering of patients with intrahepatic cholangiocarcinoma based on serum periostin may be predictive of prognosis. Oncol Lett 14:623-634. doi: 10.3892/ol.2017.6250
162. Hu WW, Chen PC, Chen JM, Wu YM, Liu PY, Lu CH, Lin YF, Tang CH and Chao CC (2017) Periostin promotes epithelial-mesenchymal transition via the MAPK/miR-381 axis in lung cancer. Oncotarget 8:62248-62260. doi: 10.18632/oncotarget.19273
163. Hu Q, Tong S, Zhao X, Ding W, Gou Y, Xu K, Sun C and Xia G (2015) Periostin Mediates TGF-β-Induced Epithelial Mesenchymal Transition in Prostate Cancer Cells. Cell Physiol Biochem 36:799-809. doi: 10.1159/000430139
164. Kim CJ, Sakamoto K, Tambe Y and Inoue H (2011) Opposite regulation of epithelial-to-mesenchymal transition and cell invasiveness by periostin between prostate and bladder cancer cells. Int J Oncol 38:1759-66. doi: 10.3892/ijo.2011.997
165. Ori A, Wilkinson MC and Fernig DG (2008) The heparanome and regulation of cell function: structures, functions and challenges. Front Biosci 13:4309-38. doi: 10.2741/3007
166. Harmer NJ, Ilag LL, Mulloy B, Pellegrini L, Robinson CV and Blundell TL (2004) Towards a resolution of the stoichiometry of the fibroblast growth factor (FGF)-FGF receptor-heparin complex. J Mol Biol 339:821-34. doi: 10.1016/j.jmb.2004.04.031
167. Eswarakumar VP, Lax I and Schlessinger J (2005) Cellular signaling by fibroblast growth factor receptors. Cytokine Growth Factor Rev 16:139-49. doi: 10.1016/j.cytogfr.2005.01.001
168. Altomare DA and Testa JR (2005) Perturbations of the AKT signaling pathway in human cancer. Oncogene 24:7455-64. doi: 10.1038/sj.onc.1209085
169. Peters KG, Marie J, Wilson E, Ives HE, Escobedo J, Del Rosario M, Mirda D and Williams LT (1992) Point mutation of an FGF receptor abolishes phosphatidylinositol turnover and Ca2+ flux but not mitogenesis. Nature 358:678-81. doi: 10.1038/358678a0
170. Klint P and Claesson-Welsh L (1999) Signal transduction by fibroblast growth factor receptors. Front Biosci 4:D165-77. doi: 10.2741/klint
171. Hart KC, Robertson SC, Kanemitsu MY, Meyer AN, Tynan JA and Donoghue DJ (2000) Transformation and Stat activation by derivatives of FGFR1, FGFR3, and FGFR4. Oncogene 19:3309-20. doi: 10.1038/sj.onc.1203650
172. Kang S, Elf S, Dong S, Hitosugi T, Lythgoe K, Guo A, Ruan H, Lonial S, Khoury HJ, Williams IR, Lee BH, Roesel JL, Karsenty G, Hanauer A, Taunton J, Boggon TJ, Gu TL and Chen J (2009)

Fibroblast growth factor receptor 3 associates with and tyrosine phosphorylates p90 RSK2, leading to RSK2 activation that mediates hematopoietic transformation. Mol Cell Biol 29:2105-17. doi: 10.1128/mcb.00998-08
173. Cappellen D, De Oliveira C, Ricol D, de Medina S, Bourdin J, Sastre-Garau X, Chopin D, Thiery JP and Radvanyi F (1999) Frequent activating mutations of FGFR3 in human bladder and cervix carcinomas. Nat Genet 23:18-20. doi: 10.1038/12615
174. di Martino E, L'Hôte CG, Kennedy W, Tomlinson DC and Knowles MA (2009) Mutant fibroblast growth factor receptor 3 induces intracellular signaling and cellular transformation in a cell type- and mutation-specific manner. Oncogene 28:4306-16. doi: 10.1038/onc.2009.280
175. Birrer MJ, Johnson ME, Hao K, Wong KK, Park DC, Bell A, Welch WR, Berkowitz RS and Mok SC (2007) Whole genome oligonucleotide-based array comparative genomic hybridization analysis identified fibroblast growth factor 1 as a prognostic marker for advanced-stage serous ovarian adenocarcinomas. J Clin Oncol 25:2281-7. doi: 10.1200/jco.2006.09.0795
176. Presta M, Dell'Era P, Mitola S, Moroni E, Ronca R and Rusnati M (2005) Fibroblast growth factor/fibroblast growth factor receptor system in angiogenesis. Cytokine Growth Factor Rev 16:159-78. doi: 10.1016/j.cytogfr.2005.01.004
177. Ratajczak-Wielgomas K, Grzegrzolka J, Piotrowska A, Matkowski R, Wojnar A, Rys J, Ugorski M and Dziegiel P (2017) Expression of periostin in breast cancer cells. Int J Oncol 51:1300-1310. doi: 10.3892/ijo.2017.4109
178. Yan W and Shao R (2006) Transduction of a mesenchyme-specific gene periostin into 293T cells induces cell invasive activity through epithelial-mesenchymal transformation. J Biol Chem 281:19700-8. doi: 10.1074/jbc.M601856200
179. Wu SZ, Roden DL, Wang C, Holliday H, Harvey K, Cazet AS, Murphy KJ, Pereira B, Al-Eryani G, Bartonicek N, Hou R, Torpy JR, Junankar S, Chan CL, Lam CE, Hui MN, Gluch L, Beith J, Parker A, Robbins E, Segara D, Mak C, Cooper C, Warrier S, Forrest A, Powell J, O'Toole S, Cox TR, Timpson P, Lim E, Liu XS and Swarbrick A (2020) Stromal cell diversity associated with immune evasion in human triple-negative breast cancer. Embo j 39:e104063. doi: 10.15252/embj.2019104063
180. Hao Y, Hao S, Andersen-Nissen E, Mauck WM, Zheng S, Butler A, Lee MJ, Wilk AJ, Darby C, Zagar M, Hoffman P, Stoeckius M, Papalexi E, Mimitou EP, Jain J, Srivastava A, Stuart T, Fleming LB, Yeung B, Rogers AJ, McElrath JM, Blish CA, Gottardo R, Smibert P and Satija R (2020) Integrated analysis of multimodal single-cell data.2020.10.12.335331. doi: 10.1101/2020.10.12.335331 %J bioRxiv
181. Hafemeister C and Satija R (2019) Normalization and variance stabilization of single-cell RNA-seq data using regularized negative binomial regression. Genome Biology 20:296. doi: 10.1186/s13059-019-1874-1
182. Bray NL, Pimentel H, Melsted P and Pachter L (2016) Near-optimal probabilistic RNA-seq quantification. Nat Biotechnol 34:525-7. doi: 10.1038/nbt.3519
183. Pimentel H, Bray NL, Puente S, Melsted P and Pachter L (2017) Differential analysis of RNA-seq incorporating quantification uncertainty. Nat Methods 14:687-690. doi: 10.1038/nmeth.4324
184. Schubert M, Klinger B, Klünemann M, Sieber A, Uhlitz F, Sauer S, Garnett MJ, Blüthgen N and Saez-Rodriguez J (2018) Perturbation-response genes reveal signaling footprints in cancer gene expression. Nat Commun 9:20. doi: 10.1038/s41467-017-02391-6
185. Sriram R, Lo V, Pryce B, Antonova L, Mears AJ, Daneshmand M, McKay B, Conway SJ, Muller WJ and Sabourin LA (2015) Loss of periostin/OSF-2 in ErbB2/Neu-driven tumors results in androgen receptor-positive molecular apocrine-like tumors with reduced Notch1 activity. Breast Cancer Res 17:7. doi: 10.1186/s13058-014-0513-8
186. Shao R, Bao S, Bai X, Blanchette C, Anderson RM, Dang T, Gishizky ML, Marks JR and Wang XF (2004) Acquired expression of periostin by human breast cancers promotes tumor angiogenesis through up-regulation of vascular endothelial growth factor receptor 2 expression. Mol Cell Biol 24:3992-4003.

187. Rachner TD, Göbel A, Hoffmann O, Erdmann K, Kasimir-Bauer S, Breining D, Kimmig R, Hofbauer LC and Bittner AK (2020) High serum levels of periostin are associated with a poor survival in breast cancer. Breast Cancer Res Treat 180:515-524. doi: 10.1007/s10549-020-05570-0
188. Balmain A (2002) Cancer as a complex genetic trait: tumor susceptibility in humans and mouse models. Cell 108:145-52. doi: 10.1016/s0092-8674(02)00622-0
189. Lee YJ, Kim IS, Park SA, Kim Y, Lee JE, Noh DY, Kim KT, Ryu SH and Suh PG (2013) Periostin-binding DNA aptamer inhibits breast cancer growth and metastasis. Mol Ther 21:1004-13. doi: 10.1038/mt.2013.30
190. Rios H, Koushik SV, Wang H, Wang J, Zhou HM, Lindsley A, Rogers R, Chen Z, Maeda M, Kruzynska-Frejtag A, Feng JQ and Conway SJ (2005) periostin null mice exhibit dwarfism, incisor enamel defects, and an early-onset periodontal disease-like phenotype. Mol Cell Biol 25:11131-44. doi: 10.1128/MCB.25.24.11131-11144.2005
191. Lipponen P, Aaltomaa S, Kosma VM and Syrjänen K (1994) Apoptosis in breast cancer as related to histopathological characteristics and prognosis. Eur J Cancer 30a:2068-73. doi: 10.1016/0959-8049(94)00342-3
192. Houthuijzen JM and Jonkers J (2018) Cancer-associated fibroblasts as key regulators of the breast cancer tumor microenvironment. Cancer Metastasis Rev 37:577-597. doi: 10.1007/s10555-018-9768-3
193. Lambrechts A, Van Troys M and Ampe C (2004) The actin cytoskeleton in normal and pathological cell motility. Int J Biochem Cell Biol 36:1890-909. doi: 10.1016/j.biocel.2004.01.024
194. Jeon M, You D, Bae SY, Kim SW, Nam SJ, Kim HH, Kim S and Lee JE (2017) Dimerization of EGFR and HER2 induces breast cancer cell motility through STAT1-dependent ACTA2 induction. Oncotarget 8:50570-50581. doi: 10.18632/oncotarget.10843
195. Carvalho I, Milanezi F, Martins A, Reis RM and Schmitt F (2005) Overexpression of platelet-derived growth factor receptor alpha in breast cancer is associated with tumour progression. Breast Cancer Res 7:R788-95. doi: 10.1186/bcr1304
196. Gilles C, Polette M, Mestdagt M, Nawrocki-Raby B, Ruggeri P, Birembaut P and Foidart JM (2003) Transactivation of vimentin by beta-catenin in human breast cancer cells. Cancer Res 63:2658-64.
197. Korsching E, Packeisen J, Liedtke C, Hungermann D, Wülfing P, van Diest PJ, Brandt B, Boecker W and Buerger H (2005) The origin of vimentin expression in invasive breast cancer: epithelial-mesenchymal transition, myoepithelial histogenesis or histogenesis from progenitor cells with bilinear differentiation potential? J Pathol 206:451-7. doi: 10.1002/path.1797
198. Manuel M, Tredan O, Bachelot T, Clapisson G, Courtier A, Parmentier G, Rabeony T, Grives A, Perez S, Mouret JF, Perol D, Chabaud S, Ray-Coquard I, Labidi-Galy I, Heudel P, Pierga JY, Caux C, Blay JY, Pasqual N and Ménétrier-Caux C (2012) Lymphopenia combined with low TCR diversity (divpenia) predicts poor overall survival in metastatic breast cancer patients. Oncoimmunology 1:432-440. doi: 10.4161/onci.19545
199. Denkert C, von Minckwitz G, Brase JC, Sinn BV, Gade S, Kronenwett R, Pfitzner BM, Salat C, Loi S, Schmitt WD, Schem C, Fisch K, Darb-Esfahani S, Mehta K, Sotiriou C, Wienert S, Klare P, André F, Klauschen F, Blohmer JU, Krappmann K, Schmidt M, Tesch H, Kümmel S, Sinn P, Jackisch C, Dietel M, Reimer T, Untch M and Loibl S (2015) Tumor-infiltrating lymphocytes and response to neoadjuvant chemotherapy with or without carboplatin in human epidermal growth factor receptor 2-positive and triple-negative primary breast cancers. J Clin Oncol 33:983-91. doi: 10.1200/jco.2014.58.1967
200. Ali HR, Chlon L, Pharoah PD, Markowetz F and Caldas C (2016) Patterns of Immune Infiltration in Breast Cancer and Their Clinical Implications: A Gene-Expression-Based Retrospective Study. PLoS Med 13:e1002194. doi: 10.1371/journal.pmed.1002194
201. Liu J, Shen JX, Wu HT, Li XL, Wen XF, Du CW and Zhang GJ (2018) Collagen 1A1 (COL1A1) promotes metastasis of breast cancer and is a potential therapeutic target. Discov Med 25:211-223.

202. Nolan J, Mahdi AF, Dunne CP and Kiely PA (2020) Collagen and fibronectin promote an aggressive cancer phenotype in breast cancer cells but drive autonomous gene expression patterns. Gene 761:145024. doi: 10.1016/j.gene.2020.145024
203. Liu GX, Xi HQ, Sun XY and Wei B (2015) Role of periostin and its antagonist PNDA-3 in gastric cancer metastasis. World J Gastroenterol 21:2605-13. doi: 10.3748/wjg.v21.i9.2605
204. Wei WF, Chen XJ, Liang LJ, Yu L, Wu XG, Zhou CF, Wang ZC, Fan LS, Hu Z, Liang L and Wang W (2021) Periostin(+) cancer-associated fibroblasts promote lymph node metastasis by impairing the lymphatic endothelial barriers in cervical squamous cell carcinoma. Mol Oncol 15:210-227. doi: 10.1002/1878-0261.12837
205. Wu Z, Dai W, Wang P, Zhang X, Tang Y, Liu L, Wang Q, Li M and Tang C (2018) Periostin promotes migration, proliferation, and differentiation of human periodontal ligament mesenchymal stem cells. Connect Tissue Res 59:108-119. doi: 10.1080/03008207.2017.1306060
206. Yue H, Li W, Chen R, Wang J, Lu X and Li J (2021) Stromal POSTN induced by TGF-β1 facilitates the migration and invasion of ovarian cancer. Gynecol Oncol 160:530-538. doi: 10.1016/j.ygyno.2020.11.026
207. Shaw FL, Harrison H, Spence K, Ablett MP, Simões BM, Farnie G and Clarke RB (2012) A Detailed Mammosphere Assay Protocol for the Quantification of Breast Stem Cell Activity. Journal of Mammary Gland Biology and Neoplasia 17:111-117. doi: 10.1007/s10911-012-9255-3
208. Nuzzo PV, Rubagotti A, Zinoli L, Salvi S, Boccardo S and Boccardo F (2016) The prognostic value of stromal and epithelial periostin expression in human breast cancer: correlation with clinical pathological features and mortality outcome. BMC Cancer 16:95. doi: 10.1186/s12885-016-2139-y
209. Serrano-Carbajal EA, Espinal-Enríquez J and Hernández-Lemus E (2020) Targeting Metabolic Deregulation Landscapes in Breast Cancer Subtypes. Front Oncol 10:97. doi: 10.3389/fonc.2020.00097
210. Bower JJ, Vance LD, Psioda M, Smith-Roe SL, Simpson DA, Ibrahim JG, Hoadley KA, Perou CM and Kaufmann WK (2017) Patterns of cell cycle checkpoint deregulation associated with intrinsic molecular subtypes of human breast cancer cells. npj Breast Cancer 3:9. doi: 10.1038/s41523-017-0009-7
211. Li G, Oparil S, Sanders JM, Zhang L, Dai M, Chen LB, Conway SJ, McNamara CA and Sarembock IJ (2006) Phosphatidylinositol-3-kinase signaling mediates vascular smooth muscle cell expression of periostin in vivo and in vitro. Atherosclerosis 188:292-300. doi: 10.1016/j.atherosclerosis.2005.11.002
212. Lee MJ, Heo SC, Shin SH, Kwon YW, Do EK, Suh DS, Yoon MS and Kim JH (2013) Oncostatin M promotes mesenchymal stem cell-stimulated tumor growth through a paracrine mechanism involving periostin and TGFBI. Int J Biochem Cell Biol 45:1869-77. doi: 10.1016/j.biocel.2013.05.027
213. Rani S, Barbe MF, Barr AE and Litivn J (2010) Role of TNF alpha and PLF in bone remodeling in a rat model of repetitive reaching and grasping. J Cell Physiol 225:152-67. doi: 10.1002/jcp.22208
214. Ouyang G, Liu M, Ruan K, Song G, Mao Y and Bao S (2009) Upregulated expression of periostin by hypoxia in non-small-cell lung cancer cells promotes cell survival via the Akt/PKB pathway. Cancer Lett 281:213-9. doi: 10.1016/j.canlet.2009.02.030
215. Ouanouki A, Lamy S and Annabi B (2018) Periostin, a signal transduction intermediate in TGF-β-induced EMT in U-87MG human glioblastoma cells, and its inhibition by anthocyanidins. Oncotarget 9:22023-22037. doi: 10.18632/oncotarget.25153
216. Powers CJ, McLeskey SW and Wellstein A (2000) Fibroblast growth factors, their receptors and signaling. Endocr Relat Cancer 7:165-97. doi: 10.1677/erc.0.0070165
217. Hamidi A, Song J, Thakur N, Itoh S, Marcusson A, Bergh A, Heldin CH and Landström M (2017) TGF-β promotes PI3K-AKT signaling and prostate cancer cell migration through the TRAF6-mediated ubiquitylation of p85α. Sci Signal 10. doi: 10.1126/scisignal.aal4186

218. Noorolyai S, Shajari N, Baghbani E, Sadreddini S and Baradaran B (2019) The relation between PI3K/AKT signalling pathway and cancer. Gene 698:120-128. doi: 10.1016/j.gene.2019.02.076
219. Utispan K, Sonongbua J, Thuwajit P, Chau-In S, Pairojkul C, Wongkham S and Thuwajit C (2012) Periostin activates integrin α5β1 through a PI3K/AKT-dependent pathway in invasion of cholangiocarcinoma. Int J Oncol 41:1110-8. doi: 10.3892/ijo.2012.1530
220. Hsu AH, Lum MA, Shim KS, Frederick PJ, Morrison CD, Chen B, Lele SM, Sheinin YM, Daikoku T, Dey SK, Leone G, Black AR and Black JD (2018) Crosstalk between PKCα and PI3K/AKT Signaling Is Tumor Suppressive in the Endometrium. Cell Rep 24:655-669. doi: 10.1016/j.celrep.2018.06.067
221. Ziemba BP, Burke JE, Masson G, Williams RL and Falke JJ (2016) Regulation of PI3K by PKC and MARCKS: Single-Molecule Analysis of a Reconstituted Signaling Pathway. Biophys J 110:1811-1825. doi: 10.1016/j.bpj.2016.03.001
222. Rexer BN and Arteaga CL (2012) Intrinsic and acquired resistance to HER2-targeted therapies in HER2 gene-amplified breast cancer: mechanisms and clinical implications. Crit Rev Oncog 17:1-16. doi: 10.1615/critrevoncog.v17.i1.20
223. Cheng N, Chytil A, Shyr Y, Joly A and Moses HL (2008) Transforming growth factor-beta signaling-deficient fibroblasts enhance hepatocyte growth factor signaling in mammary carcinoma cells to promote scattering and invasion. Mol Cancer Res 6:1521-33. doi: 10.1158/1541-7786.Mcr-07-2203
224. Bhowmick NA, Neilson EG and Moses HL (2004) Stromal fibroblasts in cancer initiation and progression. Nature 432:332-7. doi: 10.1038/nature03096
225. Hanahan D and Weinberg RA (2011) Hallmarks of cancer: the next generation. Cell 144:646-74. doi: 10.1016/j.cell.2011.02.013
226. Sonongbua J, Siritungyong S, Thongchot S, Kamolhan T, Utispan K, Thuwajit P, Pongpaibul A, Wongkham S and Thuwajit C (2020) Periostin induces epithelial-to-mesenchymal transition via the integrin α5β1/TWIST-2 axis in cholangiocarcinoma. Oncol Rep 43:1147-1158. doi: 10.3892/or.2020.7485
227. Watanabe T, Yasue A, Fujihara S and Tanaka E (2012) PERIOSTIN regulates MMP-2 expression via the αvβ3 integrin/ERK pathway in human periodontal ligament cells. Arch Oral Biol 57:52-9. doi: 10.1016/j.archoralbio.2011.07.010
228. Roy R, Morad G, Jedinak A and Moses MA (2020) Metalloproteinases and their roles in human cancer. Anat Rec (Hoboken) 303:1557-1572. doi: 10.1002/ar.24188
229. Izuhara K, Arima K, Ohta S, Suzuki S, Inamitsu M and Yamamoto K (2014) Periostin in allergic inflammation. Allergol Int 63:143-51. doi: 10.2332/allergolint.13-RAI-0663
230. Chen CC, Young JL, Monzon RI, Chen N, Todorović V and Lau LF (2007) Cytotoxicity of TNFalpha is regulated by integrin-mediated matrix signaling. Embo j 26:1257-67. doi: 10.1038/sj.emboj.7601596
231. Shimoyama Y, Tamai K, Shibuya R, Nakamura M, Mochizuki M, Yamaguchi K, Kakuta Y, Kinouchi Y, Sato I, Kudo A, Shimosegawa T and Satoh K (2018) Periostin attenuates tumor growth by inducing apoptosis in colitis-related colorectal cancer. Oncotarget 9:20008-20017. doi: 10.18632/oncotarget.25026
232. Vi L, Feng L, Zhu RD, Wu Y, Satish L, Gan BS and O'Gorman DB (2009) Periostin differentially induces proliferation, contraction and apoptosis of primary Dupuytren's disease and adjacent palmar fascia cells. Exp Cell Res 315:3574-86. doi: 10.1016/j.yexcr.2009.07.015
233. Xu X, Chang W, Yuan J, Han X, Tan X, Ding Y, Luo Y, Cai H, Liu Y, Gao X, Liu Q, Yu Y, Du Y, Wang H, Ma L, Wang J, Chen K, Ding Y, Fu C and Cao G (2016) Periostin expression in intratumoral stromal cells is prognostic and predictive for colorectal carcinoma via creating a cancer-supportive niche. Oncotarget 7:798-813. doi: 10.18632/oncotarget.5985

234. McCormack VA and dos Santos Silva I (2006) Breast density and parenchymal patterns as markers of breast cancer risk: a meta-analysis. Cancer Epidemiol Biomarkers Prev 15:1159-69. doi: 10.1158/1055-9965.Epi-06-0034
235. Boyd NF, Lockwood GA, Byng JW, Tritchler DL and Yaffe MJ (1998) Mammographic densities and breast cancer risk. Cancer Epidemiol Biomarkers Prev 7:1133-44.
236. Li T, Sun L, Miller N, Nicklee T, Woo J, Hulse-Smith L, Tsao MS, Khokha R, Martin L and Boyd N (2005) The association of measured breast tissue characteristics with mammographic density and other risk factors for breast cancer. Cancer Epidemiol Biomarkers Prev 14:343-9. doi: 10.1158/1055-9965.Epi-04-0490
237. Alowami S, Troup S, Al-Haddad S, Kirkpatrick I and Watson PH (2003) Mammographic density is related to stroma and stromal proteoglycan expression. Breast Cancer Res 5:R129-35. doi: 10.1186/bcr622
238. Provenzano PP, Inman DR, Eliceiri KW, Knittel JG, Yan L, Rueden CT, White JG and Keely PJ (2008) Collagen density promotes mammary tumor initiation and progression. BMC Med 6:11. doi: 10.1186/1741-7015-6-11
239. Taufalele PV, VanderBurgh JA, Muñoz A, Zanotelli MR and Reinhart-King CA (2019) Fiber alignment drives changes in architectural and mechanical features in collagen matrices. PLoS One 14:e0216537. doi: 10.1371/journal.pone.0216537
240. Gilkes DM, Semenza GL and Wirtz D (2014) Hypoxia and the extracellular matrix: drivers of tumour metastasis. Nat Rev Cancer 14:430-9. doi: 10.1038/nrc3726
241. Gabriel EM, Fisher DT, Evans S, Takabe K and Skitzki JJ (2018) Intravital microscopy in the study of the tumor microenvironment: from bench to human application. Oncotarget 9:20165-20178. doi: 10.18632/oncotarget.24957
242. Levental KR, Yu H, Kass L, Lakins JN, Egeblad M, Erler JT, Fong SF, Csiszar K, Giaccia A, Weninger W, Yamauchi M, Gasser DL and Weaver VM (2009) Matrix crosslinking forces tumor progression by enhancing integrin signaling. Cell 139:891-906. doi: 10.1016/j.cell.2009.10.027
243. Diermeier SD, Chang KC, Freier SM, Song J, El Demerdash O, Krasnitz A, Rigo F, Bennett CF and Spector DL (2016) Mammary Tumor-Associated RNAs Impact Tumor Cell Proliferation, Invasion, and Migration. Cell Rep 17:261-274. doi: 10.1016/j.celrep.2016.08.081
244. Lin EY, Jones JG, Li P, Zhu L, Whitney KD, Muller WJ and Pollard JW (2003) Progression to malignancy in the polyoma middle T oncoprotein mouse breast cancer model provides a reliable model for human diseases. Am J Pathol 163:2113-26. doi: 10.1016/s0002-9440(10)63568-7
245. Du J, Zu Y, Li J, Du S, Xu Y, Zhang L, Jiang L, Wang Z, Chien S and Yang C (2016) Extracellular matrix stiffness dictates Wnt expression through integrin pathway. Sci Rep 6:20395. doi: 10.1038/srep20395
246. Puglisi F, Puppin C, Pegolo E, Andreetta C, Pascoletti G, D'Aurizio F, Pandolfi M, Fasola G, Piga A, Damante G and Di Loreto C (2008) Expression of periostin in human breast cancer. J Clin Pathol 61:494-8. doi: 10.1136/jcp.2007.052506
247. Li C, Xu J, Wang Q, Geng S, Yan Z, You J, Li Z and Zou X (2018) Prognostic value of periostin in early-stage breast cancer treated with conserving surgery and radiotherapy. Oncol Lett 15:8072-8078. doi: 10.3892/ol.2018.8310
248. Nakazawa Y, Taniyama Y, Sanada F, Morishita R, Nakamori S, Morimoto K, Yeung KT and Yang J (2018) Periostin blockade overcomes chemoresistance via restricting the expansion of mesenchymal tumor subpopulations in breast cancer. Sci Rep 8:4013. doi: 10.1038/s41598-018-22340-7
249. Kakarala M and Wicha MS (2008) Implications of the cancer stem-cell hypothesis for breast cancer prevention and therapy. J Clin Oncol 26:2813-20. doi: 10.1200/jco.2008.16.3931
250. Butti R, Gunasekaran VP, Kumar TVS, Banerjee P and Kundu GC (2019) Breast cancer stem cells: Biology and therapeutic implications. Int J Biochem Cell Biol 107:38-52. doi: 10.1016/j.biocel.2018.12.001

251. Wang X, Liu J, Wang Z, Huang Y, Liu W, Zhu X, Cai Y, Fang X, Lin S, Yuan L and Ouyang G (2013) Periostin contributes to the acquisition of multipotent stem cell-like properties in human mammary epithelial cells and breast cancer cells. PLoS One 8:e72962. doi: 10.1371/journal.pone.0072962
252. Targow AM (1934) THE EFFECT OF A GROWTH-PROMOTING EXTRACT OF THE ANTERIOR PITUITARY ON THE EARLY GROWTH OF THE ALBINO RAT. J Exp Med 59:699-710. doi: 10.1084/jem.59.6.699
253. Trowell O and Willmer EJJoEB (1939) Studies on the Growth of Tissues in vitro: VI. The Effects of some Tissue Extracts on the Growth of Periosteal Fibroblasts. 16:60-70.
254. Armelin HA (1973) Pituitary extracts and steroid hormones in the control of 3T3 cell growth. Proc Natl Acad Sci U S A 70:2702-6. doi: 10.1073/pnas.70.9.2702
255. Gospodarowicz D (1975) Purification of a fibroblast growth factor from bovine pituitary. J Biol Chem 250:2515-20.
256. Lemmon SK and Bradshaw RA (1983) Purification and partial characterization of bovine pituitary fibroblast growth factor. J Cell Biochem 21:195-208. doi: 10.1002/jcb.240210302
257. Ye X, Tam WL, Shibue T, Kaygusuz Y, Reinhardt F, Ng Eaton E and Weinberg RA (2015) Distinct EMT programs control normal mammary stem cells and tumour-initiating cells. Nature 525:256-60. doi: 10.1038/nature14897
258. Xu J, Acharya S, Sahin O, Zhang Q, Saito Y, Yao J, Wang H, Li P, Zhang L, Lowery FJ, Kuo WL, Xiao Y, Ensor J, Sahin AA, Zhang XH, Hung MC, Zhang JD and Yu D (2015) 14-3-3ζ turns TGF-β's function from tumor suppressor to metastasis promoter in breast cancer by contextual changes of Smad partners from p53 to Gli2. Cancer Cell 27:177-92. doi: 10.1016/j.ccell.2014.11.025
259. He BW, Guo JJ, Jiang ZY and Zhang SZ (1984) Selection of a beta-amylase-producing strain and its fermentation conditions. Ann N Y Acad Sci 434:275-7.
260. Kim SS, Jackson-Boeters L, Darling MR, Rieder MJ and Hamilton DW (2013) Nifedipine induces periostin expression in gingival fibroblasts through TGF-beta. J Dent Res 92:1022-8. doi: 10.1177/0022034513503659
261. Nanri Y, Nunomura S, Terasaki Y, Yoshihara T, Hirano Y, Yokosaki Y, Yamaguchi Y, Feghali-Bostwick C, Ajito K, Murakami S, Conway SJ and Izuhara K (2020) Cross-Talk between Transforming Growth Factor-β and Periostin Can Be Targeted for Pulmonary Fibrosis. Am J Respir Cell Mol Biol 62:204-216. doi: 10.1165/rcmb.2019-0245OC
262. Chen G, Nakamura I, Dhanasekaran R, Iguchi E, Tolosa EJ, Romecin PA, Vera RE, Almada LL, Miamen AG, Chaiteerakij R, Zhou M, Asiedu MK, Moser CD, Han S, Hu C, Banini BA, Oseini AM, Chen Y, Fang Y, Yang D, Shaleh HM, Wang S, Wu D, Song T, Lee JS, Thorgeirsson SS, Chevet E, Shah VH, Fernandez-Zapico ME and Roberts LR (2017) Transcriptional Induction of Periostin by a Sulfatase 2-TGFβ1-SMAD Signaling Axis Mediates Tumor Angiogenesis in Hepatocellular Carcinoma. Cancer Res 77:632-645. doi: 10.1158/0008-5472.Can-15-2556
263. Swallow CJ, Partridge EA, Macmillan JC, Tajirian T, DiGuglielmo GM, Hay K, Szweras M, Jahnen-Dechent W, Wrana JL, Redston M, Gallinger S and Dennis JW (2004) alpha2HS-glycoprotein, an antagonist of transforming growth factor beta in vivo, inhibits intestinal tumor progression. Cancer Res 64:6402-9. doi: 10.1158/0008-5472.Can-04-1117
264. Qi L, Zhou B, Chen J, Hu W, Bai R, Ye C, Weng X and Zheng S (2019) Significant prognostic values of differentially expressed-aberrantly methylated hub genes in breast cancer. J Cancer 10:6618-6634. doi: 10.7150/jca.33433
265. Zhou M, Sutliff RL, Paul RJ, Lorenz JN, Hoying JB, Haudenschild CC, Yin M, Coffin JD, Kong L, Kranias EG, Luo W, Boivin GP, Duffy JJ, Pawlowski SA and Doetschman T (1998) Fibroblast growth factor 2 control of vascular tone. Nat Med 4:201-7. doi: 10.1038/nm0298-201
266. Ortega S, Ittmann M, Tsang SH, Ehrlich M and Basilico C (1998) Neuronal defects and delayed wound healing in mice lacking fibroblast growth factor 2. Proc Natl Acad Sci U S A 95:5672-7. doi: 10.1073/pnas.95.10.5672

267. Homer-Bouthiette C, Doetschman T, Xiao L and Hurley MM (2014) Knockout of nuclear high molecular weight FGF2 isoforms in mice modulates bone and phosphate homeostasis. J Biol Chem 289:36303-14. doi: 10.1074/jbc.M114.619569
268. Montero A, Okada Y, Tomita M, Ito M, Tsurukami H, Nakamura T, Doetschman T, Coffin JD and Hurley MM (2000) Disruption of the fibroblast growth factor-2 gene results in decreased bone mass and bone formation. J Clin Invest 105:1085-93. doi: 10.1172/jci8641
269. Markwald RR, Moreno-Rodriguez RA, Ghatak S, Misra S, Norris RA and Sugi Y (2019) Role of Periostin in Cardiac Valve Development. Adv Exp Med Biol 1132:177-191. doi: 10.1007/978-981-13-6657-4_17
270. Nikoloudaki G, Creber K and Hamilton DW (2020) Wound healing and fibrosis: a contrasting role for periostin in skin and the oral mucosa. Am J Physiol Cell Physiol 318:C1065-c1077. doi: 10.1152/ajpcell.00035.2020
271. Duchamp de Lageneste O and Colnot C (2019) Periostin in Bone Regeneration. Adv Exp Med Biol 1132:49-61. doi: 10.1007/978-981-13-6657-4_6
272. Siegel-Axel DI, Ullrich S, Stefan N, Rittig K, Gerst F, Klingler C, Schmidt U, Schreiner B, Randrianarisoa E, Schaller HE, Stock UA, Weigert C, Königsrainer A and Häring HU (2014) Fetuin-A influences vascular cell growth and production of proinflammatory and angiogenic proteins by human perivascular fat cells. Diabetologia 57:1057-66. doi: 10.1007/s00125-014-3177-0
273. Engelman JA (2009) Targeting PI3K signalling in cancer: opportunities, challenges and limitations. Nat Rev Cancer 9:550-62. doi: 10.1038/nrc2664
274. Verret B, Cortes J, Bachelot T, Andre F and Arnedos M (2019) Efficacy of PI3K inhibitors in advanced breast cancer. Ann Oncol 30:x12-x20. doi: 10.1093/annonc/mdz381
275. Levine DA, Bogomolniy F, Yee CJ, Lash A, Barakat RR, Borgen PI and Boyd J (2005) Frequent mutation of the PIK3CA gene in ovarian and breast cancers. Clin Cancer Res 11:2875-8. doi: 10.1158/1078-0432.Ccr-04-2142
276. Zheng QM, Lu JJ, Zhao J, Wei X, Wang L and Liu PS (2016) Periostin Facilitates the Epithelial-Mesenchymal Transition of Endometrial Epithelial Cells through ILK-Akt Signaling Pathway. Biomed Res Int 2016:9842619. doi: 10.1155/2016/9842619
277. Jiang N, Dai Q, Su X, Fu J, Feng X and Peng J (2020) Role of PI3K/AKT pathway in cancer: the framework of malignant behavior. Mol Biol Rep 47:4587-4629. doi: 10.1007/s11033-020-05435-1
278. Liu WT, Huang KY, Lu MC, Huang HL, Chen CY, Cheng YL, Yu HC, Liu SQ, Lai NS and Huang HB (2017) TGF-β upregulates the translation of USP15 via the PI3K/AKT pathway to promote p53 stability. Oncogene 36:2715-2723. doi: 10.1038/onc.2016.424
279. Yi JY, Shin I and Arteaga CL (2005) Type I transforming growth factor beta receptor binds to and activates phosphatidylinositol 3-kinase. J Biol Chem 280:10870-6. doi: 10.1074/jbc.M413223200
280. Remy I, Montmarquette A and Michnick SW (2004) PKB/Akt modulates TGF-beta signalling through a direct interaction with Smad3. Nat Cell Biol 6:358-65. doi: 10.1038/ncb1113
281. Conery AR, Cao Y, Thompson EA, Townsend CM, Jr., Ko TC and Luo K (2004) Akt interacts directly with Smad3 to regulate the sensitivity to TGF-beta induced apoptosis. Nat Cell Biol 6:366-72. doi: 10.1038/ncb1117
282. Xie F, Jin K, Shao L, Fan Y, Tu Y, Li Y, Yang B, van Dam H, Ten Dijke P, Weng H, Dooley S, Wang S, Jia J, Jin J, Zhou F and Zhang L (2017) FAF1 phosphorylation by AKT accumulates TGF-β type II receptor and drives breast cancer metastasis. Nat Commun 8:15021. doi: 10.1038/ncomms15021
283. Kattla JJ, Carew RM, Heljic M, Godson C and Brazil DP (2008) Protein kinase B/Akt activity is involved in renal TGF-beta1-driven epithelial-mesenchymal transition in vitro and in vivo. Am J Physiol Renal Physiol 295:F215-25. doi: 10.1152/ajprenal.00548.2007
284. Isakov N (2018) Protein kinase C (PKC) isoforms in cancer, tumor promotion and tumor suppression. Semin Cancer Biol 48:36-52. doi: 10.1016/j.semcancer.2017.04.012

285. Namciu S, Lieberman MA and Stavnezer E (1994) Induction of the c-ski proto-oncogene by phorbol ester correlates with induction of megakaryocyte differentiation. Oncogene 9:1407-16.
286. El-Brolosy MA and Stainier DYR (2017) Genetic compensation: A phenomenon in search of mechanisms. PLoS Genet 13:e1006780. doi: 10.1371/journal.pgen.1006780